Pb ISOTOPE SYSTEMATICS IN CENOZOIC IGNEOUS ROCKS FROM THE RIO GRANDE RIFT REGION, USA

by

CHERYLYN E. HEIKOOP, B.A., M.S.

A thesis

Submitted to the School of Graduate Studies

in Partial Fulfilment of the Requirements

for the Degree

Doctor of Philosophy

McMaster University

Pb ISOTOPES IN IGNEOUS ROCKS FROM THE RIO GRANDE RIFT REGION

DOCTOR OF PHILOSOPHY (1997)
(Geology)

McMaster University
Hamilton, Ontario

TITLE: Pb isotope systematics in Cenozoic igenous rocks from the Rio Grande Rift region, USA

AUTHOR: Cherylyn E. Heikoop
B.A. (Geology), Douglass College (Rutgers University)
New Brunswick, New Jersey, USA
M.S. (Geology), University of Texas
Arlington, Texas, USA

SUPERVISOR: Professor A.P. Dickin

NUMBER OF PAGES: xiii, 178

Abstract

The Rio Grande Rift is a major tectonomagmatic feature of the North American craton. Physiographically, the present rift is recognized as a series of grabens and half-grabens which extend for over 1000 km from south-central Colorado into Chihuahua, Mexico. Rift structures, however, are recognized as far north as the Colorado-Wyoming border. Basaltic magmatism within the rift began by 30 Ma in southern New Mexico, and by 25 Ma in northern New Mexico and Colorado. Within-rift magmatism is low in volume in comparison to rift-related activity on the rift shoulders and flanks.

Petrologic studies of Rio Grande Rift-related volcanics are numerous, yet focus primarily on suites erupted in north-central New Mexico and Colorado. However, recently published abstracts suggest areas of southern New Mexico are receiving much needed attention. Initial attempts at characterizing the petrologic diversity and mantle sources of rift-related volcanics have concentrated on major and trace element data, as well as the application of Sr and Nd isotopes. Only minor attention has been given to Pb isotope variations.

This thesis contains the most recent compilation of Pb isotope data for volcanic rocks erupted within the Rio Grande Rift region. The oldest rocks included in this work are monzonite stocks erupted c. 60 Ma within the Colorado Mineral Belt. Using Pb isotope data in combination with trace element variations and Sr-Nd isotopes, a model is developed which suggests the stocks were initially derived from mantle sources with geochemical properties similar to those which produced rift-related basaltic volcanics in northwest Colorado beginning at 25 Ma.

Two chapters of the thesis are devoted to exploring the utility of Pb isotopes as tracers of crustal influence in continental basaltic volcanism. One deals specifically with documenting Pb isotope variations in the northwest Colorado region, whereas the second focuses on variations in the Española Basin of north-central New Mexico. Major results of the northwest Colorado study 1) suggest that the asthenosphere contributed to early rift (25 Ma volcanism), 2) better characterize the geochemical signature of lithospheric and asthenospheric sources during periods of active volcanism, and 3) confirm earlier suspicions regarding the effects of crustal contamination in several rock suites. Work on basaltic components of volcanism in the Española Basin indicate that crustal contamination was also an important process in producing the observed Pb and Sr isotopic variations in both early and later rift lavas.

The remaining chapter of the thesis is a synthesis of all available rift data, from northern Colorado to southern New Mexico. An analysis of changes in the Pb isotopic composition of the lithosphere with latitude is presented, as well as a cross-rift transect of the central rift region. Further, a model which combines previously published ideas on the tectonomagmatic development of the Rio Grande Rift and the Basin and Range province is proposed. The most important results of the combined model are the proposition that rifting began earlier than previously thought, and that the timing of extension and magmatism in the Rio Grande Rift is very similar to that of the Basin and Range province. Additional data from the rift, particularly the southern region, will help to confirm or deny this model.

Acknowledgements

I owe a very large debt of gratitute to my supervisor, Alan Dickin, for continually fielding questions regarding mass spectrometry, clean lab techniques, and isotope geochemistry. I would also like to acknowledge the critical but fair reviews of the research by the remaining members of my supervisory committee, including Bob McNutt, Paul Clifford, Mike Risk, and Brian Clarke. John Wolff, formerly my M.S. thesis supervisor, has provided additional advice on petrologic problems.

It is only fair to recognize technical assistance from other individuals. Departmental technicians Tuong Ngyuen, Catharina Jager, and Jim McAndrew are thanked for advice on numerous aspects of chemistry and mass spectrometry. Friendly and efficient office staff, including Angela Antanavicius and Edna Cutler, are thanked for help and guidance through the technical maze of graduate studies rules and regulations. Joyce Allen is acknowledged for making sure my degree requirements were fulfilled.

Samples analyzed during the course of this research were supplied in the form of powders by P.T. Leat, R.N. Thompson, S.A. Gibson, J.A. Wolff, and N.J. McMillan, and are part of collaborative research projects developed by A.P. Dickin. These individuals are co-authors on the various papers that will be developed from the chapters of the thesis and are acknowledged for their critical reviews.

My tenure at McMaster was made more enjoyable by the friendships of my past and present officemates, Mingze Zhai, and Scott Smith, respectively. Work in the clean lab would not have been the same without the companionship of Karen Goodger and Chris Martin. I would also like to thank my parents for their continual support,

despite the fact that they were never quite sure just what exactly I was doing. Lastly, I must thank my husband, Jeff, for celebrating my accomplishments, and for pulling me through the setbacks and giving me a shoulder to cry on, as needed.

The research described herein was generously funded from several sources, including departmental scholarships and research grants to Alan P. Dickin, Robert H. McNutt, and Michael J. Risk. Additional financial support from a part-time technician position with Derek Ford is also acknowledged.

TABLE OF CONTENTS

PREFACE

Chapters 3 - 6 have been organized in publication format. The following information describes the contribution of this candidate to each paper, as well indentifying co-authors and journals to which each paper is or will be submitted to.

CHAPTER 3: Rio Grande Rift-related volcanism in Northwest Colorado: refinement of source characteristics using Pb isotopes
Authors: C.E. Heikoop, A.P. Dickin, R.N. Thompson, P.T. Leat, and S.A. Gibson
Journal: Chemical Geology (submitted)

All Pb isotope ratio and isotope dilution analyses were performed by the candidate except for data from the Elkheads Igneous Province, which was previously published by Leat et al. (1988a) and Thompson et al. (1989). Comments and revisions were suggested by all co-authors.

CHAPTER 4: Identification of crustal contaminants in mafic volcanics of the Española Basin, Rio Grande Rift, using Pb isotopes
Authors: C.E. Heikoop, J.A.Wolff, A.P.Dickin, S.A. Gibson, and R.N. Thompson
Journal: Contributions to Mineralogy and Petrology (to be submitted)

All Pb isotope ratio and isotope dilution analyses were performed by the candidate. Comments and revisions were suggested by all co-authors.

CHAPTER 5: Spatial and temporal review of Pb isotopes in mafic rocks from the Rio Grande Rift
Authors: C.E. Heikoop, N.J. McMillan, and A.P. Dickin
Journal: Journal of Petrology (to be submitted)

Pb isotope ratio and isotope dilution analyses were performed by the candidate, with the exception of those samples supplied by N.J. McMillan, and data derived from the literature. The majority of McMillan samples were processed in the clean lab by C. Jager and analyzed by A.P. Dickin. Comments and revisions were suggested by all co-authors.

CHAPTER 6: Sr-Nd-Pb isotope evidence for potential mantle derivation of monzonites near Central City, Colorado (Colorado Mineral Belt)
Authors: C.E. Heikoop, A.P. Dickin, C.M. Rice
Journal: Lithos (to be submitted)

All Pb isotope ratio analyses were performed by the candidate. The ideas presented in this paper were originally envisaged and drafted by A.P. Dickin, emphasizing Nd isotopes only. Comments and revisions were suggested by all co-authors.

LIST OF FIGURES

LIST OF TABLES

Chapter 1: Introduction

1.1 Overview

On the North American craton, the Basin and Range Province and the Rio Grande Rift (RGR) are areas of major extensional activity. Prior to the onset of extension, vast areas of western North America witnessed the emplacement of large batholiths and smaller stocks, primarily between 70-60 Ma, which became important sites of mineralization, including the Colorado Mineral Belt (e.g., Lipman, 1980). This intense magmatism and later extensional activity are thought to be directly related to the tectonic regime at the time, that is the ongoing eastward subduction of the Farallon plate beneath the westward moving North American plate.

In the Basin and Range Province, extension began c. 53 Ma in the Pacific Northwest, and was accompanied by intermediate to silicic volcanism (Wernicke et al., 1987). Between 38 - 30 Ma, extension began in the Great Basin region, and is recognized on the basis of fault patterns in metamorphic core complexes and through extensive igneous activity which produced large volumes of ignimbrite. The southward migration of activity in the Basin and Range followed a decrease in the westward motion of the North American plate, although it is still under debate as to whether or not there is a genetic link between these events (Hamilton, 1987). In contrast, extension within the RGR region is widely cited as beginning as early as 32 Ma in southern New Mexico and as late as 25 Ma in Colorado (e.g. Lipman and Mehnert, 1975; Chapin, 1979), and was accompanied by basaltic volcanism. However, more recent work by Mack et al. (1996) revises the estimated time of initial extension in the southern RGR to 35 Ma. A lag in the

timing of initial extensional activity in the RGR (32 -35 Ma) versus the Great Basin (38 Ma) also translates to a period of reduced magmatism followed by renewed extension in each region. In the Basin and Range, this lull in magmatic and extensional activity took place 20 -17 Ma (Wernicke et al., 1987), whereas in the RGR, the lull took place 18 - 13 Ma (Morgan et al., 1986). Basin and range topography developed in the Basin and Range and RGR following these lulls.

Many workers view the RGR as part of the Basin and Range, however models developed for the Basin and Range do not adequately describe the tectonomagmatic history of the RGR. For example, Coney (1987) maintains that the Basin and Range Province as well as the RGR are no older than 17 Ma, yet a substantial body of evidence suggests otherwise (e.g., Lipman and Mehnert, 1975; Eaton, 1979; Tweto, 1979; Morgan et al., 1986; Baldridge et al., 1991; Miller et al., 1992; Axen et al., 1993; Chapin and Cather, 1994). Magmatic models for the Basin and Range which document a change from lithospheric to asthenospheric sources around 5 Ma are not applicable to the RGR, as Gibson et al. (1992, 1993) and this author (Chapter 3) show that asthenospheric sources were tapped throughout the history of the RGR.

Although the geologic histories of the Basin and Range Province and the RGR are probably related, present day physiographic, tectonic, and magmatic characteristics of the RGR combine to make it a unique region. As noted by Seager and Morgan (1979), the RGR is distinguished from the Basin and Range region by its higher heat flow, late Quaternary volcanism, abundant Pliocene and Quaternary faulting, and exceptionally deep basins. These features are related to the existence of a large continental ridge, termed the Alvarado Ridge, of which the RGR system constitutes the

axial basin (Eaton, 1987). The Basin and Range Province resides on the western flank of this ridge. Geophysical studies suggest that at the present time, the asthenosphere has upwarped against the base of the lithosphere beneath the axis of the rift (Cordell, 1978; Eaton, 1979; Seager and Morgan, 1979; Davis et al., 1984; Parker et al., 1984). Overall uplift of the RGR and surrounding regions has been attributed to various causes, including lithospheric thinning and emplacement of hot asthenosphere beneath the uplifted regions (Coney, 1987; Eaton, 1987; Angevine and Flanagan, 1987).

Recent petrologic syntheses for both the Basin and Range Province and RGR allow for documentation of spatial and temporal changes in magma sources (e.g., Fitton et al., 1988, 1991; Perry et al., 1987, 1988; Daley and DePaolo, 1992; Gibson et al., 1992, 1993; Bradshaw et al., 1993; Leeman and Harry, 1993). Many of these studies discuss the incompatible trace element and Sr-Nd isotope variations in extension-related lavas. Kempton et al. (1991), however, do present Pb isotope data for Basin and Range basalts, relating combined Sr-Nd-Pb data trends to lithospheric or asthenospheric sources and the effects of crustal contamination.

1.2 Scope of thesis

This thesis embodies the most current synthesis of Pb isotopic data for the RGR system. Previously, Everson (1979) compiled a regional Pb isotope data base for the southwestern U.S.A. which included a number of samples from the RGR region, but focused primarily on the Basin and Range. In contrast, this work concentrates exclusively on the RGR. To construct a database, an intensive literature search was conducted, as well as the analysis by the author of nearly 100 samples from the collection of A.P. Dickin. Samples for analysis were chosen on the basis of the completeness of existing major and trace element data, as well as available Sr-Nd

isotope data. Analytical procedures are outlined in the Appendix 1 and all data are listed in Appendix 2.

Theoretical concepts regarding the interpretation of trace element and isotope data are addressed in Chapter 2. Potential mantle magma source components in the continental realm and the effects of crustal contamination are discussed. A discussion on the isotope systematics of Pb is presented, as it is the focus of the thesis. Also, the isotope systematics of the radiogenic isotopes Sr, Nd, and Hf are briefly reviewed, as each of these isotopes is incorporated in some degree into the interpretations of the current data set.

Chapter 3 presents Pb isotope data on Miocene - Recent basic volcanic rocks from Northwest Colorado, which are believed to represent the northernmost manifestation of Rio Grande Rift-related activity. In addition, Sr-Nd-Pb inter-isotope variations are also documented. The results of this chapter redefine a mantle source for the Northwest Colorado volcanics, and strongly suggest the availability of a previously undetected asthenospheric source component in the early rift-stage volcanics.

In Chapter 4, Pb isotopes in mafic lavas from the Española Basin, north-central New Mexico, are presented. Variations in Pb isotope ratios are attributed to variable degrees of crustal contamination, specifically by upper crust in the early rift stage lavas, and lower crust for compositions from the late rift Cerros del Rio volcanic center. The results of this chapter emphasize the sensitivity of Pb isotope ratios in mantle-derived rocks to contamination by crustal components.

Chapter 5 is a synthesis of the available Pb isotope data for the RGR. Spatial and temporal changes in lithospheric and asthenospheric sources on a regional scale are considered. A tectonomagmatic model based on extension models for the

Great Basin and RGR is presented.

Pb isotope variations in a group of monzonite stocks from the Colorado Mineral Belt are the subject of Chapter 6. The monzonites are Laramide in age and were emplaced prior to RGR activity. The location of the stocks is approximately 100 km from the volcanic centers in Northwest Colorado discussed in Chapter 3. Data from the Northwest Colorado volcanics and potassic rocks of Eocene age from Montana (O'Brien et al., 1991, 1995) are used as proxies for mantle components which have contributed to the petrogenesis of the monzonites. A model is suggested in which the monzonites were ultimately derived from a mantle source, rather than a crustal source.

Chapter 2: Theories and Methodologies

The approach taken in this thesis is to use combined trace element and isotope relationships to (1) determine if previous interpretations regarding petrogenesis of specific volcanic suites are consistent with Pb data presented here, (2) further characterize or establish magma sources and their possible contaminants using Pb data, and (3) reconcile the Pb data to theories on mantle structure and dynamics pertinent to the Rio Grande Rift (RGR) region of the United States. In order to accomplish these goals, it is necessary to review the trace element and isotopic characteristics of the available magma sources and contaminants, and resolve any changes in magma source chemistry over time. This chapter begins with an overview of basic magma sources and contaminants, then outlines the theory and methodology regarding use of incompatible element diagrams. The concluding section considers the use of radiogenic isotopes as petrogenetic tools, focusing especially on Pb.

2.1 Potential magma sources and contaminants

Basic magmas are thought to originate in the upper mantle. Before proceeding with the description of relevant sources of magma for RGR volcanism, it is useful to clarify the terminology used to delineate the structure of the upper mantle, in terms of lithospheric and asthenospheric components.

McKenzie and Bickle (1988) and McKenzie (1989) discuss the structure of the upper mantle in terms of its thermal properties and the relevant terminology has been adopted in this thesis. The lithosphere can be divided into two distinct parts. A mechanical boundary layer (MBL) forms the upper layer of the lithosphere (including the

crust). The MBL is relatively cool and rigid, and transfers heat entirely through conduction (Fig. 2.1). These properties allow the MBL to remain physically isolated for geologically long periods of time from the convective asthenosphere, which in turn promotes the development of distinctive elemental and isotopic characteristics. In contrast, the thermal boundary layer (TBL) separates the MBL from the asthenosphere (Fig. 2.1), transferring heat via conduction at its upper contact and via convection at its lower contact. The TBL has the potential to undergo convective overturn into the asthenosphere, thus the chemical composition of the TBL is equivalent to that of the underlying asthenosphere. Some workers have postulated that if a change in tectonic regime were to occur, the upper mantle structure might change, allowing the geochemical character of the TBL to remain distinct from the asthenosphere until convective overturn occurred (e.g., Leat et al., 1988a).

The potential mantle sources for RGR volcanism include the lower to middle portions of the MBL, the TBL, and the convecting asthenosphere. The geochemical composition of the asthenosphere and the TBL during rifting is contentious. In order to explain the observed geochemical variations in rift-related volcanism of Northwest Colorado, Leat et al. (1988a, 1989, 1990, 1991) proposed that during the first phase of rifting, c. 30 - 18 Ma, the convecting asthenosphere and the TBL beneath Northwest Colorado had subduction- processed qualities as a result of dehydration of the underlying Farallon plate. By the second phase of rifting, c. 10 Ma - present, the asthenospheric volume above the subducted Farallon plate had changed to a predominantly oceanic island basalt, or OIB - like composition, with the TBL still retaining the subduction- processed qualities. Newly acquired Pb data presented in Chapter 3 cast doubt on this interpretation, however, as it is shown that OIB-like magmas were

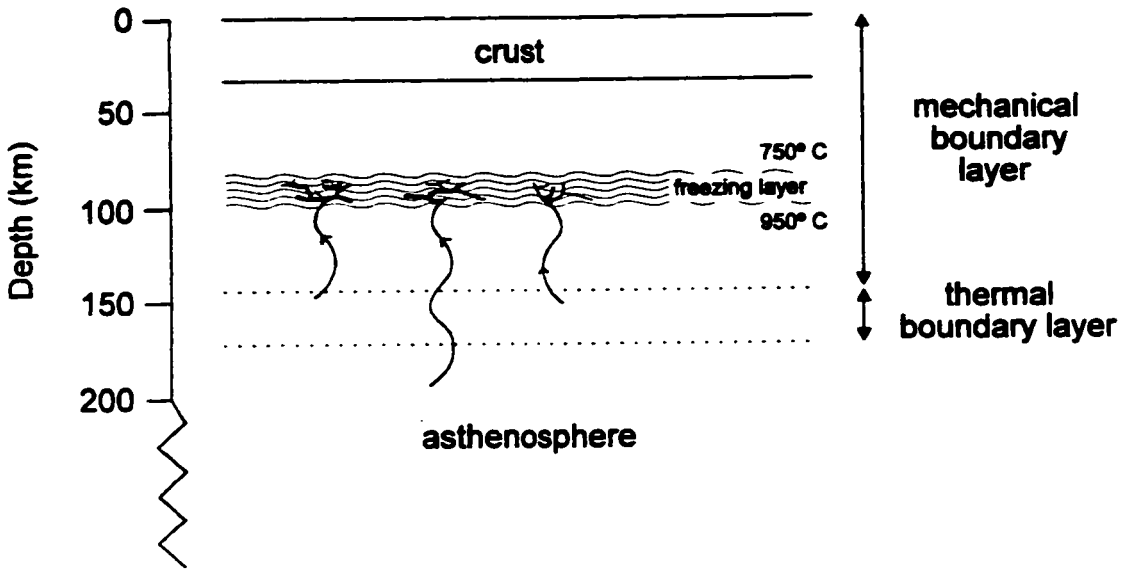

Fig. 2.1 Structure of the crust and upper mantle, following the model of McKenzie (1989). Vein networks in the mechanical boundary layer are thought to be a potential source of ultrapotassic rocks.

available *during the first* rifting phase. This latter explanation is also more in keeping with the upper mantle composition promoted by Gibson et al. (1993) for the central rift region during the earlier rifting phase, and presents a unified model for upper mantle structure in the RGR region.

The geochemical composition of the MBL may be variable. McKenzie (1989) has shown that, theoretically, small melt fractions (< 1%) are capable of escaping the asthenosphere by moving upwards into the MBL to form complex vein networks (Fig. 2.1). This process could be promoted by dehydration of a subducted slab which could provide additional volatiles and incompatible elements to the asthenosphere. Vein networks, enriched in incompatible elements and volatiles, would melt readily upon decompression or heating from below. Melts derived from the vein networks are believed by many to represent the source of ultrapotassic magmas (McKenzie, 1989; Thompson et al, 1989b; Foley and Peccerillo, 1992; Foley, 1992). Where present, the incompatible element-rich veins have the potential to mix with other mantle components (lithospheric or asthenospheric) during melting to form magmas with complex trace element and isotopic characteristics.

Several studies have indicated that OIB-like asthenosphere underlies continents (e.g Fitton and Dunlop, 1985; Fitton et al. 1988; Thompson et al. 1990). Combined radiogenic isotope studies have indicated that mixing between several OIB sources is required to explain the isotopic and trace element variations in OIB (e.g., Sun, 1980; White and Hofmann, 1982; Zindler et al., 1982; White, 1985; Zindler and Hart, 1986). The existence of enriched OIB mantle sources has been attributed to metasomatism and crustal recycling (see Dickin, 1995 for review). Contamination of non-enriched OIB components within the continental lithosphere may potentially produce

trace element and isotopic signatures similar to enriched OIB. Therefore, in this thesis reference to an asthenospheric source will be to OIB, with no specific connotations to any OIB components.

The potential contribution of mantle plumes to RGR magmatism must also be assessed. Leat et al. (1991) have suggested that advection of the asthenosphere beneath Northwest Colorado within the Yellowstone plume affected the resultant geochemistry of the later rift (< 10 Ma) asthenosphere- derived magmas . Geist and Richards (1993) document the first surface expression of the Yellowstone plume at 17.2 Ma, marking the eruption of the Columbia River Basalt. Numerical modeling by Thompson et al. (1989a) implied that the influence of the Yellowstone plume would eventually be recognized over 1000 km away, as the plume head spreads out radially beneath the North American plate. This theory is considered further in Chapter 5, in which the Pb isotopic signatures of basic magmas from the entire RGR region are analyzed. More relevant here is the suggestion noted above that OIB-like sources were tapped during the early rifting phase in Northwest Colorado. In Chapter 3 it is proposed that 'plums' or 'blobs' of plume-like material were present within the asthenosphere prior to the evolution and surface expression of the Yellowstone plume proper, thus supplying the region with Yellowstone plume-like OIB.

The number of potential contaminants to a mantle-derived magma is dependent in part on where the magma originated. For example, an asthenospheric magma could potentially be contaminated by components of the lithosphere and crust. Lithospheric magmas could be contaminated by incompatible element-rich melts from veins within the lithosphere or by crust. The distinction between upper and lower crustal contamination is made using specific trace element data and isotope ratios. For

example, the lower crust is expected to have undergone granulite facies metamorphism, which would effectively strip it of mobile elements such as U and Rb. These elements would accumulate in the upper crust. Over geologic time, this process would result in lower isotopic Pb and Sr ratios for lower crustal rocks, in comparison to radiogenic Pb and Sr isotopic signatures in the upper crust. These properties discussed further in section 2.3.

2.2 Incompatible elements

An element is considered incompatible if it has a low distribution coefficient relative to a phenocryst assemblage undergoing crystallization or one which is undergoing partial melting. In other words, incompatible elements prefer the melt phase relative to the crystalline phase and will remain in, or escape to, a melt as long as or as soon as possible, respectively. Traditionally, igneous petrologists have used chondrite normalized rare earth element (REE) diagrams in discussions regarding the petrogenesis of magmatic suites. The effect of normalization is to smooth an otherwise zig zag pattern that results from cosmic abundance variations. A group of elements with similar abundance ratios to chondrite will produce an essentially flat pattern if normalized.

Sun et al. (1979) expanded the REE diagram to include other incompatible elements, such as large ion lithophile elements (e.g. Rb, K, and Ba), and also several high field strength elements, including Zr and Hf, all of which are incompatible during partial melting to generate mid-ocean ridge basalt (MORB). This expanded trace element plot is now widely used for a variety of compositions in both the continental and oceanic environments. The terminology used to describe this type of plot is variable, and includes "mantle normalizing diagram" (Sun and McDonough, 1989), "spider-

diagram" or "spidergram" if referring to a specific pattern (Thompson et al., 1983), and an "extended Coryell - Masuda diagram" (Hofmann et al., 1986). The phrase "incompatible element diagram" is most unambiguous and is utilized throughout this thesis.

Normalizing parameters and the order of elements on an incompatible element diagram are varied. Sun et al. (1979) introduced chondrite normalized incompatible element diagrams for normal and enriched (plume-influenced) MORB. The order of the elements is one of increasing incompatibility from right to left in a partial melt of a four phase lherzolite assemblage (ol - opx - cpx - gt/spinel) so as to produce the smoothest possible pattern. The normalization factors for Rb, K, and P are normalized to primitive terrestrial mantle rather than chondritic abundances, since K and Rb may have been volatile during Earth formation and P may be partly contained in the core. A similar normalization scheme and sequence was adopted by Thompson (1982), however there are minor differences from the Sun et al. normalization, such as slight changes in the order of elements and the normalization factors themselves. Pearce (1983) employs MORB-normalized patterns for studying arc lavas. The ordering of elements on a MORB-normalized plot is based on ionic potential, a measure of mobility in aqueous fluids, and the bulk distribution coefficient in a garnet lherzolite melt, a measure of incompatibility. Mobile elements are plotted on the left-hand side of the diagram, whereas immobile elements are on the right, with the degree of incompatibility increasing towards the center of the diagram.

An awareness of diverse normalization schemes is critical in terms of data comparison. An accurate comparison of results provided by different workers is only possible where the same normalization schemes are employed. In some cases it may

be necessary to renormalize published data so that reliable interpretations result. In this thesis, the normalization scheme of Thompson (1982) is used exclusively. An example of this normalization scheme is shown in Fig. 2.2.

2.3 Radiogenic isotopes

Use of radiogenic isotopes as petrogenetic indicators has become commonplace in igneous petrology. In this thesis, previously published isotopic Sr, Nd, and Hf data provide a starting point for the interpretation of isotopic Pb data. The isotope systematics of Sr, Nd, Hf, and Pb are reviewed in detail by Faure (1986), DePaolo (1988), and Dickin (1995). In the following sections, the pertinent characteristics of these systems are explained, with emphasis on Pb, the principle focus of this thesis.

2.3.1 Sr-Nd

The isotopic pair $^{87}Sr/^{86}Sr$ and $^{143}Nd/^{144}Nd$ are the most commonly used isotope ratios in igneous petrology. As in all radiogenic systems, the variation in observed ratios is assumed to be the result of closed system radioactive decay following magmatic differentiation or metamorphism. Beta decay of ^{87}Rb to ^{87}Sr results in an increase in the $^{87}Sr/^{86}Sr$ ratio. The half-life and decay constant of this process is given in Table 2.1. From this, it is apparent that a rock or mineral with a high Rb/Sr ratio has the potential to produce a high time-integrated $^{87}Sr/^{86}Sr$ ratio. Rb is depleted in most mantle rocks and the lower crust but enriched in the upper crust. Depletion of Rb in the mantle is due to its incompatibility, whereas in the lower crust, Rb is mobilized during granulite facies metamorphism. Therefore, in unaltered samples, we can expect to find relatively low $^{87}Sr/^{86}Sr$ (c. 0.703 - 0.7045) in MORB, oceanic island basalts (OIB), and the lower crust, and relatively high $^{87}Sr/^{86}Sr$ (c. > 0.708) in the upper crust. Complicating factors in

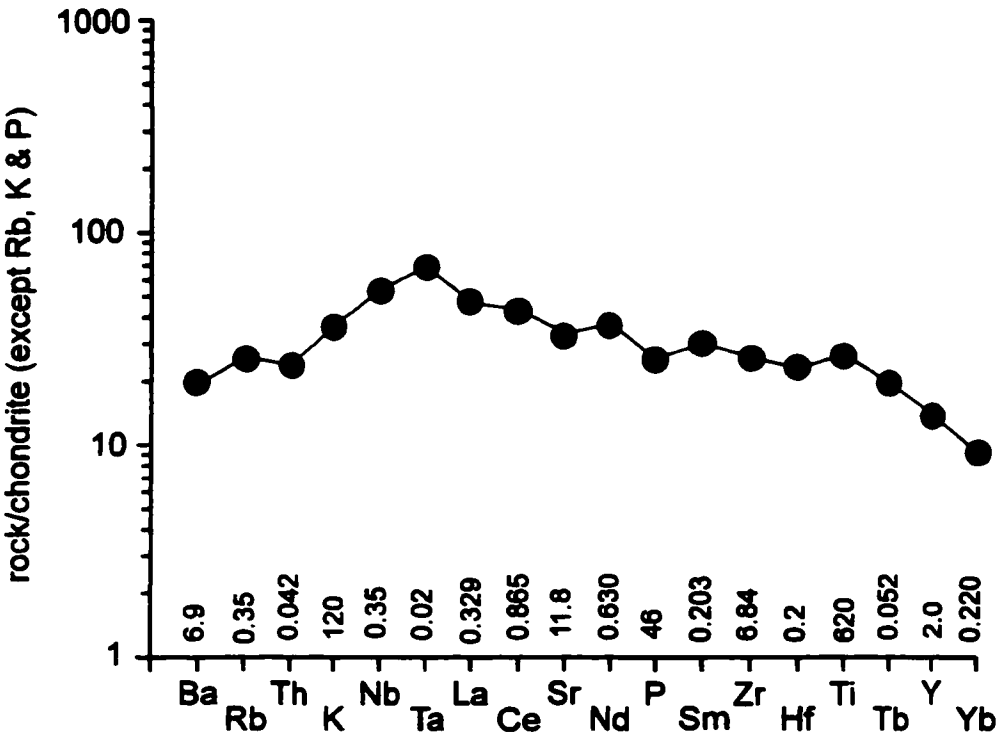

Fig. 2.2 Example of an incompatible element diagram using the International standard BHVO-1. Trace element abundance data from Chen and Frey (1985) and Sun et al. (1979). Normalization factors are shown above each element and are from Thompson et al. (1983).

Table 2.1 Half-lives and decay constants of Sr, Nd, Hf, and Pb isotopes

Isotope	half-life ($t_{½}$), Ga	decay constant	Reference
$^{87}Rb \rightarrow {}^{87}Sr$	48.8	1.42×10^{-11} yr^{-1}	1
$^{147}Sm \rightarrow {}^{143}Nd$	106	6.45×10^{-12} yr^{-1}	2
$^{176}Lu \rightarrow {}^{176}Hf$	35.7	1.94×10^{-11} yr^{-1}	3
$^{238}U \rightarrow {}^{206}Pb$	4.47	1.55×10^{-10} yr^{-1}	4
$^{235}U \rightarrow {}^{207}Pb$	0.704	9.85×10^{-10} yr^{-1}	4
$^{232}Th \rightarrow {}^{208}Pb$	14.01	0.49×10^{-10} yr^{-1}	4

1: Steiger and Jager (1977)
2: Lugmair and Marti (1978)
3: Tatsumoto et al. (1981)
4: Jaffey et al. (1971)

this model are the existence of enriched OIB components with $^{87}Sr/^{86}Sr$ as high as 0.7065 (e.g., Zindler and Hart, 1986), and possible metasomatic enrichment of the MBL of the lithosphere (Nelson, 1992).

Alpha decay of radioactive ^{147}Sm to ^{143}Nd (Table 2.1) is the basis for analysis of the $^{143}Nd/^{144}Nd$ ratio. Both Sm and Nd are rare earth elements and generally have similar geochemical properties, including resistance to change during metamorphism. With increasing degree of differentiation of a magma body, the concentrations of both elements increase, but the Sm/Nd ratio decreases due to the slightly higher compatibility of Sm over Nd. As a result of this fractionation, an evolved crustal rock (e.g. granite) with a low Sm/Nd ratio is expected to have a lower $^{143}Nd/^{144}Nd$ ratio than a mantle-derived rock with higher Sm/Nd. Upper mantle rocks unaffected by metasomatism tend to have $^{143}Nd/^{144}Nd$ ratios > 0.513, whereas this ratio in differentiated crustal rocks usually does not exceed 0.512.

Fig. 2.3 is a schematic drawing showing the coupled Sr-Nd relationships of various crust and mantle reservoirs. As with incompatible element diagrams, caution must be used when comparing published isotopic data from different laboratories, in that there is no unique international standard normalization factor in use. This is particularly true for Nd data. The use of the ε_{Nd} notation is useful in this regard. This notation indicates a relative deviation from a Bulk Earth value (Fig. 2.3). The magnitude of the deviation will be the same regardless of which fractionation scheme is employed, thus data from various sources can quickly be compared with no ambiguities.

2.3.2 Hf

Radioactive ^{176}Lu transforms to ^{176}Hf by beta decay (Table 2.1) and to ^{176}Yb by electron capture. The latter process represents only a small percentage of the

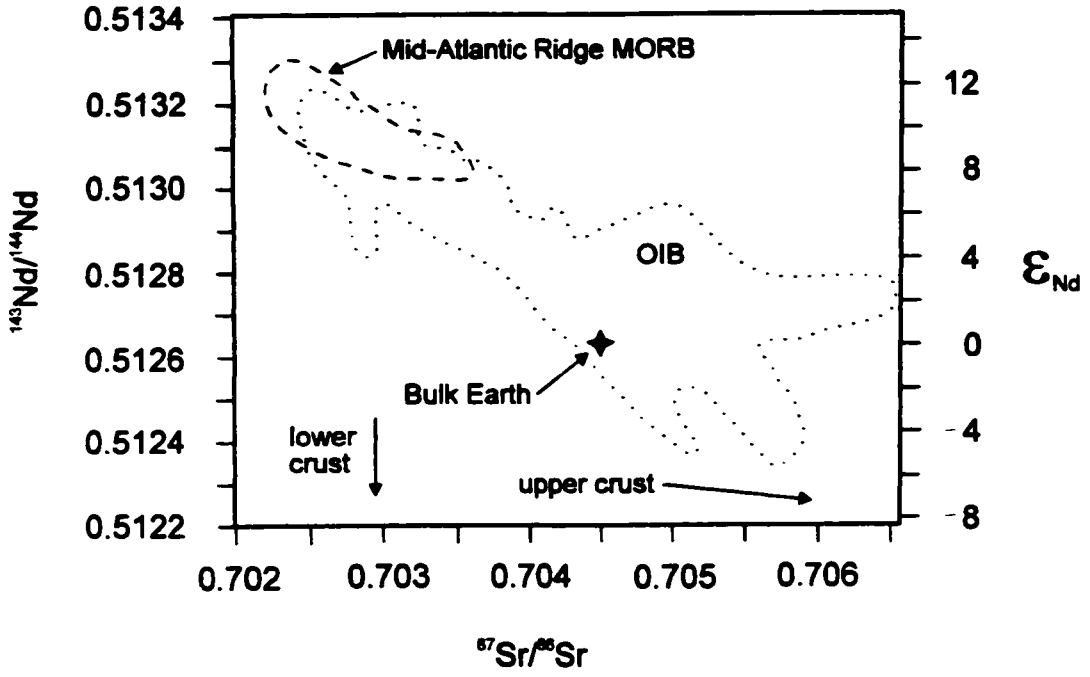

Fig. 2.3 Schematic Sr-Nd isotopic relationships for mantle and crustal compositions. The Bulk Earth value represents the isotopic composition of non-fractionated mantle. The ε_{Nd} parameter is calculated as follows:

$$\varepsilon_{Nd}(t) = \left[\frac{(^{143}Nd/^{144}Nd)_{sample}(t)}{(^{143}Nd/^{144}Nd)_{CHUR}(t)} - 1 \right] \times 10^4$$

where (t) indicates the time at which ε_{Nd} is calculated, and CHUR is the Chondritic Uniform Reservoir, believed to represent the closest compositional estimate to the solar nebula (DePaolo and Wasserburg, 1976).

activity and can be more or less ignored. Hf, like Nd, is somewhat more incompatible than Lu, therefore igneous processes promote higher Lu/Hf ratios in mantle rocks and lower Lu/Hf in differentiated crustal rocks. Because shifts in the $^{176}Hf/^{177}Hf$ ratio due to radioactive decay are small, the ε notation is also useful here. The similarity between the Sm-Nd and Lu-Hf systems produces a positive correlation between their isotopic ratios. Despite their similarities, the Lu-Hf and Sm-Nd systems are different enough geochemically to serve separate purposes. Lu is a heavy rare earth element that is often sequestered in garnet, whereas Hf is readily incorporated into refractory zircon. Nd is more easily mobilized during magmatic processes, as it is contained in a variety of less refractory rock-forming minerals. Therefore, the Sm-Nd system is more useful for considering crustal processes, whereas a more practical use of the Lu-Hf system is determining source mineralogies.

2.3.3 Pb

There are four stable isotopes of Pb: ^{204}Pb, ^{206}Pb, ^{207}Pb, and ^{208}Pb (Faure, 1986; Dickin, 1995). The latter three are the products of complex decay schemes from ^{238}U, ^{235}U, and ^{232}Th (Table 2.1). Table 2.1 lists only the initial and final products of the decay schemes; the intermediate members are inconsequential when the time scale under consideration is in the millions of years. The half-life of ^{235}U is relatively short in comparison to the other parental isotopes of Pb listed in Table 2.1. As a result, nearly all of the primordial ^{235}U has decayed to ^{207}Pb, and the range in measured $^{207}Pb/^{204}Pb$ is accordingly restricted in post-Archean rocks. Isotopic data are usually presented on $^{207}Pb/^{204}Pb$ vs. $^{206}Pb/^{204}Pb$ and $^{208}Pb/^{204}Pb$ vs. $^{206}Pb/^{204}Pb$ diagrams.

U, Th, and Pb are incompatible during magmatic differentiation, although to varying degrees. U and Th are lithophile elements, and tend to concentrate in

accessory silicate minerals. In contrast, Pb has lithophile and chalcophile tendencies, and is distributed in major rock forming silicates and ore deposits. All three elements are susceptible to open system behavior, including low grade metamorphism and surface weathering. This holds especially true for U, which can assume a +6 valencey state by complexing with oxygen to form water-soluble uranyl ions (UO_2^{+2}; Faure, 1986).

Interpretation of radiogenic Pb data requires not only an understanding of the potential changes that can occur during petrogenesis, but also a framework into which the data can be placed relative to terrestrial Pb isotope evolution models. A general evolution model for terrestrial Pb (Holmes, 1946; Houtermans, 1946) was developed to resolve the time at which Pb incorporated into a common Pb mineral (e.g. galena) was isolated from a source undergoing closed system radioactive decay since the formation of the Earth. This process is one of "single-stage" growth, that is, once Pb is incorporated into galena, its isotopic composition does not change, as parental U and Th are excluded from the mineral lattice. A significant drawback to this (Holmes-Houtermans) model is that there is only a small number of galenas that conform to it. In contrast, sulphide ores derived from conformable stratigraphic sequences in island arcs and greenstone belts do tend to follow a single stage closed system growth model (Stanton and Russell, 1959).

The ability of a closed system single stage growth model to produce meaningful ages in conformable deposits was called into question when it was found that the difference between accepted and model ages was small for older deposits, i.e., Archean, but that the difference increased markedly with decreasing accepted age (Oversby, 1974). In order to rectify the discrepancy, open system models were proposed. Initial attempts at open system models were single stage (Oversby, 1974;

Cumming and Richards, 1975), and tended to under-estimate the age of the Earth relative to the age determined from a Pb-Pb meteorite isochron (Patterson, 1956).

Stacey and Kramers (1975) introduced a two stage open system growth model. Although the Stacey-Kramers model provides a reasonable estimate of terrestrial Pb evolution, it is recognized as an approximation. For example, a rigid definition of the start of the second stage (t_1=3.7 Ga) implies that a worldwide differentiation event occurred in the Archean, instantaneously resetting the $^{238}U/^{204}Pb$, or μ, ratio in the mantle. Given the available data which imply variable t_1 values, it is more appropriate to suggest that mantle μ values changed throughout the Archean but have been relatively constant since c. 3.8 Ga.

The "Plumbotectonics" model, developed by Doe and Zartman (1979), is a more complex terrestrial Pb evolution model that emphasizes dynamic interaction, or bi-directional transport between crust and mantle reservoirs. Following continental accretion at 4 Ga, Plumbotectonics requires orogenies at 400 Ma intervals. During an orogeny, U, Th, and Pb are extracted, mixed, and redistributed to the upper crust, lower crust, and upper mantle reservoirs (Fig. 2.4). Evolution of the isotopic composition of the model reservoirs is constrained to accommodate galena ore data, represented by the orogene (Fig. 2.5). Uranium loss resulting from high grade metamorphism produces an unradiogenic Pb isotope signature in the lower crust. In a complimentary fashion, a radiogenic reservoir is established in the upper crust, which becomes enriched in U during orogeny. Within the Plumbotectonics model, the radiogenic growth of Pb within an average upper mantle component has a calculated μ value similar to that for total crust. However, the vast majority of actual oceanic isotopic Pb data is unsupported, i.e., the data plot to the right of the Geochron at higher $^{206}Pb/^{204}Pb$, indicating that the μ value

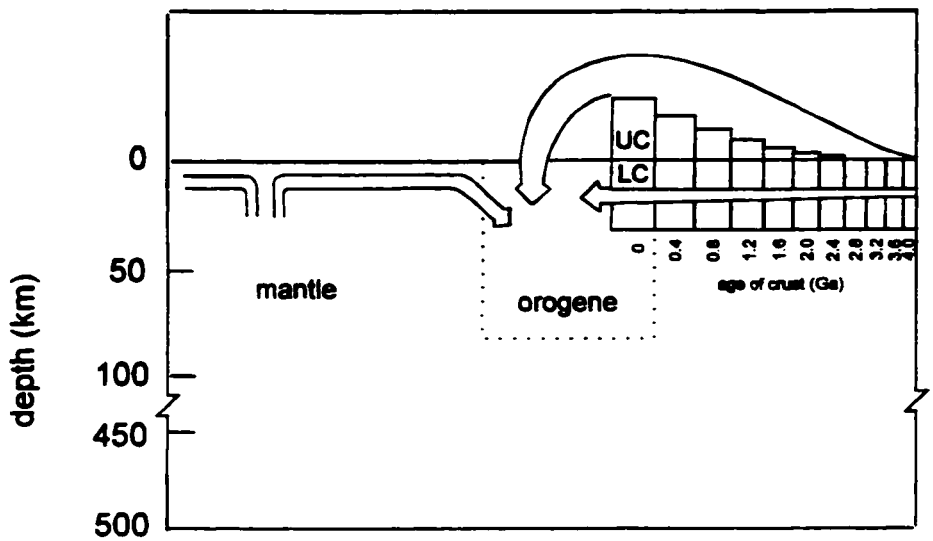

Fig. 2.4 Configuration of the reservoirs in the Plumbotectonics model of Doe and Zartman (1979). UC=upper crust, LC=lower crust.

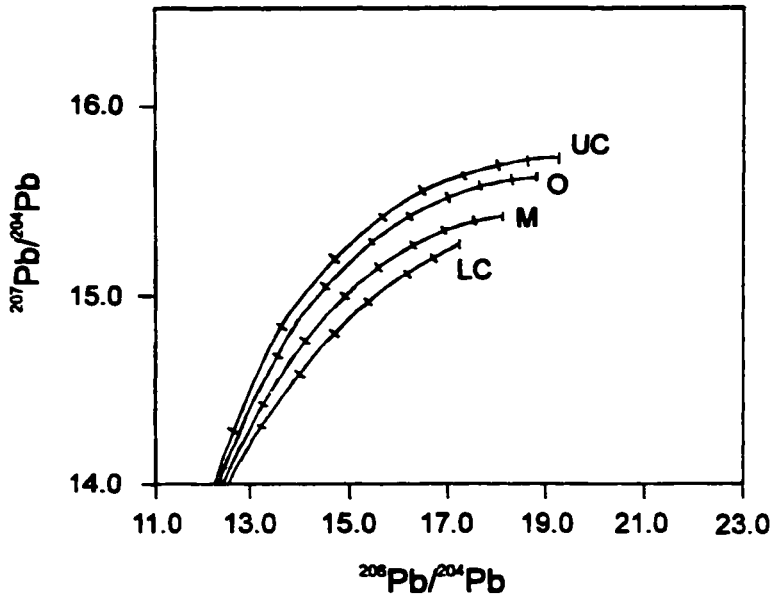

Fig. 2.5 Isotopic evolution of the reservoirs in the Plumbotectonics model of Doe and Zartman (1979). Variations in $^{208}Pb/^{204}Pb$ versus $^{206}Pb/^{204}Pb$ space approximate straight lines. UC=upper crust; O=orogene; M=mantle; LC=lower crust. Tick marks are at 0.4 Ga intervals.

has increased over time. This discrepancy exposes a deficiency of the Plumbotectonics model. Current theory explains the apparent increase in μ with time as resulting from recycling of radiogenic Pb from the continental and oceanic lithosphere (see below). The Plumbotectonics model, however restricts chemical and isotopic transfer between the crust and mantle reservoirs to times of orogeny, and does not take into account the extreme isotopic variations which may develop within the lithospheric realm. Despite these shortcomings, the Plumbotectonics model represents a good approximation to terrestrial Pb evolution.

In this thesis, a large number of samples are considered to be wholly or partially asthenospheric in origin. Yet in the continental realm, isotopic values of asthenosphere-derived magmas may potentially be modified by interaction with subcontinental lithospheric mantle or continental crust. In order to facilitate analysis of Pb data from asthenosphere-derived RGR magmas, it is useful to consider Pb isotopic data from oceanic volcanic rocks, which are devoid of continental contamination.

The asthenosphere is now largely regarded as having one major large-ion-lithophile depleted source and several enriched sources (see Zindler and Hart, 1986, and Dickin, 1995 for review). The depleted component is recognized at mid-ocean ridge segments not influenced by plume activity. Isotopically, mid-ocean ridge basalt (MORB) has high $^{143}Nd/^{144}Nd$, and low $^{87}Sr/^{86}Sr$ and $^{206}Pb/^{204}Pb$ (Fig. 2.6). Recycling of various lithospheric and crustal components has produced three enriched sources in the upper convecting mantle. HIMU, so named for its high μ value, can be created by mixing oceanic lithosphere (± oceanic crust) from which Pb has preferentially been extracted (e.g., Weaver, 1991), back into the upper mantle. As shown in Fig. 2.6, HIMU has low $^{87}Sr/^{86}Sr$, intermediate $^{143}Nd/^{144}Nd$, and high $^{206}Pb/^{204}Pb$. EMI, or "enriched mantle I" is

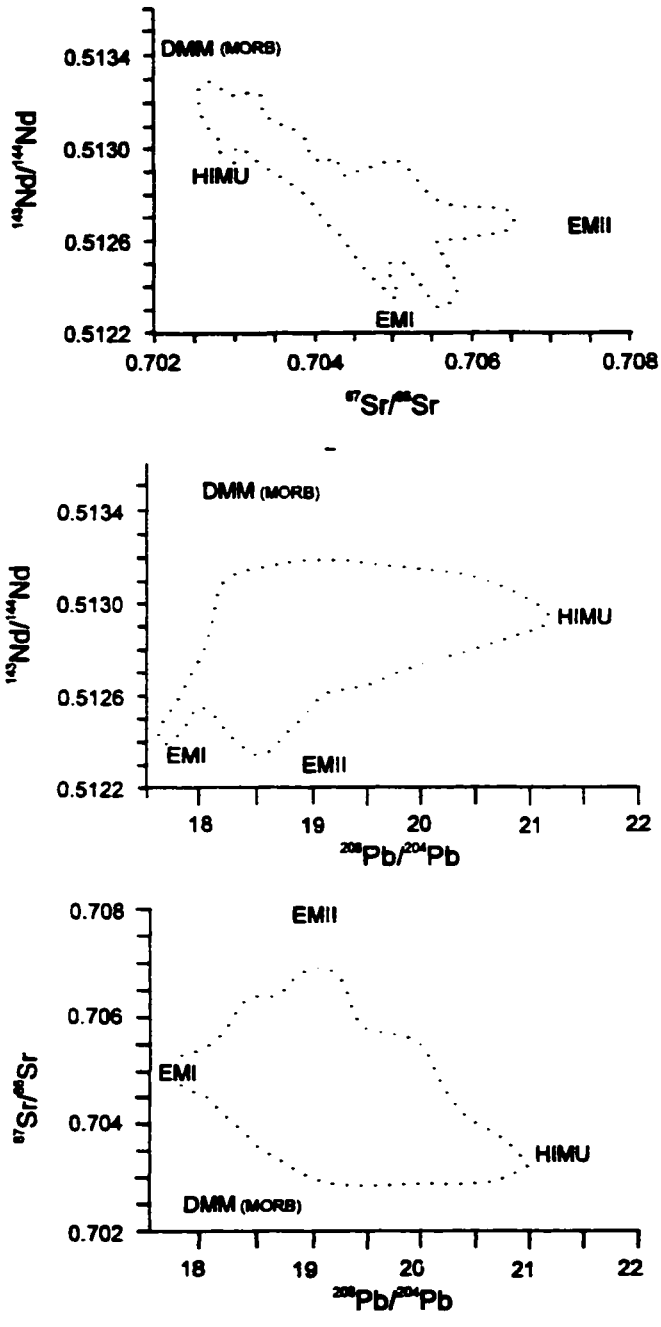

Fig. 2.6 Sr-Nd-Pb variation diagrams showing the relationships between asthenospheric sources discussed in text. DMM=depleted MORB mantle. Dotted line encloses field for OIB. Figures modified from Zindler and Hart (1986).

likely the product of recycling of the subcontinental lithosphere, whereas EMII (enriched mantle II) is ascribed to recycling of continental sediments. The characteristic isotopic signatures of the EM sources include low $^{206}Pb/^{204}Pb$ and $^{143}Nd/^{144}Nd$ in EMI, and elevated $^{87}Sr/^{86}Sr$ with intermediate $^{143}Nd/^{144}Nd$ and $^{206}Pb/^{204}Pb$ in EMII. Mixing between the various sources is usually invoked to explain the radiogenic isotope signatures in groups of oceanic magmas.

Hart (1984) noted the colinearity of a number of Northern Hemisphere MORB and OIB in isotopic Pb-Pb space. Lines drawn through the data originally were partial criteria for evaluating a large scale isotopic anomaly first recognized in the Indian Ocean (Dupre and Allègre, 1983). Current usage of the Northern Hemisphere Reference Line (NHRL) in either $^{206}Pb/^{204}Pb$ vs. $^{207}Pb/^{204}Pb$ or $^{206}Pb/^{204}Pb$ vs. $^{208}Pb/^{204}Pb$ space (Fig. 2.7) permits rapid comparison of large amounts of data. For this reason, the NHRL as well as the Geochron are plotted on Pb-Pb diagrams. It should be noted however that proximity to the NHRL may suggest an asthenospheric origin for a suite of samples, but does not imply a strict relationship to any specific asthenospheric component, as identified above. Any presumed relationship to a specific mantle source must be confirmed using additional isotope data as well as incompatible element data. In this thesis, reference to the asthenosphere as a source will be restricted to the term OIB.

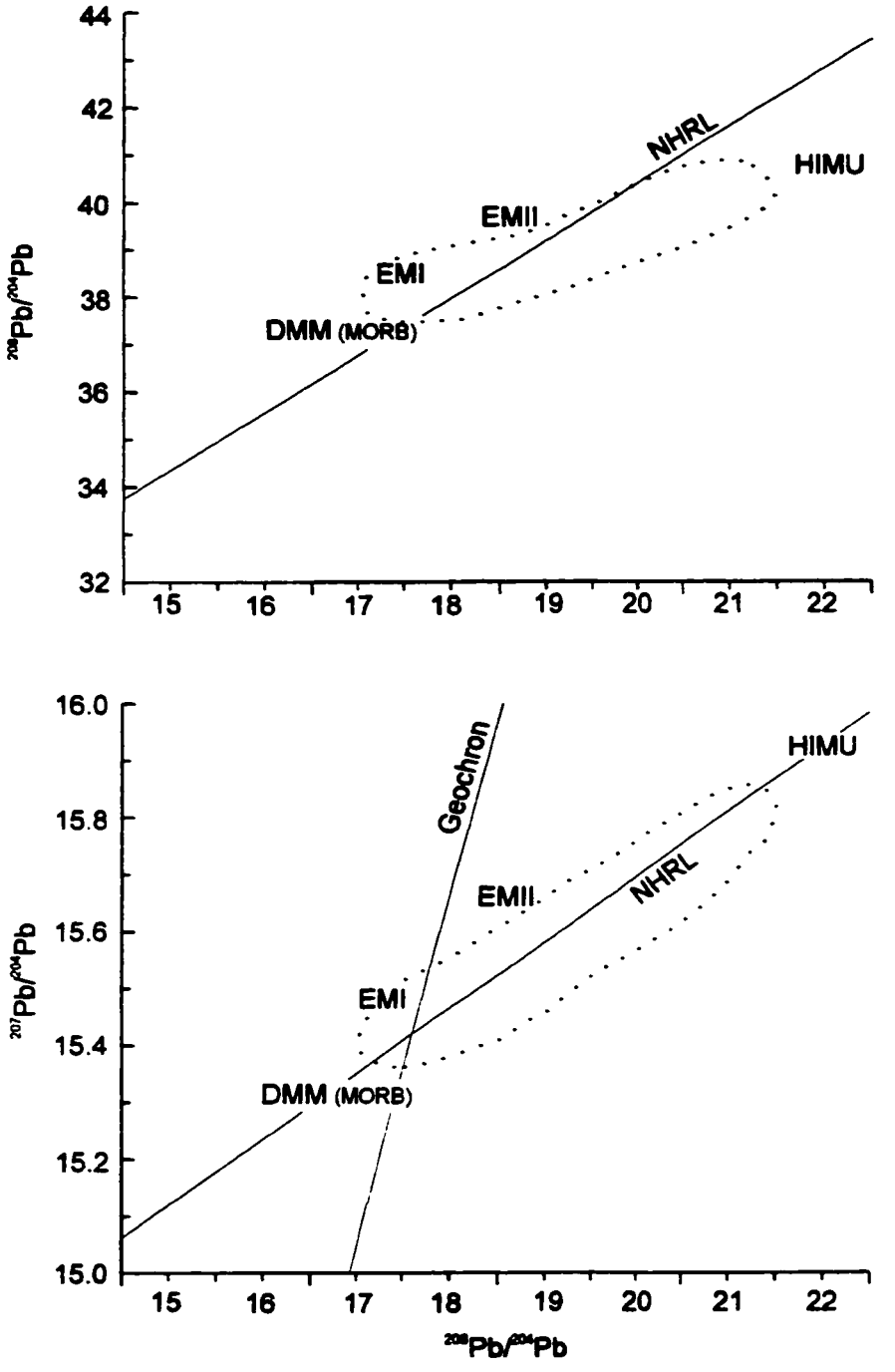

Fig. 2.7 Location of the Northern Hemisphere Reference Line (NHRL) and 4.55 Ga Geochron relative to the oceanic basalt field (dotted line) and asthenospheric sources discussed in the text. Basalt fields from Zindler and Hart (1986), NHRL from Hart (1984).

Chapter 3: Rio Grande Rift-related volcanism in Northwest Colorado: refinement of source characteristics using Pb isotopes

3.1 Abstract

Rio Grande Rift-related basic volcanic rocks in Northwest Colorado exhibit a range of Pb isotope compositions consistent with magma sources both within the asthenosphere and subcontinental lithosphere. Previous work, based on incompatible trace element and Sr-Nd isotope ratios, has categorized the magma sources as three specific groups. Group 1 exhibits characteristics similar to oceanic island basalts (OIB), Group 2 shows strong affinities to the subcontinental lithospheric melts, and Group 3 displays attributes generally associated with subduction-related magmas. On Pb-Pb plots, the majority of data from specific localities tend to cluster in fields that are approximately parallel to the Northern Hemisphere Reference Line (NHRL). On plots of $^{206}Pb/^{204}Pb$ vs. $^{207}Pb/^{204}Pb$, data from seven localities considered here are approximately centered on the Geochron. OIB-like asthenospheric Group 1 magmas from Yampa are relatively enriched, with $^{206}Pb/^{204}Pb$, $^{207}Pb/^{204}Pb$, and $^{208}Pb/^{204}Pb$ ratios as high as 18.31, 15.55, and 37.81, respectively. In contrast, lithospheric mantle-derived Group 2 minettes from the Miocene Elkheads Igneous Province are relatively depleted, with $^{206}Pb/^{204}Pb$, $^{207}Pb/^{204}Pb$, and $^{208}Pb/^{204}Pb$ ratios as low as 17.24, 15.45, 36.63, respectively. Group 3 subduction-related magmas have ratios that are, for the most part intermediate between Groups 1 and 2.

In most cases, the Pb isotope systematics from individual localities support previous interpretations regarding petrogenesis. One notable exception is the Pb

isotopic character of Yarmony basalts, a 'type' locality for Group 3 subduction-related magmas. Elevated $^{206}Pb/^{204}Pb$ and $^{208}Pb/^{204}Pb$ ratios within this sample suite, in addition to radiogenic Sr, strongly suggests that the Pb and Sr isotopic composition was imprinted at crustal levels during the development of the Yarmony magmatic system. As a result, Group 3 is redefined as being most clearly represented by the Miocene Flat Tops magmas. The geochemistry of alkali and tholeiitic basalt samples from the Glenwood Springs area is shown to have OIB characteristics, and to have been strongly affected by crustal input of variable composition. The influence of upper crust is also apparent in the Quaternary suite. Inter-isotope relationships suggest that 23 Ma Walton Peak magmas, previously regarded as mixtures of Groups 2 and 3, may contain a Group 1 component. If so, revision of current models regarding the geochemistry of the available contributing mantle sources during the initial rifting phase in Northwest Colorado is required. Recently published Hf isotope data, together with the Pb data presented here, may reflect a predominant subcontinental lithospheric mantle component in the geochemistry of the early rift-related magmas in the northernmost part of the rift.

3.2 Scope and objectives

Geochemical characteristics of Rio Grande Rift-related basic magmatism in Northwest Colorado (NWCO) have recently been described in a series of papers by Leat, Thompson, Gibson, and co-workers (e.g.. Leat et al., 1988a; Gibson et al., 1991; Thompson et al., 1993). These workers utilized incompatible element variations and Sr-Nd isotopic ratios to designate magma sources and possible contaminants. Crustal assimilation was often recognized, usually as a minor component in the basic magmas, but had little effect on the overall conclusion of primary derivation from mantle sources.

In this chapter, the Pb isotopic compositions of Miocene-Recent basic lavas from NWCO are reported. In general, Pb isotopes support previous conclusions about the geochemical evolution of the various volcanic centers. Certain discrepancies can be explained as the result of interaction with upper crust. As a consequence of one such discrepancy, the type locality of magmas that were largely derived from a compositionally distinct mantle source, is redefined. Revisions to previous interpretations regarding the mantle sources of several volcanic suites are suggested, and an alternative model for the geochemical structure of the mantle beneath NWCO at 20 - 24 Ma is offered. Also, the geochemistry of 8-10 Ma alkalic and tholeiitic lavas from the Glenwood Springs area are analyzed, and are modeled as having geochemical affinities to enriched oceanic island basalt (OIB).

3.3 Geological setting

The Rio Grande Rift (RGR) system is a prominent physiographic feature in the Southwest U.S.A., primarily recognized as a series of en echelon basins that traverse over 1000 km from south-central Colorado, southward into Mexico. During periods of rift-related faulting and sedimentation, the Southern Rocky Mountain region underwent epeirogenic uplift (Eaton, 1986), which may have been in response to regional delamination of the subcontinental lithosphere after 10 Ma (Angevine and Flanagan, 1987; Eaton, 1987). Thus, in the region north of 39° latitude (Fig. 3.1), rift grabens are not well-developed, and the rift system is recognized as a series of faults that continue northward, terminating at the Wyoming border (Tweto, 1979). The development of the rift is thought to be related to a change in the tectonic regime of the west coast of the U.S.A., specifically one of subduction to eventual strike-slip motion (Christiansen & Lipman, 1973; Lipman, 1980). This change in tectonic regime is

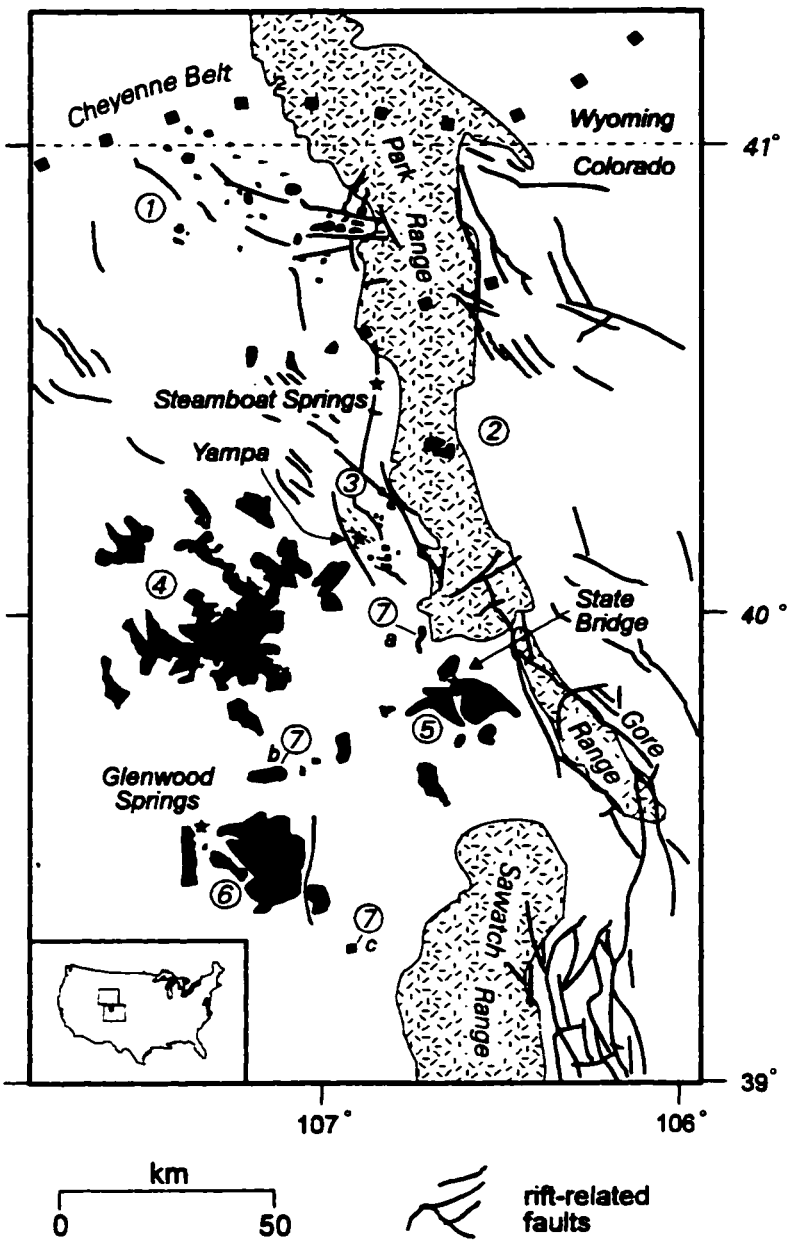

Fig. 3.1 Geologic sketch map of the Northwest Colorado region showing location of volcanic centers discussed in text. Numbered locations are: (1) Elkhead Igneous Province; (2) Walton Peak; (3) Yampa; (4) Flat Tops; (5) Yarmony; (6) Glenwood Springs; (7) Qyaternary sites a) McCoy, b) Willow Peak, c) Triangle Peak. The Cheyenne Belt is a crustal suture separating Archean craton to the north from Proterozoic craton to the south. A small shear zone is also present to the northeast of Steamboat Springs. See text for discussion.

believed to have affected the geochemistry of the subcontinental mantle of the western U.S.A., as reflected in the geochemistry of volcanic products in this region (e.g.. Lipman, 1980). Rifting is considered to be a continuous process over the past 30 Ma. In a simplistic sense, two major phases can be defined, one at c. 30 - 18 Ma and the other at c. 13 Ma - present, each with associated magmatism and a distinct tectonic style (Eaton, 1979; Morgan et al., 1986). A lull in magmatism took place for the most part c. 18 - 13 Ma..

In Colorado, rift-related magmatism north of 39° latitude occurs primarily to the west of the rift system and the Park, Gore, and Sawatch Ranges (Fig. 3.1). This implies that deep fractures with orientations different from the rift system controlled the distribution of the volcanic centers (Tweto, 1979). The Park Range consists mainly of Proterozoic metavolcanic and metasedimentary crystalline rocks intruded by batholiths approximately 1700 Ma and 1430 Ma (Snyder and Hedge, 1978; Hedge et al., 1986). To the north, a major shear zone, the Cheyenne Belt, separates the Archean terrane of the Wyoming Province from the Proterozoic terrane to the south (Karlstrom and Houston, 1984). In the original model proposed by Hills and Houston (1979), the Cheyenne Belt formed as a result of collision of island arcs with the Wyoming craton, culminating around 1700 Ma. It was estimated that approximately one half of the Proterozoic terranes south of the Cheyenne Belt are felsic, and that they formed above a south dipping subduction zone. The hypothesis regarding the orientation of the subduction zone is supported by more recent geophysical data. Gravity and seismic profiles constructed by Johnson et al., (1984) confirm that the suture zone does dip to the south, and that a change in crustal thickness occurs across the zone. This has important implications for the geochemical signatures of magmas produced in this area,

i.e., any magma erupted in the region suspected to overlie the Cheyenne suture may be influenced by Archean as well as Proterozoic components. In terms of crustal thickness, geophysical data suggest a southward thickening, from c. 40 km in the Archean craton to c. 50 km in the Proterozoic (Prodehl and Pakiser, 1980; Johnson et al., 1984). Snyder and Hedge (1978) also note the existence of a much smaller but pervasive shear zone northeast of Steamboat Springs (Fig. 3.1).

3.3.1 Magma groups

Volcanic fields included in the scope of this chapter are denoted in Fig. 3.1. With the exception of lavas from the Glenwood Springs area, the petrology, major and trace element, and Sr & Nd isotope geochemistry of these fields have been explored in detail (Leat et al., 1988a&b,1989, 1990, 1991; Gibson, 1991;Thompson et al., 1989, 1993) and will be briefly reviewed in section 3.4.2.4. One significant conclusion of the initial study by Leat et al. (1988a) was that the geochemical variation in the NWCO basic lavas could be explained by variable degrees of interaction of three mantle sources, or Groups, with minor degrees of crustal contamination. Each Group has a definable set of elemental and isotopic characteristics that cannot be produced via mixing, fractional crystallization, or crustal contamination of any other Group.

3.3.1.1 Group 1

The Group 1 source was originally defined as an OIB-like, and believed to reside within the asthenosphere. This may have attained its geochemical characteristics through interaction with the Yellowstone plume (Leat et al. 1991). Smith and Braile (1994) cite the linear age progression of silicic volcanic centers spanning 16 Ma along the Yellowstone-Snake River Plain as straightforward evidence of plume-plate interaction, although Geist and Richards (1993) suggested a somewhat earlier age of

17.2 Ma, marking the beginning of the eruption of the Columbia River Basalt. More recently, Camp (1995) has documented the propagation of the plume within the Columbia River basalt region using a model for plume behavior beneath continental lithosphere of variable thickness that was proposed by Thompson and Gibson (1991). This implies that, in the NWCO lavas, a Group 1 source influenced by the Yellowstone plume would not have been available until the second phase of rifting and magmatism, c. 13 Ma - present. The 'type' locality for the Group 1 source is the Yampa Volcanic Field (Fig. 3.1), dated at 5.8 Ma (Thompson et al., 1993) . Incompatible element data (Fig. 3.2) as well as Sr and Nd isotopic variations (Fig. 3.3) are consistent with derivation of Group 1 melts from a Hawaii-like OIB source similar in composition to that which produced basanites at Loihi seamount, but which has also experienced minor and variable degrees of mixing with lithospheric mafic magma compositions as well as crustal contamination (Leat et al., 1988a, 1991). In order to define the composition of this end-member with the effects of lithospheric interaction removed, the Group 1 magma type is represented by Hawaiian OIB in Fig. 3.3 and subsequent isotope diagrams.

3.3.1.2 Group 2

Readily fusible, volatile- and K-rich mafic melts from the mechanical boundary layer of the subcontinental lithosphere, with time-integrated LREE enrichment relative to bulk Earth, are representative of the Group 2 source in NWCO and are manifest in the minette component of the Elkhead Mountains Igneous Province (Fig. 3.1). Incompatible element variations, in particular low La/Nb and Nb/Zr ratios, suggest a link to subduction (Leat et al., 1988). The Sr and Nd isotopic character of this component (Fig. 3.3) is similar to that found in mafic magmas from Wyoming-Montana

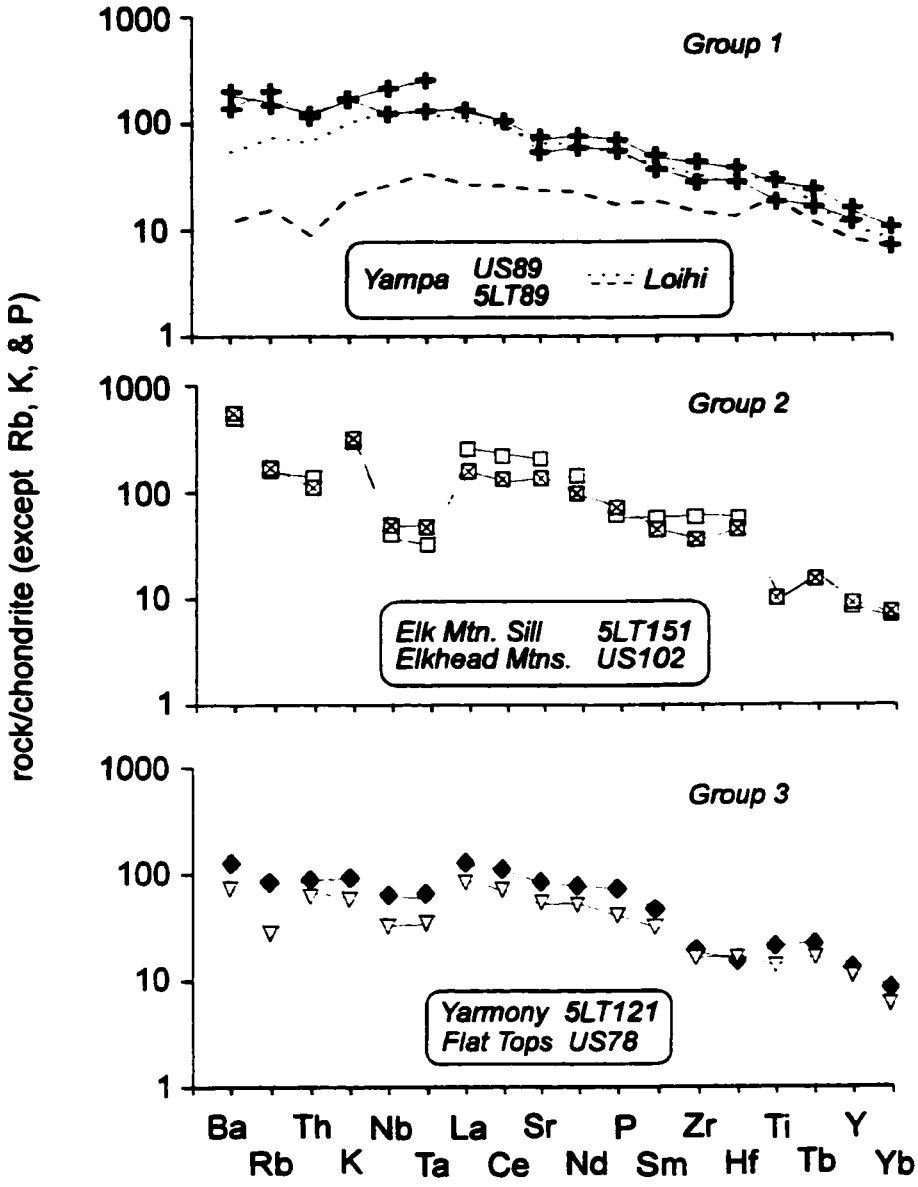

Fig. 3.2 Representative chondrite normalized incompatible element diagrams for magma source groups discussed in text. Loihi patterns depict Group 1 compositions unaffected by continental lithosphere or crust: tholeiite (29-10), dashed pattern, basanite (15-4), dotted pattern; data are from Frey and Clague (1983). Normalizing parameters from Thompson et al. (1984).

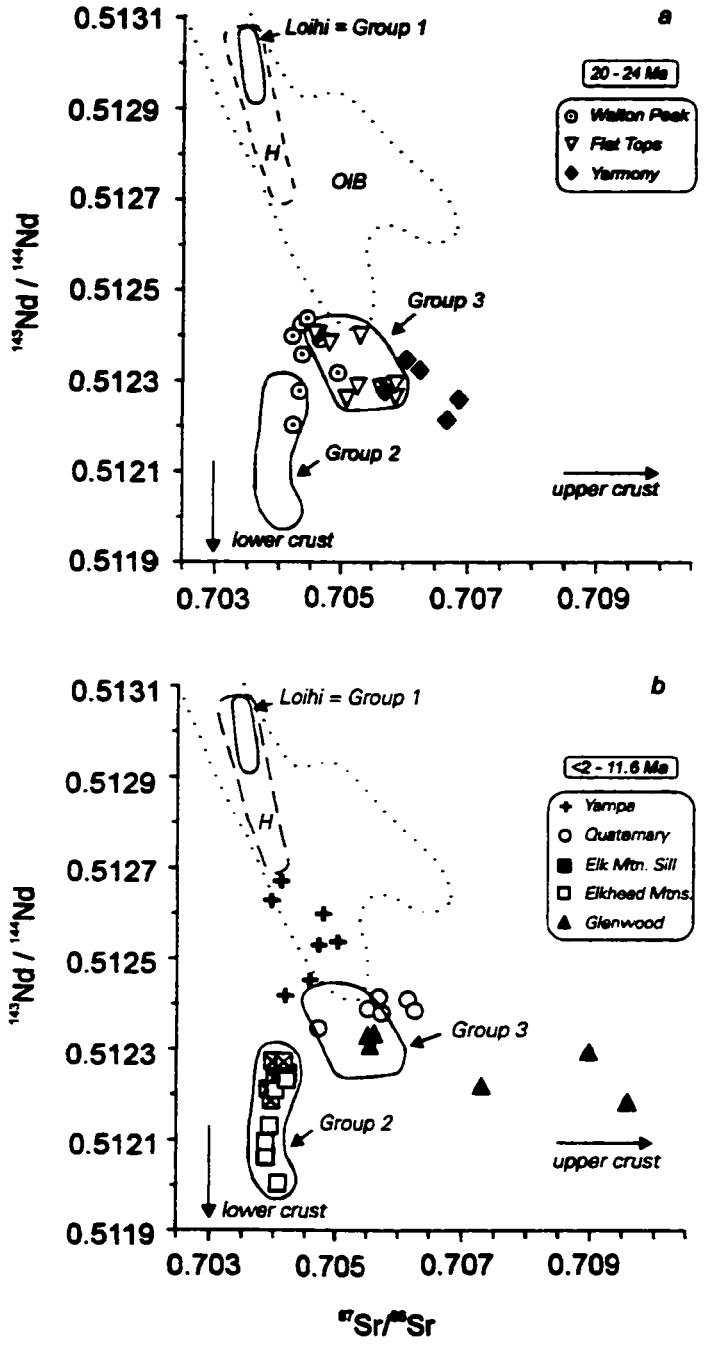

Fig. 3.3 Sr-Nd isotopic variations in NWCO volcanics; (a) early rift, (b) later rift. OIB field shown for reference. Mantle source Groups discussed in text are highlighted. NWCO data are from Gibson et al. (1991; 1992; 1993), Leat et al. (1988a,b; 1989; 1990; 1991), Thompson et al. (1989; 1993), and this study. Loihi data are from Staudigel et al. (1984), additional Hawaii data (H) from Stille et al (1983).

potassic province (Vollmer et al., 1984; Fraser et al., 1985; Dudás et al., 1987; Meen and Eggler, 1987). It is probable that the subduction event associated with the accretion of Proterozoic island arcs to the southward dipping Archean craton of Wyoming 1.5 - 1.8 Ga (Karlstrom and Houston, 1984) influenced the geochemistry of the lithosphere of NWCO. In particular, migration of very small volume partial melts from the asthenosphere into the overlying lithosphere may have produced regions containing volatile-rich, compositionally diverse, ultrapotassic veins (McKenzie, 1989). Such volatile-charged regions would melt readily upon decompression or if heated from below by upwelling of comparatively larger volume partial melts from the asthenosphere (e.g. Thompson et al., 1989). More recent subduction events in Mesozoic or Cenozoic times may also have contributed to the metasomatism of the lithosphere. If this were the case, it is expected that analyzed $^{143}Nd/^{144}Nd$ ratios would be more radiogenic relative to their Proterozoic analogues.

3.3.1.3 Group 3: definition and reappraisal

The Group 3 source is more enigmatic. Trace element variations within this group are similar to subduction-related magmas erupted on continental margins, exhibiting Nb-Ta depletion and LREE enrichments (Fig. 3.2); however, the distinctive enrichments in Ba and Th are lacking (Pearce, 1983; Thompson et al., 1984). Low abundances of highly incompatible elements in Group 3 are thought to be the result of a previous episode of melt extraction, prior to the generation of melts that contribute to the NWCO lavas. Alternatively, Duncker et al. (1991) suggest dehydration of the mantle induced by CO_2 migration may be responsible for the depletion of alkali elements in the geochemically similar lavas from the Cerros del Rio field in North-Central New Mexico. Isotopically, Group 3 magmas are similar to subduction-related magmas from the

Andes, South America and low $^{143}Nd/^{144}Nd$ OIB (Fig. 3.3).

Leat et al. (1988a; 1990) chose the volcanic field developed around State Bridge (Fig. 3.1) and on Yarmony Mountain as the 'type' locality for this Group. The initial interpretation by Leat et al. (1988a,1990) held that the Group 3 source mantle occupied the convecting asthenosphere as well as the thermal boundary layer of the lithosphere until the latter stages of rifting, by which time it had been confined to the thermal boundary layer. Newly acquired Pb isotope data presented here, in conjunction with previously published Sr-Nd data, may necessitate revision of this model. Inter-isotope relationships, in addition to trace element variations, argue for a potential role for a Group 1 component in samples from Walton Peak (Fig. 3.1), a volcanic field that developed concurrently with Yarmony during the early stage of rifting (section 3.4.1.1). The availability of an asthenospheric OIB-like source during the early rifting phase in NWCO requires the Group 3 source to be restricted to the lithosphere by that time. Gibson et al. (1992) have shown that OIB-like magmas were erupted at least locally within the axis of the RGR proper throughout its development. Thus, the proposed change to the chemical geometry of the mantle beneath NWCO would serve to establish a harmonized picture of the mantle structure beneath the entire rift region.

Pb isotope data from Yarmony, discussed below, are similar to ratios obtained from local Proterozoic crust. This observation, taken together with elevated $^{87}Sr/^{86}Sr$ ratios (Fig. 3.3) seems to suggest that Pb and Sr isotopic values were imprinted at crustal levels as the Yarmony magmatic system evolved, and are therefore not representative of a Group 3 *mantle* source. As such, the composition of the Group 3 source is redefined as being best represented by the 21-23 Ma lavas from the Flat Tops Volcanic Field (Gibson et al., 1991), which are similar in terms of incompatible trace

elements, have similar $^{143}Nd/^{144}Nd$ values, and less radiogenic Sr and Pb ratios to the Yarmony suite.

3.4 NWCO volcanic fields

In order to place the Pb isotope data from NWCO in a functional context, it is necessary to briefly review published geochemical and age data on each of the relevant volcanic fields.

3.4.1 Early rift magmatism: 20 - 24 Ma

Towards the end of the first period of extension of the RGR (c. 30-18 Ma), magmatism in NWCO produced volcanic successions at Walton Peak, Flat Tops, and in the State Bridge area. The Walton Peak volcanic field developed on the Proterozoic Park Range horst , whereas Flat Tops and the lavas near State Bridge formed to the southwest and south, respectively (Fig. 3.1). In the TAS classification scheme (Le Maitre, 1989), the early rift lavas include basalt, potassic trachybasalt, basaltic andesite, shoshonite, and trachydacite.

3.4.1.1 Walton Peak

Thompson et al. (1993) discuss the petrogenesis of lavas erupted at Walton Peak, c.22.8 ± 0.3 Ma. In particular, a composite flow of trachydacite containing pillow-like basic masses was examined. The pillow-like basic components of this flow consist of high-Nb and low-Nb varieties, which cannot be related by models that appeal to variable degrees of partial melting of a lithospheric mantle source. Based on incompatible element variations, the primary source of lavas at Walton Peak was determined most likely to be Group 3 subduction- processed asthenosphere. Processes of fractional crystallization and crustal assimilation affecting Group 3 low-Nb basic magma produced the trachydacite component, whereas contamination by up to 15

% lamproitic melt, a Group 2 source, produced the high-Nb basic pillow component. As noted above, variations in radiogenic isotopes at Walton Peak favor interaction between Group 1 and Group 2 sources (Fig. 3.3). This possibility will be explored below (section 3.5.3).

3.4.1.2 Yarmony

The succession near State Bridge reaches a maximum thickness at Yarmony Mountain; hereafter this locality will be referred to as Yarmony. Lavas at Yarmony, dated at 21.5 ± 1.0 to 24.0 ± 1.0 Ma (York et al., 1971), are the oldest Cenozoic volcanic rocks west of the Park Range. Leat et al. (1990) discuss the geochemistry of this volcanic center. The majority of lavas at Yarmony exhibit characteristics of the Group 3 source. Elemental and isotopic evidence require input of a Group 2 component in at least one of the lavas, though petrographic evidence for mixing was not found. The $^{87}Sr/^{86}Sr$ ratios of the Yarmony lavas are the highest found within this age group (Fig. 3.3). Although Leat et al. (1990) argued against crustal contamination as a means of producing elevated $^{87}Sr/^{86}Sr$ within the lava flow succession, combined Sr and Pb isotope data discussed below imply that crustal contamination affected the entire magmatic system prior to and immediately before the eruption of individual lava flows.

3.4.1.3 Flat Tops

The Flat Tops Volcanic Field consists of two successions of lava flows, each of which erupted during discrete time intervals. Gibson et al. (1991) discuss the petrology and geochemistry of the older series, dated at 20.6 ± 0.8 to 23 ± 1.0 Ma (Larson et al., 1975). Although no obvious petrographic evidence of mixing was encountered, a minimum of five geochemical cycles can be recognized in the lava pile,

and are attributed to replenishment fractional crystallization processes. Variations in incompatible elements reflect a predominant Group 3 component in the lavas. Combined elemental and Sr-Nd isotopic data (Fig. 3.3) suggest that minor upper crustal contamination occurred during the lifetime of the magmatic system, and that several of the lava flows contain a Group 2 component.

3.4.1.4 Does a mixing relationship exist among the early-rift lavas?

Isotopic variations among the early rift lavas (Fig. 3.3a) may be indicative of a possible relationship via mixing of melts derived from different mantle sources. In Fig. 3.4, incompatible element patterns for the least evolved samples from Flat Tops, Yarmony, and Walton Peak are compared. All three patterns are similar, with Flat Tops exhibiting the most enrichment, Walton Peak less enriched, and Yarmony at an intermediate position. Simple mixing of 30 % of the Flat Tops and 70% of the Walton Peak samples shown results in a pattern closely resembling that of the Yarmony basalt. Isotopically, simple mixing would not appear to work, as the Yarmony suite is more radiogenic in terms of Sr (and Pb; see below) than either Flat Tops or Walton Peak. However, it will be demonstrated that the Sr and Pb isotopic signature of the Yarmony suite was likely imprinted at crustal levels, during the establishment and evolution of the magmatic system. As the trace element patterns shown in Fig. 3.4 do not differ markedly, as would be expected if bulk rock contamination occurred, a contamination process involving a partial melt of country rock, possibly by AFC, is favored. Therefore, a scenario in which mixing between the Flat Tops and Walton Peak sources followed by crustal contamination, can readily explain the trace element and isotopic signature of the Yarmony suite.

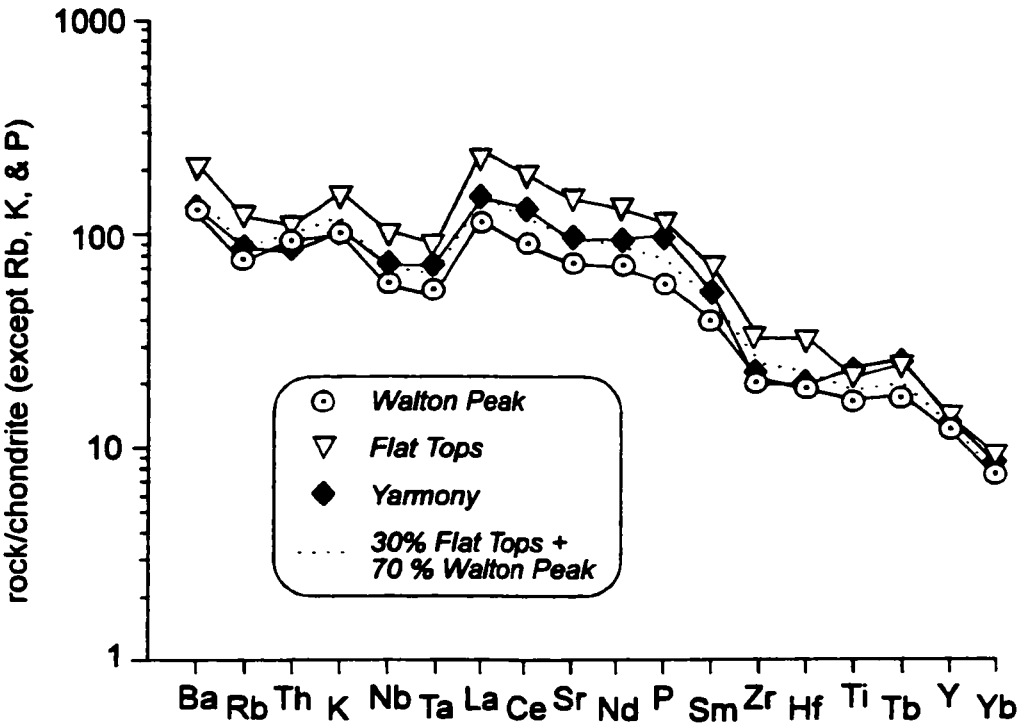

Fig. 3.4 Chondrite normalized incompatible element mixing diagram showing hypothetical mixing of least evolved compositions from Flat Tops (5LT356; Gibson et al., 1991) and Walton Peak (5LT162; Thompson et al., 1993) to produce the least evolved Yarmony sample (5LT119; Leat et al., 1990). Normalizing parameters from Thompson et al. (1984).

3.4.2 Later rift magmatism: < 2 - 11.6 Ma

Volcanic centers that developed in the second phase of rifting occur exclusively to the west of the Proterozoic uplifts shown in Fig. 3.1. The Elkhead Igneous Province is the northernmost locality under consideration here. Further south, basic magmatism occurred near Yampa, Glenwood Springs, and at scattered localities in between. Using the TAS classification scheme (Le Maitre 1989), lavas erupted at the remaining localities include basanite, basalt, potassic trachybasalt, hawaiite, shoshonite, trachydacite, and rhyolite. In addition, minettes are found within the Elkheads Igneous Province.

3.4.2.1 Yampa

The Yampa Volcanic Field consists of scattered outcrops of dikes, volcanic necks, and lavas, dated at 5.8 Ma (Thompson et al., 1993). As noted earlier, Yampa was defined as the 'type' locality for the Group 1 source; however, data from Hawaii are used here to represent Group 1 so that the effects of lithospheric contamination are removed. Results of combined elemental and Sr-Nd isotopic modeling indicate that mixing partial melts of local lithospheric mantle, in this instance the potassic Group 2 source, with OIB-like melts derived from asthenosphere advected within the Yellowstone plume, can produce the observed variations within the Yampa data set (Leat et al., 1991). Although strongly potassic rock types have not been found as dikes or sills at the present exposure level, some of the mafic volcanic fragments within Yampa diatreme-fill breccia contain phlogopite phenocrysts (R.N.Thompson, pers. comm.). This data supports the involvement of the Group 2 source in the petrogenesis of magmas at this locality. Up to 20% upper crustal contamination may also have affected some samples, producing slightly elevated $^{87}Sr/^{86}Sr$ ratios (Leat et al., 1991; Fig. 3.3).

3.4.2.2 Quaternary

From c. 2 Ma - 4 ka, volcanism in NWCO occurred at scattered localities, including Willow Peak, Triangle Peak, and McCoy (Fig. 3.1), producing mainly lava flows. Data from these areas are discussed collectively under the title 'Quaternary'. Based on incompatible element relationships, Leat et al. (1989) concluded that mixing between Groups 1, 2, and 3, together with minor amounts of crustal contamination, could account for geochemical variations in the Quaternary suite. Sr and Nd isotopic data are somewhat equivocal. $^{143}Nd/^{144}Nd$ ratios within the suite are nearly constant, which contrasts with a very large range in $^{87}Sr/^{86}Sr$ (Fig. 3.3), and there is no clear relationship to any source, save Group 3.

3.4.2.3 Elkhead Mtns & Elk Mountain Sill

Although the Elkhead Mountains Igneous Province contains a range of mafic compositions, including potassic alkali basalts to trachydacites, minettes are of primary interest here. The minettes are the clearest representatives of the Group 2 source in NWCO. Leat et al. (1988b) studied a particular locality within the province, the Elk Mountain sill, whereas Thompson et al. (1989) addressed the nature of the minettes within the province as a whole. The Elk Mountain Sill was emplaced between 7.6 - 11.1 Ma (Luedke and Smith 1978), and consists of a trachydacite host with two generations of mafic inclusions. Leat et al. (1988b) found elemental and isotopic similarities among all components of the sill, and concluded that they were related by fractional crystallization of subcontinental lithospheric mantle-derived minette. This relationship is quite similar to that developed in the composite flow at Walton Peak (section 3.1.1). Sr and Nd isotopic ratios from the Elk Mountain Sill indicate that contamination by granulite-facies crust had occurred, resulting in an overall decrease in $^{87}Sr/^{86}Sr$ and

$^{143}Nd/^{144}Nd$ with fractionation. Thompson et al. (1989), in their review of the minette geochemistry of the Province, suggested that contamination of asthenosphere-derived basalts by variable amounts of ultrapotassic melts from the lithospheric mantle could also be responsible for the resulting minette compositions. These Group 2 magmas have Sr, Nd (Fig. 3.3), and Pb isotopes that are the least radiogenic in all of the NWCO basic volcanics (Leat et al., 1988b; Thompson et al 1989).

3.4.2.4 Glenwood

Lava flows in the immediate vicinity of Glenwood Springs area (hereafter Glenwood) have been dated at 7.9 ± 0.4 - 11.1 ± 1.0 Ma (Larson et al., 1975). Because lavas were erupted periodically throughout regional uplift and river downcutting, it is possible that certain sections may exhibit an inverted age stratigraphy. For example, the most complete stratigraphic section reported on here is represented by 11 Ma samples (US73, 5LT5) which lie c. 250 m above those 8 Ma in age (5LT1 - dated, 5LT3 - inferred). 5LT7 and 9 were collected from an outlier south of Glenwood Springs and are 10 Ma. Because of the limited number of samples and the range in ages within the group, discussion of geochemical patterns from Glenwood Springs will be restricted to general observations.

Petrographic characteristics of the Glenwood lavas are varied. Olivine is ubiquitous, and the only phenocryst phase present in 5LT7 and 9. Phenocrysts of plagioclase are present in 5LT 1, whereas in US73, plagioclase, clinopyroxene and magnetite join the assemblage. Samples 5LT3 and 5LT5 contain olivine and plagioclase phenocrysts, and xenocrystic quartz with clinopyroxene reaction jackets. In addition, 5LT3 contains mafic-ultramafic microxenoliths. The presence of quartz in basic lavas in the Southern Rocky Mountain Region is not uncommon (Larsen et al., 1938;

Doe et al., 1969; Stormer, 1972; Lipman and Mehnert, 1975; Duncker et al., 1991; Leat et al., 1991; Thompson et al., 1993). Nicholls et al. (1971) have demonstrated that, for basaltic magmas, thermodynamic data permit the equilibration of quartz at temperatures of c. 1100° and pressures between 25 and 27 kbar. This implies that quartz xenocrysts may actually represent a refractory remnant of high pressure crystallization. However, the resultant lavas typically have low $^{87}Sr/^{86}Sr$, and this is not the case at Glenwood (Table 3.1, Fig. 3.3).

Major and trace element data from samples from Glenwood along, with one Sr and Nd isotope pair, were reported by Leat et al. (1988a) and Gibson et al. (1992), but have not been discussed in great detail. An abbreviated version of these data is given in Table 3.1. Geochemically, the samples from Glenwood display a range of compositions. Using the TAS nomenclature (Le Maitre, 1989), the suite includes basaltic andesite, potassic trachybasalt, and shoshonite. In terms of silica saturation, the least evolved compositions are weakly *ne*-normative (5LT5, US73) and *hy*-normative (5LT3), whereas samples displaying elemental and isotopic evidence for crustal contamination (Table 3.1) are weakly *ol*-normative (5LT1, 5LT7, 5LT9). Corrections for quartz xenocryst content would have the effect of displacing 5LT3 and 5 to more undersaturated compositions.

Chondrite normalized incompatible element patterns for the Glenwood samples are plotted in Fig. 3.5. Although the patterns closely resemble one another, the 10 Ma olivine tholeiite lavas (5LT7 and 9) are less enriched than the remaining group. Within the suite as a whole, LILE/La are generally > 1, and negative anomalies are developed at Th, Nb-Ta, Sr, Zr, and Ti. For samples 5LT 7 and 9 the Nb-Ta troughs tend to be deeper than in the remaining samples, and Rb/Ba > 1.

Table 3.1. Selected geochemical data for Glenwood Springs samples[a]

Sample #	5LT1	5LT3	5LT5	5LT7	5LT9	US73
Age (Ma)[b]	8	8	11	10	10	11
Major element oxides (wt. %)						
SiO_2	52.45	52.05	50.60	52.92	52.31	49.00
MgO	6.40	6.62	7.11	7.82	8.14	8.16
Na_2O	3.07	3.17	3.45	2.95	2.84	3.17
K_2O	1.77	2.93	2.70	1.30	1.44	2.15
Normative constituents[c]						
ne	—	—	0.81	—	—	1.28
di	10.58	14.08	12.32	9.15	8.96	14.12
hy	21.58	4.92	—	27.35	24.93	—
ol	0.29	10.92	16.20	0.23	2.87	18.46
Trace elements (ppm)						
Cr	148	174	125	224	232	220
Ni	83	101	87	149	175	147
Ba	1026	1846	1947	491	515	1094
Sr	703	767	846	389	437	930
Rb	33	75	47	37	40	45
Th	3.4	5.7	4.6	2.9	3.6	3.0
Nb	21.5	24.7	29.7	8.9	11.8	22.0
Ta	0.7	1.5	1.6	0.5	0.6	1.36
Zr	211	177	193	145	139	156
Hf	4.3	5.1	5.6	3.6	4.7	4.7
Y	33	27	30	27	27	28
La	30	43	43.5	24	22	37
Ce	69	100	90	54	56	88
Nd	34	46	52	24	27	48
Sm	6.9	8.6	9.4	4.8	5.3	8.9
Tb	1.08	1.24	1.06	0.62	—	1.27
Yb	2.55	2.18	2.19	2.45	2.28	2.0
Isotopes[d]						
$^{87}Sr/^{86}Sr$	0.707324	0.705532	0.705624	0.709563	0.708951	0.705529
$^{143}Nd/^{144}Nd$	0.512220	0.512313	0.512333	0.512184	0.512293	0.512329

[a]data sources are Leat et al. (1988a) and Gibson et al. (1992)
[b]K/Ar dates from Larsen et al. (1975); age for 5LT3 is inferred based on field relationships
[c]norms calculated using Fe_2O_3/total iron = 0.15
[d]this study; except US73 from Leat et al. (1988a)

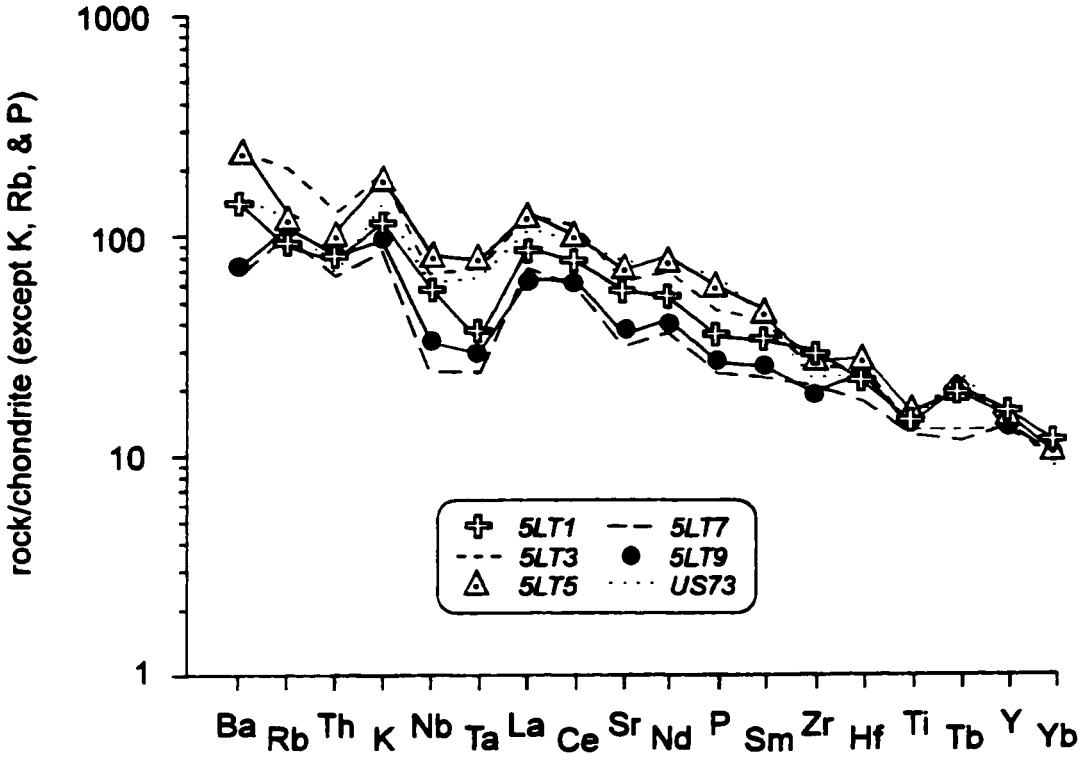

Fig. 3.5 Chondrite normalized incompatible element diagram for samples from Glenwood. Normalizing parameters from Thompson et al. (1984).

Sr and Nd isotopic variations within the Glenwood suite (Fig. 3.3) are similar to the older Flat Tops and Yarmony suites, and the younger Quaternary lavas, but have more extreme $^{87}Sr/^{86}Sr$ values. Sr contamination during alteration is ruled out by identical isotope ratios in leached and unleached duplicates. The incompatible element variations in the lavas, taken together with their Sr and Nd isotopes, implies a relationship involving crustal contamination of the OIB-like Group 1 lavas erupted at Yampa (Figs. 3.2, 3.3). Mixing models were constructed to explore this possibility. Following the premise that during this time the asthenosphere was modified via interaction with a plume component (Yellowstone) resembling compositions analyzed from Loihi, a tholeiite and a basanite from Loihi were chosen for modeling purposes. Fig. 3.6 documents the incompatible element relationships obtained by mixing 15 % minette (Group 2) with 85% Loihi tholeiite (Fig. 3.6a), and 40% minette with 60% Loihi basanite (Fig. 3.6b), and subsequently contaminating each mixture with 20 and 25 % crust, respectively. These mixing proportions are confirmed for the undersaturated lavas in terms of Sr and Nd isotopes in Fig. 3.7, however, the mixing trend for the tholeiites requires at least 30% crust. The discrepancy in the proportion of crustal component added to the Glenwood tholeiites may be the result of the incorrect estimation of the Sr content of the crustal component. If the bulk rock assimilant used in the above calculations was substituted by a partial melt which contained substantially more Sr, the amount of crust required to reproduce the isotope ratios would easily decrease.

In summary, the lavas from Glenwood consist of alkali basalt and tholeiite, both of which are products of mixing of asthenospheric and lithospheric mantle source melts (essentially Group 1 + 2) , followed by crustal contamination. These trends are

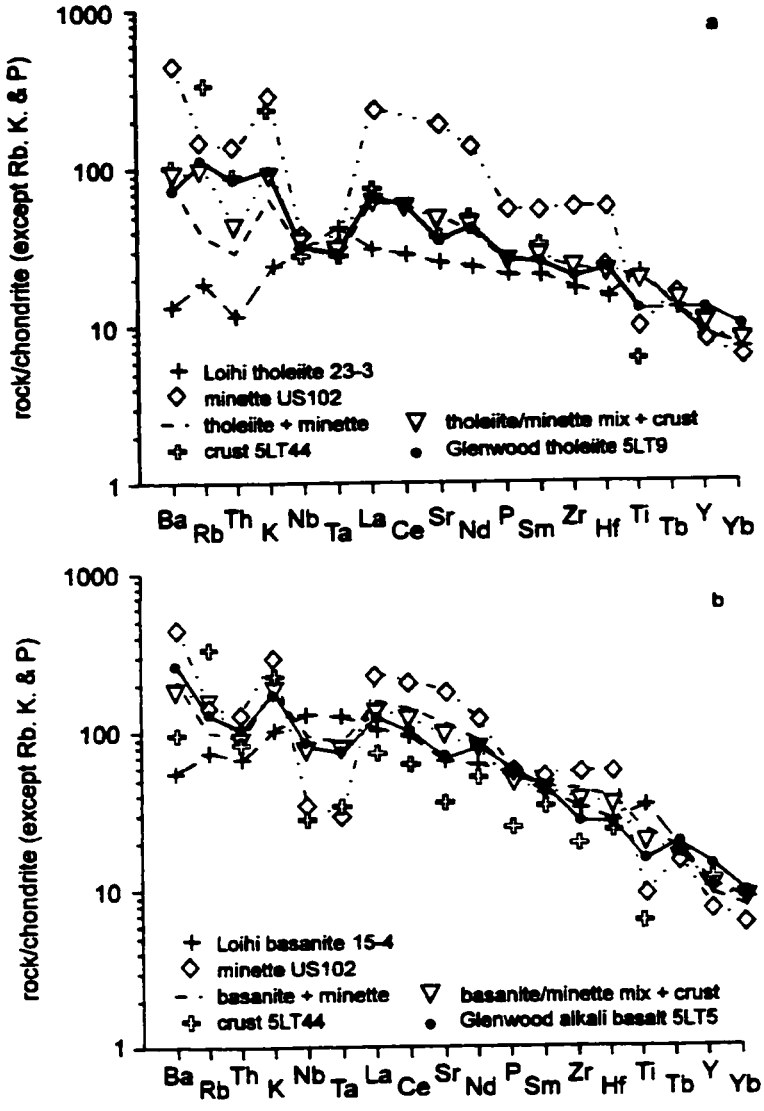

Fig. 3.6 Chondrite normalized incompatible element diagrams for Glenwood (a) tholeiites and (b) alkali basalts. In each case, a representative sample from Loihi is first mixed with minette and then contaminated by upper crust (5LT44; Leat et al., 1991). The contaminated mixtures closely resemble the patterns for the actual Glenwood samples. Loihi data from Frey and Clague (1983). Normalizing parameters from Thompson et al. (1984).

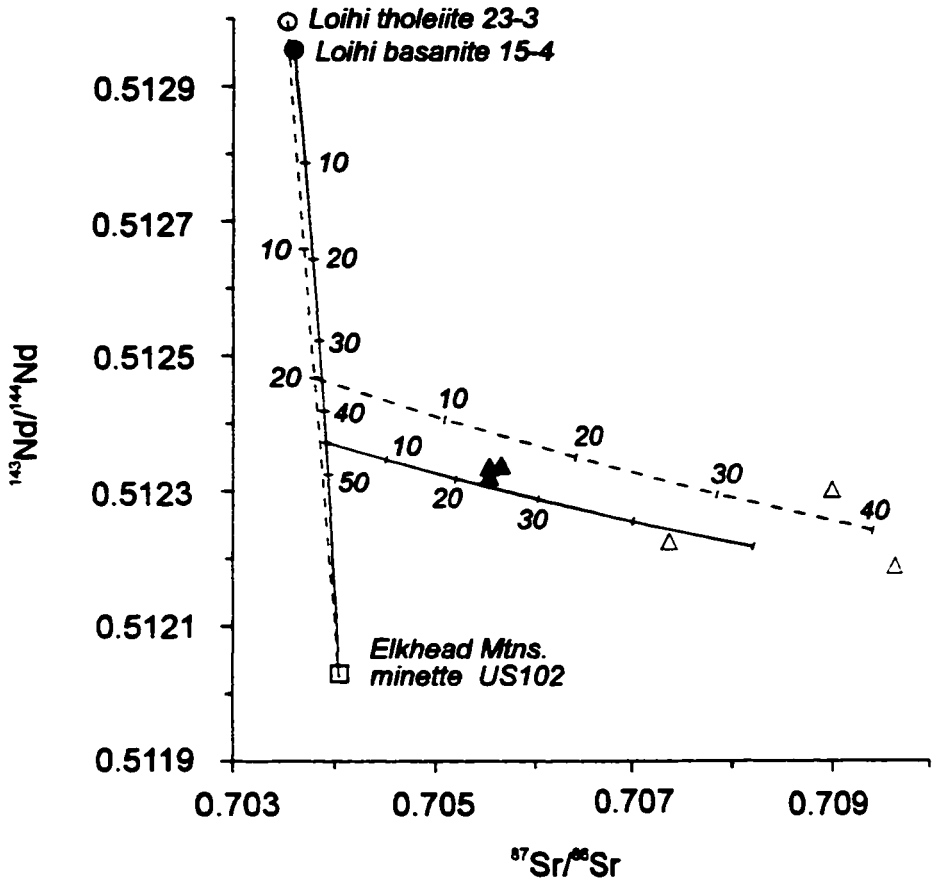

Fig. 3.7 Sr-Nd mixing results for Glenwood samples. Open triangles=tholeiites, filled triangles=alkali basalts. Tholeiite mixing trend denoted by dotted lines; alkali basalt trend by solid lines. Loihi data from Staudigel et al. (1984). Crustal data from Leat et al. (1991). See text for discussion.

confirmed in Pb isotopes also (see below). In NWCO, plume-influenced tholeiites have not previously been described.

3.5. Pb isotope results

3.5.1 Pb-Pb relationships

Pb isotope data from NWCO are plotted in Figs. 3.8 and 3.9 and listed in Appendix 2; analytical prodecures are described in Appendix 1. In $^{206}Pb/^{204}Pb$-$^{207}Pb/^{204}Pb$ space (Fig. 3.8), the NWCO data plot above the NHRL, and are approximately centered on the Geochron. $^{206}Pb/^{204}Pb$-$^{207}Pb/^{204}Pb$ compositions for local Proterozoic supracrustal rocks are similar to those in the NWCO lava suite. The largest range in $^{207}Pb/^{204}Pb$ is evident in subcontinental lithospheric mantle source Group 2 magmas, which plot to the left of the Geochron. This is consistent with derivation of this group of magmas from a relatively old lithospheric mantle component, with minor addition of lower crust. Group 1 (Hawaii) plots to the right of the Geochron, in accordance with having an asthenospheric source. Samples from Yampa, the initial Group 1 'type' locality, fall within the $^{207}Pb/^{204}Pb$ range defined by Group 2, but also overlap the OIB field.. This is to be expected if the Yampa samples represent mixtures of melts derived from asthenospheric (Hawaiian) and subcontinental lithospheric mantle (Group 2) sources. Samples from Group 3 (Flat Tops) plot at intermediate $^{206}Pb/^{204}Pb$ and similar $^{207}Pb/^{204}Pb$, relative to Groups 1 and 2. Crustal contamination is apparent in the Glenwood suite, as noted by the elevated Pb ratios. One sample from Walton Peak plots at elevated $^{206}Pb/^{204}Pb$ (5LT161; Appendix 2) relative to the remaining samples in its suite. This sample is also suspected of experiencing crustal contamination, as it has slightly elevated $^{87}Sr/^{86}Sr$ relative to the other Walton Peak samples plotted in Fig. 3.3.

Fig. 3.9 shows the relationship between $^{206}Pb/^{204}Pb$ and $^{208}Pb/^{204}Pb$ within the

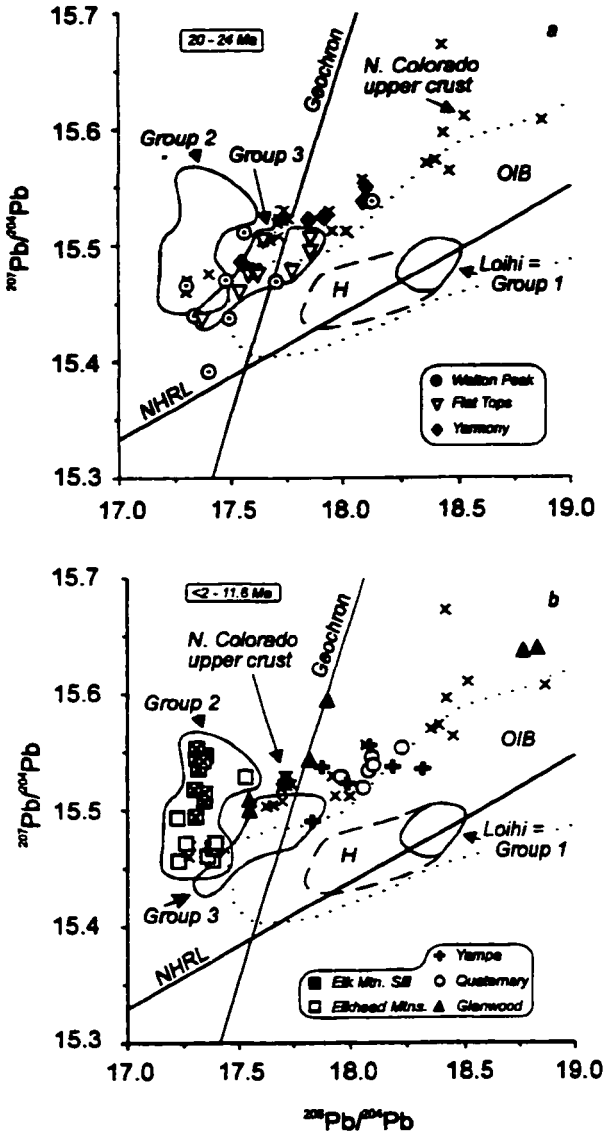

Fig. 3.8 $^{207}Pb/^{204}Pb$ vs. $^{208}Pb/^{204}Pb$ for NWCO volcanics, relative to the Northern Hemisphere Reference Line (Hart, 1984) and the Geochron; (a) early rift, (b) later rift. Elkhead Igneous Province data from Leat et al. (1988b) and Thompson et al. (1989). Hawaii data (H) from Stille et al. (1983) and Staudigel et al. (1984). Data for N. Colorado upper crust are from Aleinikoff et al. (1983) and Stein and Hannah (1985).

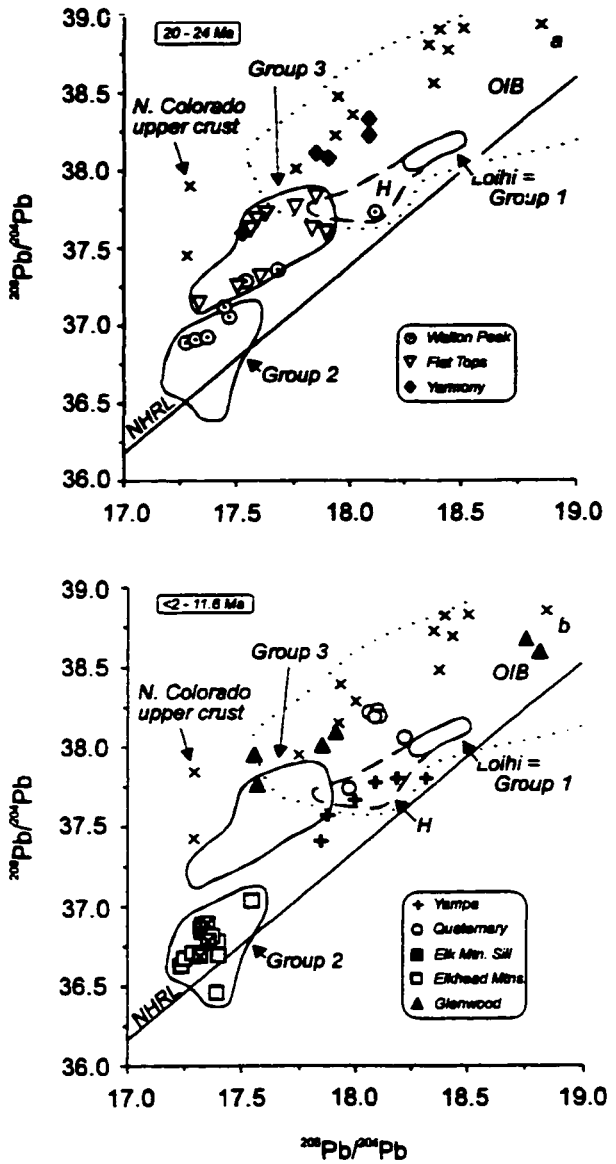

Fig. 3.9 $^{208}Pb/^{204}Pb$ vs. $^{208}Pb/^{204}Pb$ for NWCO volcanics, relative to the Northern Hemisphere Reference Line (Hart, 1984); (a) early rift, (b) later rift. Elkhead Igneous Province data from Leat et al. (1988b) and Thompson et al. (1989). Hawaii data (H) from Stille et al. (1983) and Staudigel et al. (1984). Data for N. Colorado upper crust are from Aleinikoff et al. (1993) and Stein and Hannah (1985).

NWCO data set. Approximately half of the data tend to plot in broad linear trends above the NHRL, but below the upper crustal array. The obvious exceptions to this are the Yarmony (Fig. 3.9a) and Glenwood suites (Fig. 3.9b), and to some extent the Quaternary suite (Fig. 3.9b), which plot within the crustal array. As with $^{206}Pb/^{204}Pb$ vs.$^{207}Pb/^{204}Pb$, Group 1 plots towards more radiogenic values, and Group 2 trends toward less radiogenic values. Group 3 overlaps Group 2 in terms of $^{206}Pb/^{204}Pb$, but is more radiogenic in terms of $^{208}Pb/^{204}Pb$, and cannot be produced by mixing of Groups 1 and 2. Sample 5LT161 from Walton Peak plots at noticeably higher $^{206}Pb/^{204}Pb$ and $^{208}Pb/^{204}Pb$ than other samples in its suite.

In both Figs. 3.8 and 3.9, the location of data from individual volcanic fields that previously have been interpreted as mixtures between certain Group endmembers, as well as the placement of the Group endmembers themselves, are generally internally consistent with theories on their petrogenesis (Leat et al., 1988b; 1989; 1990; Gibson et al., 1991; Thompson et al., 1989; 1993). For example, Leat et al. (1991) have shown that elemental and isotopic trends at Yampa can be modeled by mixing of an OIB-like component similar to a Loihi basanite with minette from the Elkhead Mountains Igneous Province. A similar mixing trend can be obtained for Pb isotopes, reinforcing this conclusion. However, in some cases, the Pb-Pb isotopic relationships suggest that revisions to previous models may be necessary. This will be explored in the following sections.

Samples from Glenwood are spread widely along the upper crustal Pb array. As was shown earlier, the Sr and Nd isotope and incompatible element variations within the suite are consistent with mixing of lavas geochemically similar to those erupted at Loihi with a minette composition from the Elkheads Igneous Province, followed by

contamination by upper crust. Pb isotope variation within the Glenwood suite cannot however be duplicated via this simple two- step mixing scenario. Modeling in $^{206}Pb/^{204}Pb$ versus $^{207}Pb/^{204}Pb$ space indicates 20% crustal contamination will reproduce the variations exhibited by the Glenwood suite, however, the fit for $^{208}Pb/^{204}Pb$ is poor. Contamination of the Loihi-minette mixtures with crust produces a trend roughly parallel to the Glenwood array, but at lower $^{208}Pb/^{204}Pb$. The isotopic relationships of Pb in the Glenwood suite are very similar to those in the Yarmony suite. It is likely that both data sets acquired their Pb isotopic characteristics at upper crustal levels by a component similar in composition to that used in the mixing models, but having more radiogenic $^{208}Pb/^{204}Pb$.

3.5.2 The Quaternary suite

Samples within the Quaternary suite were collected from three separate localities (Fig. 3.1). The least radiogenic sample in terms of $^{206}Pb/^{204}Pb$ is from McCoy, and is also the least radiogenic sample plotted on the Sr-Nd diagram. The most radiogenic Quaternary sample in terms of $^{206}Pb/^{204}Pb$ is from Willow Peak, and plots at intermediate Sr-Nd ratios within the Quaternary group. The remaining samples are from Triangle Peak, and tend to cluster on all Pb diagrams.

The McCoy sample was previously interpreted by Leat et al. (1989) as having a strong relationship to Group 3 subduction-related magmas. If Group 3 is redefined as being represented by the Flat Tops suite, then this interpretation still holds. In contrast, the Willow Peak sample was interpreted by Leat et al. as being the result of an approximately equal mixture of Groups 1 and 2. Pb isotopes for this sample challenge this interpretation, in that it plots furthest away from the Group 2 field. It may be more feasible that the trace element and isotopic character of the Willow Peak sample are

biased due to minor contamination by upper crust. The Triangle Peak group has also been explained as a mixture of Groups 1 and 2. In this case, the samples plot within the crustal array on Figs. 3.8 and 3.9, suggesting that their Pb isotopic signature was imprinted at crustal levels, similar to the Yarmony and Glenwood suites.

3.5.3 Reappraisal of the source of the Walton Peak lavas

In Sr-Nd space (Fig. 3.3), and on the Pb-Pb plots (Figs. 3.8 and 3.9), the position of the Walton Peak field falls approximately between Group 1 and Group 2. This would seem to indicate that the lavas at Walton Peak could be the result of mixing of melts derived from asthenospheric and subcontinental lithospheric mantle sources. Fig. 3.10 shows the incompatible element patterns produced as a result of mixing a Loihi tholeiite and a minette, followed by contamination by lamproite (madupite), another possible representative of the Group 2 source (e.g. Thompson et al. 1989). The contamination of the low-Nb basic component in the composite flow at Walton Peak by a lamproitic composition was advocated by Thompson et al. (1993) to explain the incompatible element variations of the high-Nb component (see also section 3.4.1.1). The model presented above allows for 10 % contamination of the tholeiite- minette mix by madupite to produce the low-Nb component in the composite flow. An additional 15 % contamination by madupite would produce the high-Nb component. Ideally, this hypothesis would be tested next using Sr and Nd isotopes. One difficulty encountered here is that the madupite component used in the contamination model above was collected from the Leucite Hills volcanic center, which erupted through the Archean craton in Wyoming, whereas the Walton Peak flows are located in Proterozoic terrane. The isotopic composition of a madupite derived from metasomatized Proterozoic lithosphere is not expected to be equivalent to that derived from metasomatized

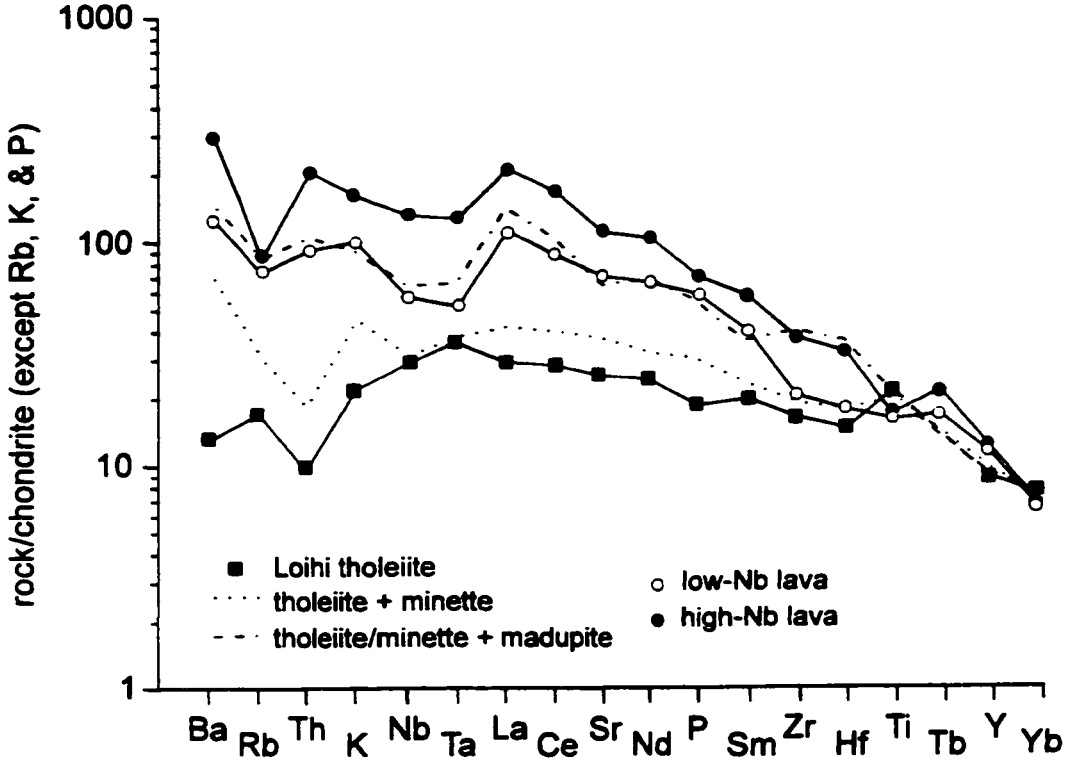

Fig. 3.10 Chondrite normalized incompatible element mixing diagram showing evolution of Walton Peak lavas. A mixture of tholeiite (Loihi 29-10; Frey and Clague, 1983) and minette (5LT154; Leat et al., 1988b) contaminated by madupite (MAD1; Thompson et al., 1984) closely resembles the pattern for the Walton Peak low-Nb (5LT162) sample. Increased contamination of the initial mixture can reproduce the high-Nb (5LT160) sample pattern. Normalizing parameters from Thompson et al. (1984).

Archean lithosphere, therefore it would not be appropriate to use the available data from the Leucite Hills madupites in a mixing model. The success of the trace element modeling implies that an enriched lamproitic component similar to madupite from the Leucite Hills exists within the lithosphere beneath NWCO.

3.6. Inter-isotope comparisons

$^{206}Pb/^{204}Pb$ is plotted against $^{143}Nd/^{144}Nd$ and $^{87}Sr/^{86}Sr$ in Figs. 3.11 and 3.12, respectively. Note that in these figures the Group 3 source is represented by the Flat Tops suite. Similar relationships between the volcanic suites exist if $^{207}Pb/^{204}Pb$ or $^{208}Pb/^{204}Pb$ is substituted for $^{206}Pb/^{204}Pb$. Within the early-rift lavas, $^{143}Nd/^{144}Nd$ varies little with increasing $^{206}Pb/^{204}Pb$ (Fig. 3.11a). Samples from Flat Tops show considerable scatter. The Walton Peak lavas exhibit two trends, originating at the position of least evolved basic lavas in the sample suite, between Groups 1 and 2. The first trend is slightly positive, with a minor decrease in $^{206}Pb/^{204}Pb$ with decreasing $^{143}Nd/^{144}Nd$, whereas the second trend is negatively correlated, with $^{206}Pb/^{204}Pb$ increasing with a slight decrease in $^{143}Nd/^{144}Nd$. The latter trend is approximately parallel to the crustal contamination trend of the Yarmony suite. As was discussed in section 3.5.3, the Walton Peak lavas appear to be the result of mixing between Groups 1 and 2, followed by contamination by lamproite. The high-Nb lavas of the Walton Peak composite flow are endmembers of the radiogenic Pb trend, i.e. trending away from the Group 2 field at enriched $^{206}Pb/^{204}Pb$. In contrast the endmembers of the slight positive trend towards Group 2 are the acid components of the composite flow at Walton Peak. An overall negative trend is also apparent for the Yarmony lavas, emphasizing that variable amounts of upper crust have influenced the isotopic composition of the Yarmony and high Nb Walton Peak lavas. This crustal effect is more apparent in $^{87}Sr/^{86}Sr$

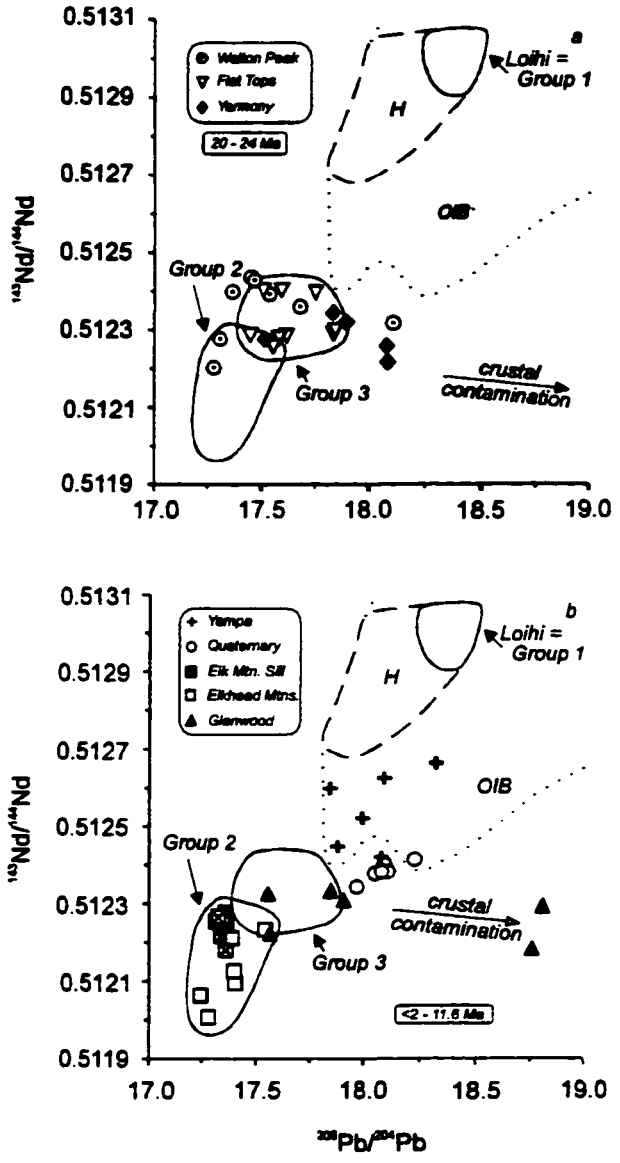

Fig. 3.11 $^{143}Nd/^{144}Nd$ vs. $^{208}Pb/^{204}Pb$ for NWCO volcanics; (a) early rift, (b) later rift. Hawaii data (H) from Stille et al. (1983) and Staudigel (1984).

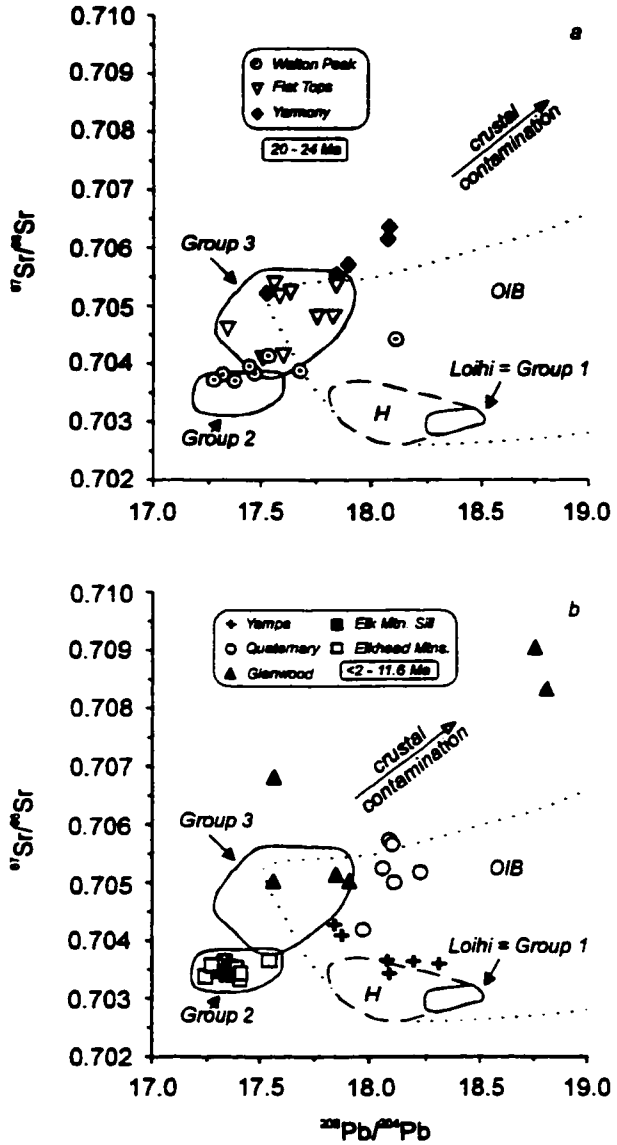

Fig. 3.12 $^{87}Sr/^{86}Sr$ vs. $^{208}Pb/^{204}Pb$ for NWCO volcanics; (a) early rift, (b) later rift. Hawaii data (H) from Stille et al. (1983) and Staudigel et al. (1984).

vs.$^{206}Pb/^{204}Pb$ space (see Fig. 3.12a, below).

A steep positive trend is evident in Fig. 3.11b for the later rift lavas. The Yampa field is one endmember of the trend, plotting at higher $^{143}Nd/^{144}Nd$ and $^{206}Pb/^{204}Pb$ than the remaining suites, consistent with its asthenospheric origin. Group 2 minettes plot at less radiogenic isotope ratios, completing the trend. Lavas from the Quaternary group extend from the Yampa field towards Group 3. The least radiogenic sample from McCoy plots close to the Group 3 field, consistent with previous interpretation. Samples from Triangle Peak and Willow Peak plot at more radiogenic values. Mixing between Groups 1 and 2 followed by crustal contamination might explain the position of these data points. The Glenwood suite exhibits similar behavior to that seen at Walton Peak and Yarmony (Fig. 3.11a), that is, decreasing isotopic Nd with increasing $^{206}Pb/^{204}Pb$, pointing to crustal contamination. Glenwood 10 Ma tholeiites are most enriched in $^{206}Pb/^{204}Pb$, whereas the alkali basalts and 8 Ma tholeiite are less enriched and plot within the main trend of the diagram.

For the NWCO lavas, plots of $^{87}Sr/^{86}Sr$ versus isotopic Pb are more instructive for examining the effects of crustal contamination. In Fig. 3.12a, $^{87}Sr/^{86}Sr$ is plotted against $^{206}Pb/^{204}Pb$ for the early rift lavas. Overall positive trends are evident for each suite of lavas. The field for Flat Tops is intermediate between the majority of less radiogenic samples from Walton Peak and the more radiogenicYarmony array. This behavior is apparent in Sr-Nd space also (Fig. 3.3). In the Walton Peak group, the acid components of the composite lava plot within the Group 2 field. In contrast, the high Nb lavas are most radiogenic, consistent with the previous interpretation of minor interaction with upper crust.

Also apparent in Fig. 3.12a is the distinct positive trend within the Yarmony

suite. $^{87}Sr/^{86}Sr$ increases with decreasing age in the sample suite. The overall elevated Sr isotopic signature of the suite in addition to a steady increase in $^{87}Sr/^{86}Sr$ over time implies that crustal input occurred during the initial development of the magmatic system as well as throughout its history. From the inter-isotope relationships for Yarmony together with its Pb isotopic composition identical to local upper crust, it is concluded that the Sr and Pb isotopic signature of this group of lavas was obtained at crustal levels and does not represent a mantle source.

For the later rift lavas, the variations in $^{87}Sr/^{86}Sr$ with $^{206}Pb/^{204}Pb$ allow more obvious distinctions between mantle and crustal influences. In Fig. 3.12b, Group 1 and Group 2 plot at similar $^{87}Sr/^{86}Sr$, with the Group 1 field at more radiogenic Pb values. The Yampa suite plots between Groups 1 and 3; this behavior is also apparent on Figs. 3.3b and 3.11b. Such trends might imply that the dominant lithospheric mantle component in the Yampa suite may be Group 3 not Group 2. However, trace element and Sr-Nd modeling by Leat et al. (1991) preclude this possibility, so the rise in $^{87}Sr/^{86}Sr$ must be due to crustal contamination. The Quaternary lavas plot in a near vertical orientation at similar Pb isotope ratios to Group 1, with increasing $^{87}Sr/^{86}Sr$. Analyses from Triangle Peak and Willow Peak plot at more radiogenic positions, consistent with minor crustal influence. Samples from the Glenwood suite show the most variation. Tholeiitic lavas plot at high $^{87}Sr/^{86}Sr$ and $^{206}Pb/^{204}Pb$, consistent with the interpretation above of upper crustal contamination. The 8 Ma Glenwood tholeiite has elevated $^{87}Sr/^{86}Sr$ at relatively unradiogenic $^{206}Pb/^{204}Pb$, indicating that the isotopic composition of possible contaminants to the NWCO volcanics are variable.

3.7 Conclusions

Pb isotope results from rift-related lavas in NWCO generally confirm previous

interpretations regarding their derivation from at least three distinct mantle sources. The analysis of lavas from the Glenwood Springs area has revealed the presence of tholeiitic magma possibly associated with the Yellowstone plume. Mixing between plume-influenced Group 1 and lithospheric mantle source Group 2, followed by contamination by lamproite is shown to be a viable hypothesis to explain the geochemistry of the Walton Peak suite. This suggests that a source similar to Group 1 was available from the convecting asthenosphere prior to the recognition of actual Yellowstone plume activity. The Group 3 subduction-related source must therefore have been confined to the thermal boundary layer of the lithosphere prior to the initiation of magmatic activity 24 Ma. This preferred chemical geometry of the mantle is consistent with proposed mantle structure in other regions of the rift for this time period (Gibson et al., 1992).

Both Groups 2 and 3 have a lithospheric mantle source, with the Group 2 source having the least radiogenic Pb component in the NWCO data set. Although the majority of NWCO lavas have similar $^{206}Pb/^{204}Pb$-$^{207}Pb/^{204}Pb$ to local upper crust, it is primarily lavas from the Yarmony suite (and to some extent the Glenwood and Quaternary lavas) that have $^{208}Pb/^{204}Pb$ ratios *within* the crustal array. Also, the trace element and isotopic signatures of the Yarmony suite could potentially represent a mixture of all three magma Groups. As such, the Group 3 source is redefined as being best represented by the c. 21-23 Ma Flat Tops suite, the Pb ratios of which plot away from the crustal array.

Beard and Johnson (1993) have analyzed a number of NWCO lavas from Yampa, Yarmony, Flat Tops, the Elkheads Igneous Province, and the Quaternary lavas for their Hf isotope composition. ε_{Hf} values range from c. 0 in the Group 1 Yampa

samples to -10 in the Group 2 minettes. Samples from Flat Tops (Group 3) yielded an average value of ε_{Hf}= -7.7 . The covariation of ε_{Nd} with ε_{Hf} in the NWCO samples was interpreted to reflect a prevalent lithospheric component in the lavas. This has two primary implications. First, samples from Yampa (Group 1) plot within the field defined by OIB in ε_{Hf} vs. ε_{Nd} space, but below the OIB field in ε_{Nd} vs. $^{87}Sr/^{86}Sr$ (Fig. 3.3). The influence of the lithosphere would help to explain this shift to lower ε_{Nd} in both cases. Second, Group 3 samples from Flat Tops have distinctly negative ε_{Hf} suggesting strong crustal or lithospheric control. This is in keeping with the conclusions reached above that the Group 3 source in the NWCO volcanics is predominantly lithospheric.

3.7.1 Regional tectonomagmatic implications

A widely quoted model developed by McKenzie and Bickle (1988) predicts the volume and composition of magma produced during periods of lithospheric extension. The potential temperature of the underlying anhydrous asthenosphere, the thickness of the lithosphere and the amount of lithospheric extension (β) are critical parameters. We have postulated above that in the early Miocene, asthenosphere-derived melts mixed with components of the lithosphere, and were erupted at Walton Peak. According to the McKenzie and Bickle model, β must exceed a value of 2.5 in order for melt to be produced from anhydrous mantle of average potential temperature (T_p=1280° C). Gibson et al. (1992) have calculated values for the apparent amount of lithospheric extension, β_a (the ratio of final to initial thickness at a given point; see McKenzie, 1984), for NWCO of 1.5 - 2. The discrepancy between the McKenzie and Bickle model value and the calculated degree of extension that we believe has yielded asthenospheric melt can be resolved if we propose that the asthenosphere beneath NWCO in the early Miocene contained an irregular distribution of volatiles which acted to reduce the

temperature of the mantle solidus. A patchy distribution of volatiles in the convecting asthenosphere is advocated by Gibson et al. (1992, 1993) to explain the presence of Oligo-Miocene aged, OIB-like tholeiitic and alkalic magmas in the Española Basin in north-central New Mexico. The continued existence of hydrous pockets within the asthenosphere beneath NWCO into the second phase of rifting and magmatism may also explain the emplacement of OIB-like alkalic and tholeiitic basalts at Glenwood Springs at 8 - 11 Ma. By c. 6 Ma, the volatile content of the asthenosphere may have been reduced such that only undersaturated magmas were erupted at Yampa.

If both the Group 2 and Group 3 sources in NWCO are lithospheric in nature, it would be useful to comment on their potential relationships. Group 2 ultrapotassic magmas are believed to originate from vein networks within the mechanical boundary layer of the lithosphere (e.g., McKenzie, 1989). We have argued above that the Group 3 source has been confined to the lithosphere throughout the magmatic history of NWCO, however, it is difficult to determine its spatial relationship to the Group 2 source. Leat et al. (1988a, 1990) speculate that the thermal boundary layer is the source region for Group 3, but we cannot unequivocally state that it is limited to this layer. The $^{143}Nd/^{144}Nd$ vs. La/Nb variations in the Group 3 Miocene Flat Tops suite versus the Group 2 Elkheads Igneous Province data set suggest some degree of separation in terms of age. Within the Flat Tops suite, $^{143}Nd/^{144}Nd$ remains relatively constant (c. 0.5123) with increasing La/Nb, whereas $^{143}Nd/^{144}Nd$ for the Elkheads Igneous Province decreases steadily (c. 0.5122 - 0.5119) with increasing La/Nb. These relationships are similar to those documented by Fitton et al. (1991) for basic magmas from the Basin and Range province. Fitton et al. interpreted the two trends as mixing between asthenosphere-derived magmas and two enriched lithospheric sources. One lithospheric source,

equivalent to our Group 3, has a Nd isotopic signature (~0.5123) similar to Pacific pelagic sediment, and obtains its enrichment via fluid fluxing from a subducted slab. The second lithospheric source, equivalent to our Group 2, trends to lower $^{143}Nd/^{144}Nd$ (~0.5115 - 0.5119), and is generated by the introduction of small-volume, highly enriched melts from the asthenosphere into the lithosphere over long periods of time. Thus it appears that in regions undergoing extension in the western U.S.A., two distinct lithospheric sources are potentially available: one comparatively ancient source with low time-integrated $^{143}Nd/^{144}Nd$, and one with a somewhat younger subduction-related signature.

Although the existence of two lithospheric sources in the northernmost extent of the RGR is similar to that advocated for the Basin and Range province, important differences exist between the two regions. For example, we argue above that asthenospheric *and* lithospheric mantle sources were tapped during the major periods of volcanism associated with rifting in NWCO. However, many workers in the Basin and Range argue for a transition from lithospheric to asthenospheric sources over time (e.g., Fitton et al., 1991; Bradshaw et al., 1993; Harry and Leeman, 1995). A detailed discussion on the tectonomagmatic distinctions between NWCO and the Basin and Range is beyond the scope of this chapter, but will be addressed in a forthcoming paper that considers Pb isotope variations in basic magmas associated with the entire RGR system.

Chapter 4: Identification of crustal contaminants in mafic volcanics of the Española Basin, Rio Grande Rift, using Pb isotopes

4.1 Abstract

Mantle-derived mafic lavas associated with the development of the Rio Grande Rift erupted in two phases in the Española Basin, north-central New Mexico. Early rift lavas, dated at 18 to 25 Ma, erupted at scattered localities in the northern section of the basin, and include alkali basalts and quartz tholeiites believed to be asthenospheric in origin. Normalized incompatible trace element abundances in these lavas suggest that they were derived from a similar source. Pb isotope values for these lavas are consistent with derivation from an asthenospheric source, followed by minor amounts of upper crustal, and possibly lithospheric mantle, contamination. During the later rifting phase, mafic volcanics were also extruded at several localities within the Española Basin, including the Cerros del Rio. Volcanic activity from 2 to 4 Ma in the northwest Cerros del Rio volcanic field produced alkali basalts with their evolved equivalents, and tholeiites. Pb isotope ratios in the Cerros volcanics are considerably less radiogenic than the early-erupted lavas, indicating that they are more heavily influenced by lower crust. Sr, Nd, and Pb isotopic variations in the asthenosphere-derived Cerros tholeiites are easily explained by contamination with relatively nonradiogenic local granite. Isotopic variations in the Cerros alkali basalts and their differentiated counterparts are more complex, requiring more than one nonradiogenic contaminant. The presence of quartz xenocrysts in the Cerros alkali basalts and evolved lavas argues favorably for some degree of upper crustal interaction.

4.2 Introduction

Magmatism in the Española Basin is directly related to the tectonomagmatic history of the Rio Grande Rift (RGR). At approximately 30 Ma, the San Andreas fault system was established following the cessation of subduction of the Farallon plate beneath the North American continent (e.g., Atwater, 1970; Lipman, 1980; Severinghaus and Atwater, 1990). As a result of the rapidly diminishing rate of subduction, asthenospheric counterflow and localized upwelling prompted the initiation of the RGR system and associated volcanism (Lipman, 1980). During the initial rifting phase (c. 30-18 Ma), volcanic activity in the Española Basin was primarily concentrated in the northern half of the Basin, and produced relatively small-volume, mafic lava flows at scattered localities. In contrast, late stage rifting (< 13 Ma) produced more voluminous volcanic fields of variable composition to the south. This report offers a comparison of the Pb isotopic character of the early rift lavas and one of the larger mafic volcanic fields, the Cerros del Rio.

Gibson et al. (1992, 1993) examined the major and trace element variations together with Sr and Nd isotopes in the early rift stage lavas (hereafter ERS), concluding that they were like those of ocean-island basic magmas (OIB) and were derived from the asthenosphere with little input from crustal or subcontinental lithosphere sources. Baldridge (1979) presented major element data on the Cerros del Rio lavas (hereafter CdR). Lack of definitive trends within the *ne*- and *hy*-normative populations on major oxide variation diagrams led Baldridge to suggest that the vast majority of CdR lavas were not related by simple fractionation or mixing processes. An exception to this petrogenetic interpretation involves silica oversaturated, evolved compositions which are the fractionated equivalents of a group of less evolved mafic lavas. This work was

subsequently enhanced by Duncker et al. (1991), who employed trace element data and Sr, Nd and O isotopes to document both OIB-like and possible lithospheric components in the CdR. Postulated contaminants of the CdR lavas include both upper and lower crust. Pb isotope data presented here, in conjunction with previously published trace element and isotope data, further refine the identification of the contaminants to the Española Basin mafic volcanics. Using these data, it will be shown that: (1) virtually none of the mafic volcanics erupted in the Española Basin escaped crustal input completely, and (2) the character of crustal influence is different in the ERS lavas relative to the CdR. It will also be suggested that a predominant component of the CdR mafic lavas is a potential lithospheric contaminant of the ERS lavas.

4.3 Regional setting

The Española Basin, in north-central New Mexico (Fig. 4.1), is one of several right-stepping en echelon basins which form the RGR proper (Golombek, 1983; Ingersoll et al., 1990; Chapin and Cather, 1994). Morgan et al. (1986) offer a thermomechanical description of rift activity in the region. The early phase of extension lasted from 30 - 18 Ma, and is characterized by low-angle faulting, broad basin development, and crustal extension, with values as high as 50% regionally and 100% locally. Extension during this phase was predominantly NE-SW and was accompanied by primarily calc-alkaline volcanism. A magmatic lull and a cessation in spreading occurred between 17 and 14 Ma. By 13 Ma, the late phase of extension had begun, with the primary direction of spreading having changed to E-W, and the nature of the volcanism switching to bimodal basalt and rhyolite. Continuous cooling following the cessation of extension and magmatism of the first rifting phase strengthened the lithosphere such that renewed extension produced narrow grabens and half-grabens bounded by high-angle normal

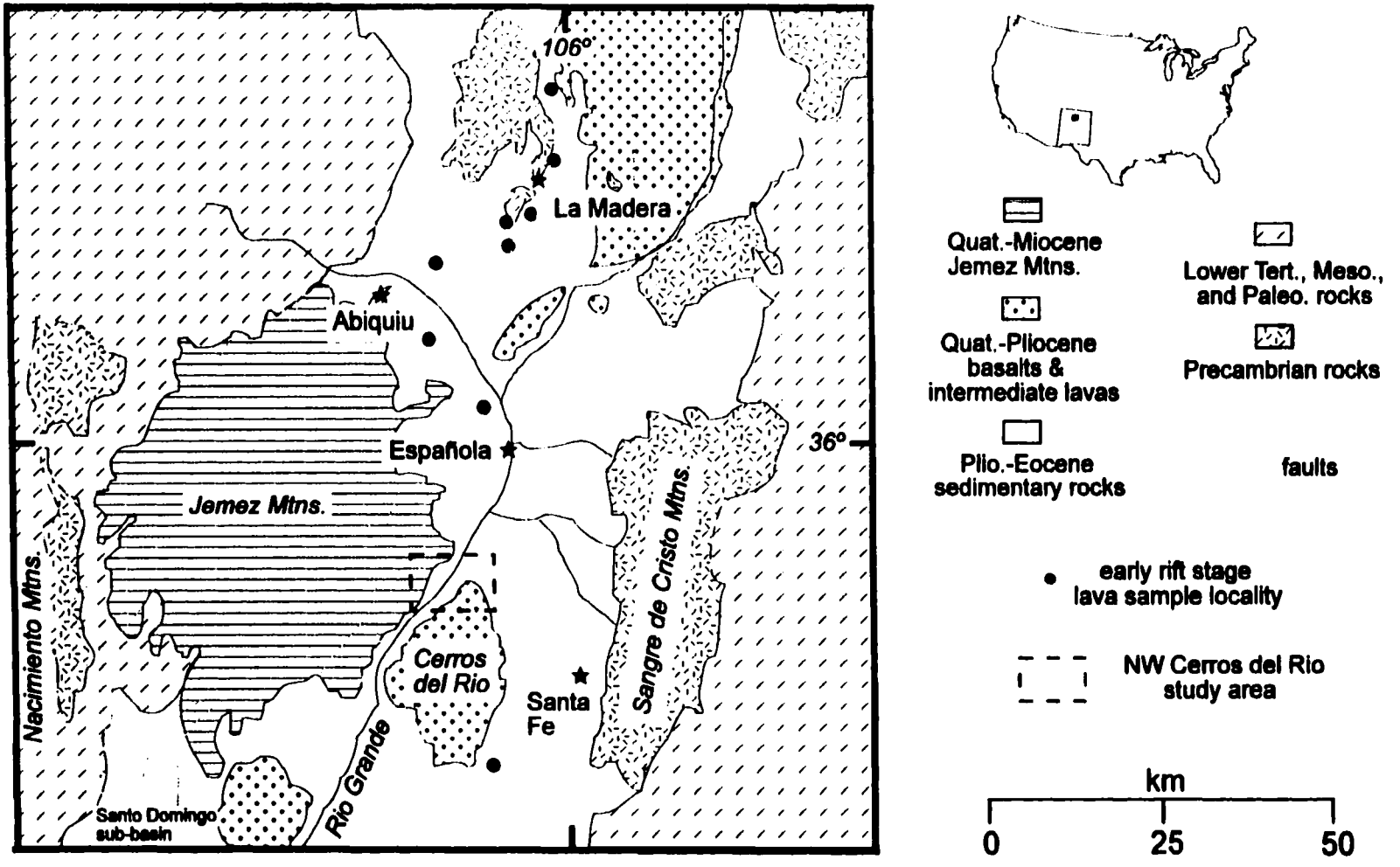

Fig. 4.1 Geologic sketch map of the Española Basin. Adapted from Manley (1979).

faults (Morgan et al., 1986). The maximum amount of extension during the latter phase is estimated at 20%, and resulted in the present rift structure recognized topographically from central Colorado southward into Mexico.

A relatively simple half graben, tilted to the west, is contained within the Española Basin (Chapin and Cather, 1994). Muehlberger (1979), citing offsets and compression deformation across adjacent fault zones, proposed that the Española block has uniformly rotated counterclockwise. However, paleomagnetic work by Salyards et al. (1994) shows that the Española block actually consists of several smaller blocks that rotate independently, albeit still in a counterclockwise sense. The western margin of the basin is delineated by a succession of northeast trending faults (Fig. 4.1), some of which are partially buried beneath young volcanic deposits in the eastern sector of the Jemez Mountains (Golombek, 1983). Manley (1979) describes the northern terminus of the basin as a northwest trending, discontinuously exposed, basement ridge extending through the town of La Madera (Fig. 4.1). The eastern margin of the basin is recognized as a depositional and faulted contact of basin fill with the Precambrian rocks of the Sangre de Cristo range (Fig. 4.1; Golombek, 1983). Published descriptions of the southern termination of the basin are variable, and may or may not include the Santo Domingo sub-basin to the southwest of the CdR field (Fig. 4.1; e.g., Manley, 1979).

Within the Española Basin, shale, sandstone, and limestone of Carboniferous to Cretaceous age overlies Precambrian basement (e.g., Smith et al., 1970). Pre-rift and syn-rift sediments of the Eocene Galisteo Formation and Oligo-Miocene Santa Fe Group are the primary basin fill which unconformably overlie the Paleozoic units. These sediments attain thicknesses of > 3 km on the western side of the Española Basin (Golombek, 1983; Ingersoll et al., 1990; Chapin and Cather, 1994). Volcanic activity

within the Jemez Mountains since > c. 13 Ma has produced the Jemez Volcanic field (Gardner and Goff, 1984), which dominates the western section of the basin. Eruption of the Bandelier Tuff in two episodes at 1.61 and 1.22 Ma (Izett and Obradovich, 1994; Spell et al. in prep.) from the central Jemez Mountains generated ignimbrites which partially overlie the northwest CdR volcanic field (Fig. 4.1).

The Española Basin is contained within the Proterozoic Mazatzal Province of Condie (1992). In general, exposed Early to Middle Proterozoic plutonic and supracrustal units can be assigned to one of five groups, including (from oldest to youngest) basalt-dominated successions (c. 1.76 Ga), older rhyolite-dominated successions, quartzite and other meta-pelitic rocks, younger rhyolite-dominated successions, and 1.4 Ga anorogenic granites (Robertson et al., 1993).

4.4 Geochemical variations: review

In this section, published geochemical data on the Española Basin volcanics is briefly reviewed, in order to provide a foundation for evaluating the available Pb isotope data.

4.4.1 Major and trace element geochemistry

Gibson et al. (1992, 1993) discuss the geochemistry of the ERS lavas, dated at 25 - 18 Ma. ERS lavas largely fall into two groups using the TAS classification (Le Maitre, 1989) and normative nomenclature. Following Gibson et al. (1993), the terms quartz tholeiite and alkali basalt are used in discussions of these silica saturated and undersaturated lavas, respectively.

Representative normalized incompatible trace element patterns for the ERS lavas are shown in Fig. 4.2. On the basis of the patterns and element concentrations, Gibson et al. (1992, 1993) consider the ERS lavas to be OIB-like. Partial melting of

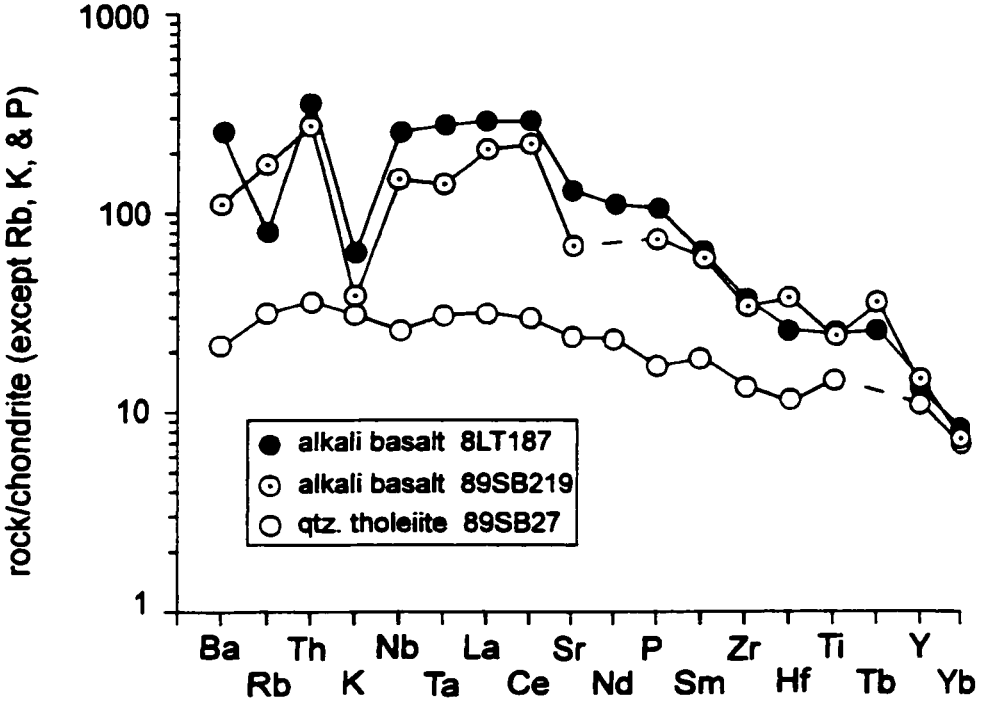

Fig. 4.2 Representative chondrite normalized incompatible element patterns for ERS alkali basalts and quartz tholeiites. Normalization parameters from Thompson et al. (1984).

localized hydrous patches within a convecting CO_2-enriched asthenosphere above the subducted Farallon plate were suggested as the source of the quartz tholeiites. In contrast, the ERS alkali basalts are thought to be the products of partial fusion of the dominantly CO_2-enriched asthenosphere. Incomplete dissolution of potassic amphibole or phlogopite in the mantle source may result in the retention of K (Fitton and Dunlop, 1985), thus producing a K-trough in the normalized trace-element patterns of the ERS alkali basalts (Gibson et al., 1993) as in manly silica-undersaturated OIBs. Deviations from expected OIB-like patterns, including $(Ta/La)_N$ >1 in a K-depleted basalt, can be attributed to contamination of the ERS alkali basalts by crust or subcontinental lithosphere.

The geochemistry of 4 - 2 Ma mafic volcanics from the northwest CdR is discussed by Duncker et al. (1991). In the TAS classification scheme (Le Maitre, 1989), the CdR volcanics fall into several categories. Following Duncker et al., compositions that are *ne*-normative are referred to as "hawaiites", and those that are *ol-hy*-normative are termed tholeiites. Incompatible element concentrations in the hawaiite group are variable, suggestive of heterogeneous source compositions, variable melt fractions, and/or interaction with diverse crustal compositions. Several samples with SiO_2 values > 52.5% have trace element characteristics similar to the more primitive hawaiites and are considered to be their evolved equivalents, and are thus referred to as evolved lavas. Most hawaiites and evolved lavas contain xenocrystic quartz of variable O-isotope composition, a hallmark of contamination by silicic crust.

Fig. 4.3 presents normalized incompatible trace element patterns for representative compositions from the CdR. Tholeiites are similar to tholeiitic OIB and are considered to be derived from the asthenosphere, with minor degrees of crustal

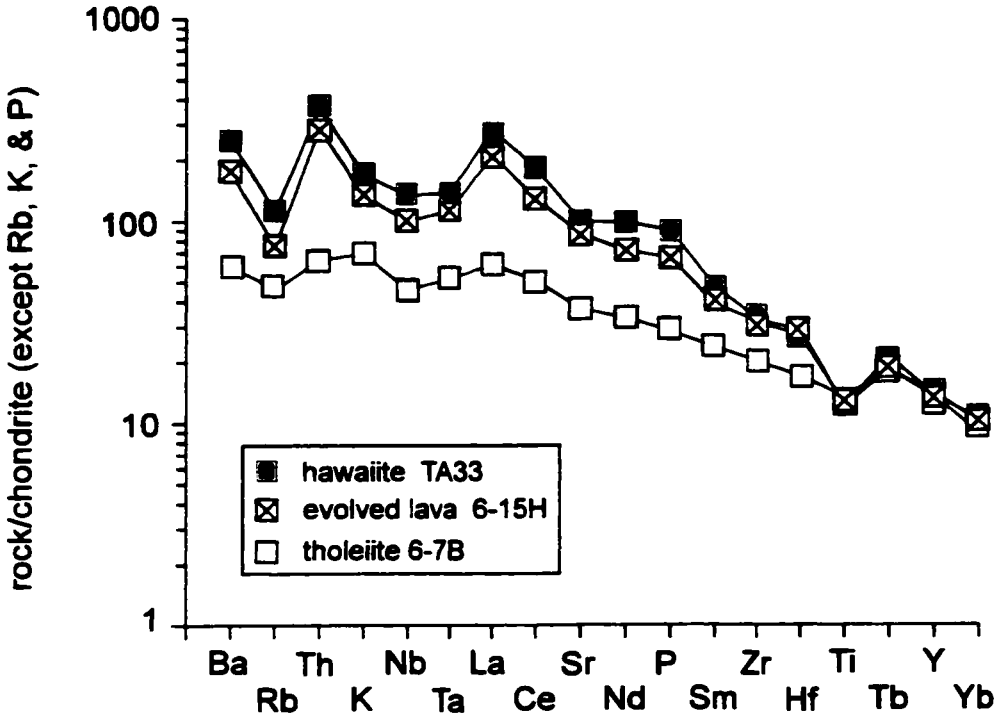

Fig. 4.3 Representative chondrite normalized incompatible element patterns for CdR hawaiites and tholeiites. Normalization parameters from Thompson et al. (1984).

contamination resulting in a weak Nb-Ta trough (Fig. 4.3). Hawaiites and evolved lavas have trace element patterns resembling those of subduction-related magmas (relative depletions in Nb and Ta), similar to the lithospheric Group 3 source of Northwest Colorado discussed by Leat et al. (1988, 1991). One difference however between the CdR hawaiites and the Group 3 magmas erupted in Northwest Colorado is the conspicuous depletion of K in the CdR lavas. Duncker et al. (1991) have attributed this characteristic to phlogopite-amphibole conversion in the thermal boundary layer during lithospheric thinning, which results in K and Rb loss. Abundances of incompatible trace elements in the evolved lavas are less than those in the parental hawaiites (Fig. 4.3). This behavior is opposite to that expected if closed system conditions prevailed during the evolution of the CdR magmas. Specifically, this argues for mixing rather than AFC-dominated, open system behavior. Isotopic data discussed below will confirm that the CdR magmatic system was affected by lower crustal contamination, resulting in incompatible element "depletions" and shifts in radiogenic isotopic composition towards regional lower crustal values.

4.4.2 Sr-Nd isotope geochemistry

ERS lavas erupted at scattered localities in the Española Basin, many of which are located near or on recognized faults (Fig. 4.1). These magmas probably originated as small-volume, low-degree partial melt fractions. In such systems, the effects of open system processes, which occur in large magma chambers (e.g., replenishment and crustal contamination) are minimized. Nevertheless, Gibson et al. (1993) recognized that contamination of some of the OIB-like ERS lavas by upper crust had occurred, based on elevated $^{87}Sr/^{86}Sr$ ratios. It has been suggested that OIB-like magmas erupted within the continental realm originate in the convecting asthenosphere

below the subcontinental lithosphere (Fitton and Dunlop, 1985; Fitton et al., 1991; Thompson et al., 1989; Gibson et al., 1992, 1993). In addition, the composition of this convecting mantle source is comparable to Northern Hemisphere OIB, specifically that from Hawaii and Iceland (Brandon and Goles, 1988; Leat et al., 1991; Draper, 1991). Thus, a range of plausible mantle compositions is available for modeling purposes. Modeling the crustal contamination of the alkali basalt and quartz tholeiite ERS lavas was attempted using data from Hawaii as starting mantle compositions, and data from local granites as contaminants (Table 4.1). Approximately 5-10% bulk contamination of Hawaiian mantle with local granite (upper crust) is necessary to reproduce the overall Sr-Nd isotopic variability within the ERS suite (Fig. 4.4). However, the mixing trends do lie above the main field of data, indicating that the model parameters have not been accurately identified. In general, this model is similar to that presented by Gibson et al. (1993), in which an OIB-like magma from the Basin and Range Province was contaminated by an isotopically extreme, ultrapotassic sample from the subcontinental lithosphere of Australia.

Also in Fig. 4.4, crustal contamination models similar to those presented by Duncker et al. (1991) for the CdR are shown. If it is assumed that the hawaiite component is representative of a relatively uncontaminated mantle source, the isotopic trends of the evolved lavas can be reproduced via simple mixing of hawaiite and up to 15 % regional lower crust, a component recognized in other RGR volcanics (Dungan et al., 1986; Johnson and Thompson, 1991). The percentage of crust required in this model is equivalent to that modeled by Duncker et al. (1991; Fig. 6, curve 1), however, the mixing trajectory is slightly offset to lower $^{87}Sr/^{86}Sr$ due to changes in mantle starting composition and a less radiogenic $^{87}Sr/^{86}Sr$ value for lower crust used here (Table 4.1).

Table 4.1. Mixing calculation endmembers

	mantle[a]						crust[b]					
	[Sr]	$^{87}Sr/^{86}Sr$	[Nd]	$^{143}Nd/^{144}Nd$	[Pb]	$^{206}Pb/^{204}Pb$	[Sr]	$^{87}Sr/^{86}Sr$	[Nd]	$^{143}Nd/^{144}Nd$	[Pb]	$^{206}Pb/^{204}Pb$
ERS												
AB 27-4	359	0.70341	18.4	0.512986	1.3	18.373	165	0.768	60.6	0.511797	25	18.77
T 23-3	318	0.70354	17.6	0.512987	0.98	18.433	280	0.745	50	0.5119	23	18.25
CdR												
H I-4	1150	0.70412	49	0.512690	6.5	18.280	1000	0.705	30	0.5118	25	17.0
KT	425	0.70406	20	0.512706	1.2	17.934	394	0.722	42.9	0.511983	21	17.76

[a] mantle values: ERS initial mantle values are from Loihi, AB=alkali basalt, T=tholeiite. Data are from Frey and Clague (1983) and Staudigel et al. (1984). CdR initial Sr-Nd mantle values for hawaiite (H) from Duncker et al. (1991); Pb data this study. Average Koolau tholeiite data (KT) calculated from four tholeiites in Roden et al. (1984), except [Pb], which was calculated using Ce/Pb=25 (Sun and McDonough, 1989). Koolau isotope data from Stille et al. (1983).

[b] crustal values: ERS alkali basalt and quartz tholeiite, and CdR tholeiite models use local granite data (samples B8, average of B4 & B8, B4, respectively) published in Duncker et al. (1991). Pb data from S. Moorbath (pers. comm.). CdR hawaiite model based on lower crustal estimates in Johnson et al. (1990)

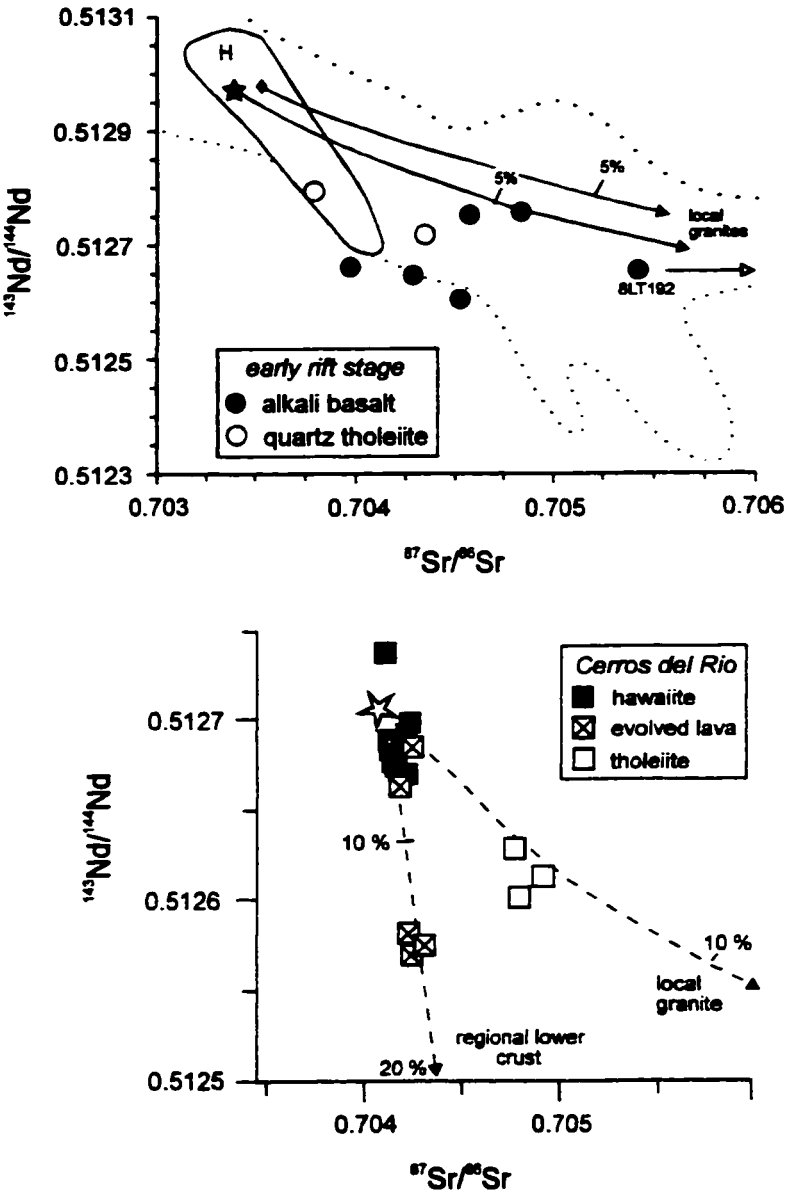

Fig. 4.4 Sr-Nd isotopic relationships in Española Basin mafic volcanics. Top: ERS data from Gibson et al. (1993). 8LT192 plots off the diagram at $^{87}Sr/^{86}Sr=0.711979$. OIB field enclosed by dotted line; solid line represents field for Hawaiian data. Filled star is Loihi alkali basalt 27-4, filled diamond is Loihi tholeiite 23-3. Bottom: CdR data from Duncker et al. (1991) and Perry et al. (1987). All crustal data are given in Table 4.1 Open star=average Koolau tholeiite. Hawaii data from Stille et al. (1983), Frey and Clague (1983), Roden et al. (1984), and Staudigel et al. (1984). All Nd isotopic data are corrected assuming a chondritic reservoir $^{143}Nd/^{144}Nd$ ratio of 0.512638.

Duncker et al. (1991) chose a lower crustal $^{87}Sr/^{86}Sr$ value of 0.707, however, model estimates for the lower crust in this region by Johnson and Thompson (1991) and Dungan et al. (1986) place the estimate of this isotopic ratio closer to 0.705. Two evolved lava samples, least radiogenic in terms of $^{143}Nd/^{144}Nd$, have > 58% SiO_2 and were probably affected by assimilation-fractional crystallization, as they are too silicic to have been generated through mixing alone (Duncker et al., 1991). For the CdR tholeiites, simple mixing of less than 10% local granite with average Koolau tholeiite (Stille et al., 1983; Roden et al., 1984) adequately reproduces their isotopic compositions. A similar trend could also be produced through mixing with regional lower crust with variable Rb/Sr.

As noted above, Gibson et al. (1993) speculate that the Sr and Nd ratios of the ERS lavas may signify that the magmas contain up to 10% of a lithospheric mantle component. The geochemical nature of the components of the CdR offer some insight to this possibility. Normalized incompatible trace element pattern shapes of the ERS alkali basalts show apparent similarities to the CdR hawaiites, including relative depletions in K, Nb, Ta, and approximately equal normalized abundances of Sr, Nd, and P (see Figs. 4.2, 4.3). This implies that the least evolved components of early and later rift activity in the Española Basin were derived from a similar source(s). The greater magnitude of normalized incompatible element depletions in the CdR hawaiites could signify that they contain a larger component of a lithospheric contaminant. Therefore, if the ERS lavas were contaminated by subcontinental lithosphere - as "represented" by the CdR hawaiites - *prior* to crustal contamination, then the similarity of the ERS and CdR trace element patterns could potentially be explained.

4.5 Pb isotope variations

4.5.1 Pb-Pb

Pb isotope data allow further characterization of the mantle and crustal components in the Española Basin mafic volcanics. Isotope ratios are listed in Appendix 2 and are plotted in Figs.4.5 and 4.6. In $^{207}Pb/^{204}Pb$ vs.$^{206}Pb/^{204}Pb$ space (Fig. 4.5), the ERS lavas plot to the right of the Geochron, nearly parallel to the Northern Hemisphere Reference Line (NHRL) of Hart (1984). In the ERS data set, there is an overall trend to more radiogenic compositions, strongly implying involvement of upper crust. In comparison, the CdR data plot as a group at less radiogenic values near the intersection of the Geochron and the NHRL. The $^{206}Pb/^{204}Pb$ ratios in the CdR evolved lavas are less radiogenic than the hawaiites. Contamination of heterogeneous CdR hawaiite parental lavas by a common non-radiogenic crustal component may explain the $^{206}Pb/^{204}Pb$ ratios of the evolved compositions, although interaction with heterogeneous lower crust is another viable explanation.

Variation in $^{208}Pb/^{204}Pb$ vs.$^{206}Pb/^{204}Pb$ for the ERS lavas is opposite to that displayed by the CdR suite (Fig. 4.6). As was shown in Fig. 4.5, the ERS lavas adopt a trend to more radiogenic values, whereas all CdR data plot in the opposite sense, following an assumed regional lower crustal vector. In summary, the Pb isotopic relationships in the mafic volcanics of the Española Basin support primarily upper crustal contamination of the ERS lavas, and essentially lower crustal input to the CdR compositions. Earlier it was proposed that the ERS lavas may contain a lithospheric component, similar to that detected in the CdR hawaiites. If so, the Pb isotopic signature imparted to the ERS lavas by minor interaction with the lithosphere has been completely overprinted by the Pb isotopic composition of the contaminating crust.

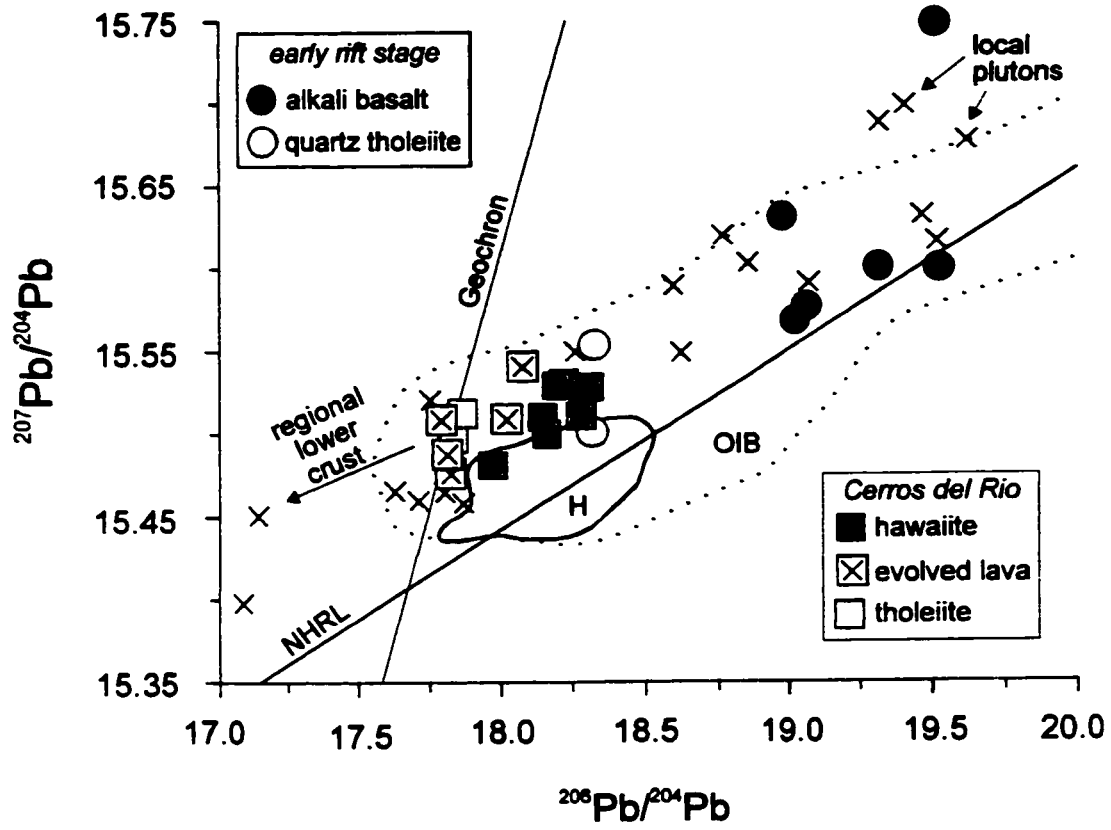

Fig. 4.5 $^{207}Pb/^{204}Pb$ vs. $^{206}Pb/^{204}Pb$ data for ERS and CdR lavas. Field for OIB denoted by dotted line; solid line encloses data for Hawaii (H). NHRL of Hart (1984) and the Geochron shown for reference. Local pluton data (all X's) from Aleinikoff et al. (1993) and S. Moorbath (pers. comm., 1990). Hawaiian data are from Stille et al. (1983), Frey and Clague (1983), Roden et al. (1984), and Staudigel et al. (1984).

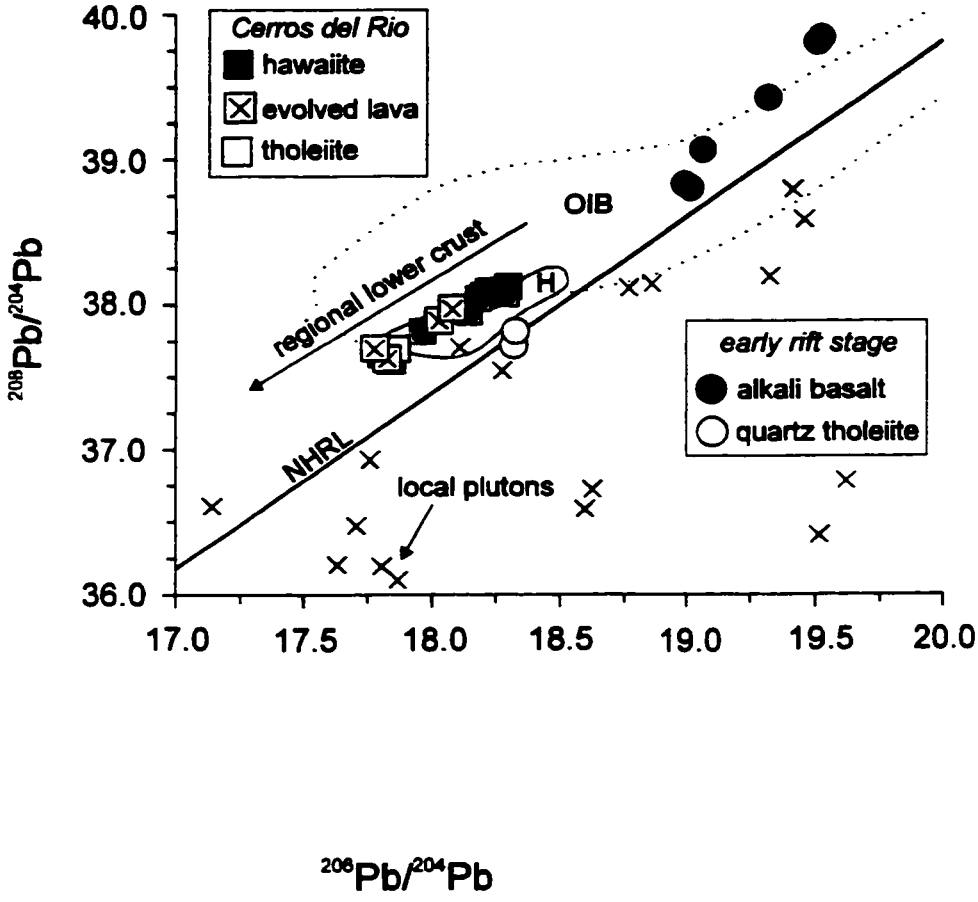

Fig. 4.6 $^{208}Pb/^{204}Pb$ vs. $^{206}Pb/^{204}Pb$ data for ERS and CdR lavas. Field for OIB denoted by dotted line; solid line encloses data for Hawaii (H). NHRL of Hart (1984) shown for reference. Local pluton data (all X's) from Aleinikoff et al. (1993) and S. Moorbath (pers. comm., 1990). Hawaiian data are from Stille et al. (1983), Frey and Clague (1983), Roden et al., (1984), and Staudigel et al. (1984).

4.5.2 Sr vs. Pb

Fig. 4.7 is a plot of $^{87}Sr/^{86}Sr$ versus $^{206}Pb/^{204}Pb$ for the Española Basin mafic volcanics. For the ERS suite, a mixing calculation using the parameters discussed in Fig. 4.4 (Sr-Nd) confirms that less than 10% crust is required to replicate the general isotopic characteristics of the alkali basalts and quartz tholeiites. As in the Sr-Nd model, the mixing trend for the alkali basalts falls away from the samples, as a contaminant more radiogenic in Pb is required. Decoupled behavior of Sr and Pb isotopes in the ERS data set is also apparent, and is suggestive of contamination by a metasedimentary unit with variable Rb/Sr.

Also shown in Fig. 4.7 are mixing calculations for the CdR volcanics, using the endmembers discussed in Fig. 4.4. In agreement with the results of the Sr-Nd mixing calculations (Fig. 4.4) the hawaiite-evolved lava trend displays a slight increase in $^{87}Sr/^{86}Sr$ with decreasing $^{206}Pb/^{204}Pb$, consistent with contamination of a hawaiite parent with about c. 15% of lower crust to produce the evolved lavas. Mixing trends for the CdR tholeiites also agree well with previous estimates on the amount of upper crust (less than 10%) required to reproduce their isotopic compositions.

4.5.3 Nd vs. Pb

In $^{143}Nd/^{144}Nd$ vs. $^{206}Pb/^{204}Pb$ space (Fig 4.8), differences in the type of crustal contamination of the ERS versus the CdR sample suite are clearly seen. There is an overall trend of decreasing $^{143}Nd/^{144}Nd$ with increasing $^{206}Pb/^{204}Pb$ in the ERS alkali basalts, whereas the $^{206}Pb/^{204}Pb$ ratios in the quartz tholeiites are nearly constant at noticeably lower isotopic Nd. In contrast, the majority of CdR data follow trends of decreasing isotopic Pb with decreasing $^{143}Nd/^{144}Nd$. Mixing proportions within the ERS alkali basalts and CdR group using the parameters discussed above are, for the most

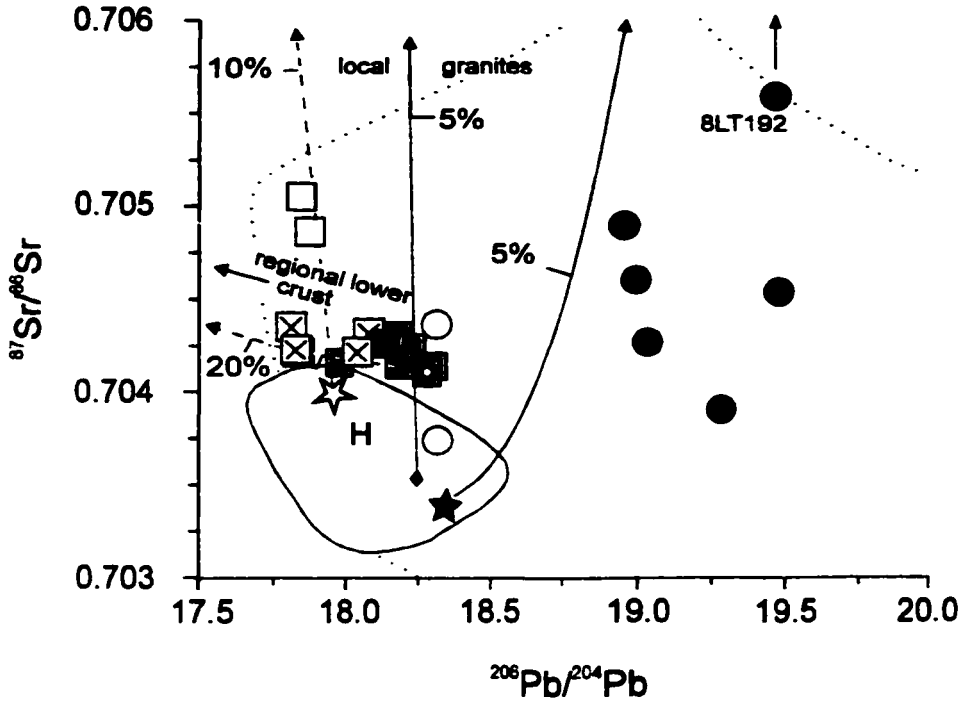

Fig. 4.7 Sr-Pb isotopic relationships in the ERS and CdR lavas. Dotted line encloses OIB data; Hawaiian data (H) enclosed by solid line. Open star=average Koolau tholeiite; filled star=Loihi alkali basalt 27-4; filled diamond=Loihi tholeiite 23-3. ERS sample 8LT192 plots off the diagram. Mixing lines generated using data in Table 4.1. Hawaii references are Stille et al. (1983), Frey and Clague (1983). Roden et al. (1984) and Staudigel et al. (1984). See text for discussion.

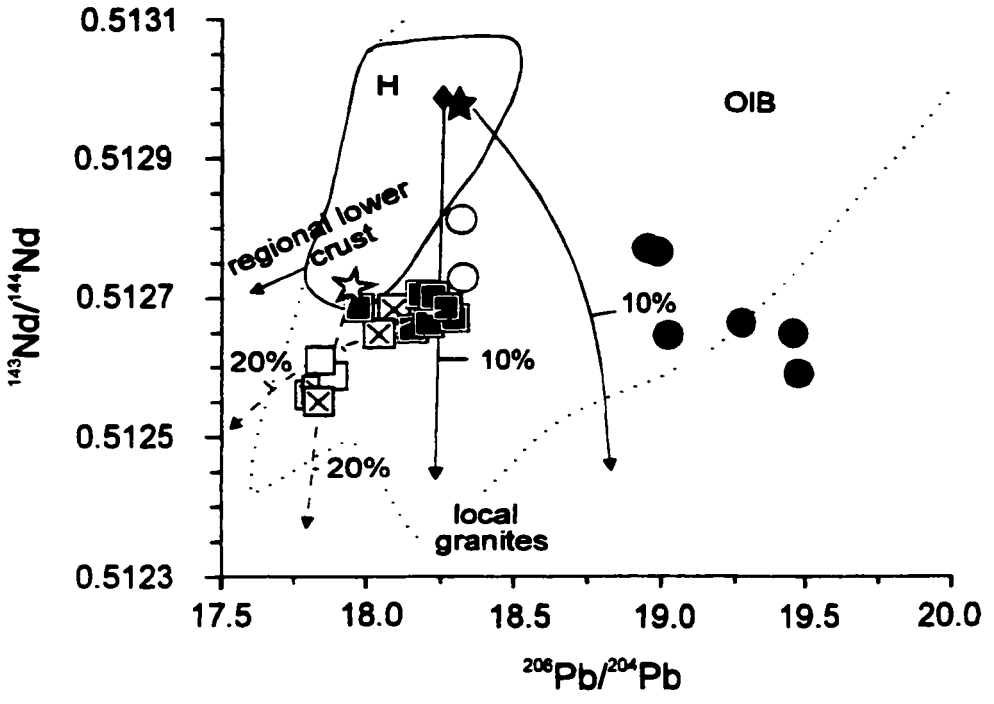

Fig. 4.8 Nd-Pb isotopic variation in ERS and CdR lavas. Contamination trends differ for each suite reflecting primarily upper and lower crustal influences in the ERS and CdR data, respectively. Symbols are as in previous diagrams. Dotted line delineates extent of OIB data; solid line is specifically for Hawaii (H). Mantle starting compositions and Hawaii references are described in Fig 4.4. See text for discussion.

part, consistent with the models presented earlier.

One sample within the CdR hawaiite group exhibits lower $^{206}Pb/^{204}Pb$, but not $^{143}Nd/^{144}Nd$ than the remaining hawaiites, hinting at the possible influence of a third contaminant composition. This potential contaminant is also recognized in Keres Group lavas and tuffs from the Jemez Mountains (Ellisor et al., 1995), which erupted just to the west of the CdR field. Ellisor et al. have defined this component as being depleted in isotopic Sr and Pb, and interpret it as being Proterozoic mafic lower crust.

4.6 Summary

The relationships among radiogenic Sr, Nd, and Pb isotopes for mantle-derived mafic volcanics from the Española Basin record two distinct crustal influences. Pb isotopes in the asthenospheric ERS lavas have been affected primarily by radiogenic upper crust, whereas Pb in the late rift stage CdR volcanics is dominated by lower crust. The isotopic composition of the ERS alkali basalts cannot be precisely modeled by simple mixing of a single crustal component with a single mantle-derived melt. This is to be expected, given the range of possible contaminant compositions as well as the probable lack of a central magmatic system for these lavas. The decoupled relationship of Sr and Pb isotopes (and to some extent Nd and Pb isotopes) in the ERS suite lends further support to the notion of variable contaminant compositions. Similarities between normalized incompatible element patterns for the ERS alkali basalts and CdR hawaiites suggest that they were derived from a similar source(s), and that both may have experienced contamination by a lithospheric component. This lithospheric component does not appear to have heavily influenced the trace element geochemistry of the ERS quartz tholeiites. Any Pb isotopic fingerprint of the lithosphere on the ERS lavas has been overwhelmed by the isotopic Pb character of the crust.

The proportion of crust within the CdR volcanics is more easily quantified. It appears that the asthenosphere-derived tholeiites, similar to those from Koolau, Hawaii, have experienced < 10% crustal contamination by relatively nonradiogenic granite or regional lower crust. In contrast, the proportion of lower crust within the hawaiites and evolved lavas approaches 15%. The variation of $^{143}Nd/^{144}Nd$ versus isotopic Pb for the hawaiites and one evolved lava suggests that another component, mafic lower crust, may have influenced their isotopic composition, although this is not strictly required.

Upper crustal contamination of the CdR hawaiites and evolved lavas did occur, despite any radical shifts in Pb or Sr isotopic composition. Quartz xenocrysts are present in most hawaiites and evolved lavas. $\delta^{18}O$ of separated quartz ranges from +6.7‰ to +10.6 ‰ (Duncker et al., 1991), requiring derivation from a heterogeneous crustal source(s). O-isotope disequilibrium between coexisting phenocrysts also indicates that the quartz is of extraneous origin. Lower values of $\delta^{18}O$ in some quartz separates are indicative of high-grade (lower crustal) protoliths, however the elevated $\delta^{18}O$ quartz must have been derived from ^{18}O-rich upper crustal units.

It was noted earlier that there is considerable heterogeneity in the Proterozoic supracrustal units exposed in New Mexico (Robertson et al., 1993). These units include basalt- and rhyolite-dominated successions, as well as quartzite and other metapelitic rocks and anorogenic granites. It is conceivable that if these compositions continue in the subsurface (see Grambling et al., 1988), than the contaminants of the Española Basin mafic volcanics may all be Proterozoic in age. Other potential contaminants include Paleozoic, Mesozoic, and lower Tertiary sedimentary units which overlie the Precambrian basement of the Basin, and Pliocene-Eocene basin-fill sediments.

Chapter 5: Spatial and temporal review of Pb isotopes in mafic magmas from the Rio Grande Rift

5.1 Abstract

Pb isotope systematics in mafic and intermediate composition volcanics associated with the development of the Rio Grande Rift are reviewed. Data from the literature are combined with approximately 100 new Pb isotope analyses on lavas from Colorado and New Mexico, and are considered in terms of latitude, age, and mantle source. Isotope transects reveal distinct differences between the Pb isotopic signatures of magmas erupted on Proterozoic versus Archean terranes. Similarities between the isotopic composition of the lithosphere beneath the rift region are also inferred. Rift extension models developed for the Great Basin and the Rio Grande Rift in New Mexico are examined, and their bearing on the geochemical signature of Rio Grande Rift magmas is evaluated. A combined model is presented which describes the evolution of Rio Grande Rift mafic magma sources. This model suggests that extension began > 5 Ma earlier than previously thought.

5.2 Introduction

Continental rifts offer an excellent opportunity to observe the physical and magmatic processes associated with continental break-up. Although studies of regions in the advanced stages of rifting, e.g. the Red Sea region, are of equal importance, subaerial rift zones are generally more accessible and therefore have the potential to provide a much larger data base of geophysical and petrologic information regarding changes to continental lithosphere during rifting. In addition to the academic value of

knowledge gained from studies of continental rifts is the awareness of geologic hazards in areas of active rifting. Earthquakes caused by movement along rift-related faults are one type of hazard; however, the potential for volcanic eruptions in populated centers that have developed within (Rinehart et al., 1979) or adjacent to rift basins (Wolff and Gardner, 1995) is probably of more concern.

The Rio Grande Rift (RGR), located in the southwestern U.S.A., is one of the Earth's currently active rift zones. Numerous studies have focused on the geochemical variations of specific volcanic fields within the rift (e.g., Leat et al., 1989; Gibson et al., 1991; Johnson and Thompson, 1991; Duncker et al., 1991; Thompson et al., 1993) or along its flanks (e.g., Gibson et al., 1993; Davis and Hawkesworth, 1993, 1994, 1995). In addition, several regional reviews have focused their attention on differences in $^{143}Nd/^{144}Nd$ ratios as related to lithospheric and asthenospheric components of the rift-related magmas (Perry et al., 1987; Gibson et al., 1992). This chapter presents a spatial and temporal compilation of published and newly acquired Pb isotope data from the RGR region. Included in this work are data from volcanic centers along the shoulders and flanks of the rift which are more representative of the composition of the underlying lithosphere during all stages of rifting.

5.3 Extension and magmatism

McKenzie and Bickle (1988; hereafter [MB]) introduced what is now a widely quoted model for basic magmatism associated with decompression melting of the asthenosphere during lithospheric extension. The model is based on an anhydrous peridotitic starting composition, and is satisfactorily applied especially in areas in which the thinning continental lithosphere during the advanced stages of extension is underlain by asthenosphere of relatively high potential temperature. Leeman and Harry (1993)

present geochemical and geophysical arguments suggesting that the [MB] model is not applicable to the initial stage of extension in many regions, such as the Great Basin area of the Basin and Range Province. The enriched trace element and radiogenic isotope characteristics of early-stage extensional basalts from the Great Basin argue for derivation from an enriched mantle source that has been isolated from the convecting mantle for a significant period of geologic time. The earliest extensional magmatic components of the Great Basin are primarily intermediate to silicic in composition, not basaltic as predicted by the [MB] model. Harry and Leeman (1995) point out that contemporaneous basaltic activity in this region did occur, acting as a heat source for crustal anatexis. In addition, the volume of silicic magmatism decreased with continuing extension, opposite to that predicted by the [MB] model.

As an alternative to the [MB] model, Leeman and Harry (1993) propose partial melting of *basaltic* components of subcontinental lithospheric mantle, introduced during previous magmatic episodes, to account for compositional changes during the magmatic history of the Great Basin. Peridotitic subcontinental lithosphere is too cold during the initial stages of extension to undergo partial melting. In contrast, the dry tholeiite solidus will be intersected during the early stages of extension, provided that advective heat gain from the convecting asthenosphere is greater than conductive heat loss in the lithosphere, and extension rates are relatively high. In this scenario, interaction of the basaltic partial melts with overlying crust results in anatexis and the production of intermediate to silicic magmas. Basaltic lavas erupted at the surface have isotopic and trace element characteristics consistent with derivation from an enriched mantle source. As extension exceeds 50%, a transition from predominantly (basaltic-melt-metasomatized) lithospheric to asthenospheric sources occurs. As with the [MB]

model, the initial thickness of the lithosphere dictates the amount of extension required to produce a melt.

5.3.1 Lithospheric magma sources

Both the [MB] model and its alternative promoted by Leeman and Harry (1993) provide a basis for analyzing the magmatic history of the RGR. However, before proceeding further it is necessary to define what is meant by the term "lithosphere" when discussing magma sources. Among the terms in use recently are mechanical and thermal boundary layers (e.g., Leat et al., 1989; Gibson et al., 1993), subcontinental lithospheric mantle (SCLM; e.g., Gibson et al., 1992), subcontinental mantle (Harry and Leeman, 1995), and perisphere (Anderson, 1994). Harry and Leeman (1995) discuss the differences and similarities between these terms; this information briefly discussed here. The lithospheric mantle is defined as that portion of the Earth which remains isolated from the convecting asthenosphere, moves with tectonic plates, and transfers heat by conduction only. McKenzie and Bickle (1988) and McKenzie (1989) have used the terms "mechanical and thermal boundary layers" (MBL and TBL, respectively) to describe portions of the lithosphere. The MBL is true lithospheric mantle, whereas the TBL is a transition zone separating the MBL from the convecting asthenosphere. The transitory character of the TBL requires it to lose heat essentially by convection at its base and conduction at its top, but not necessarily move with the MBL. Delamination of the lithosphere refers to the convective overturn of the TBL into the underlying asthenosphere. The MBL and the upper region of the TBL are isolated from the asthenosphere and are expected to develop trace element and isotopic signatures distinct from depleted mantle as a result of metasomatism. Metasomatism takes place as a result of the upward percolation of (1) small-degree carbonate-rich partial melts

from the asthenosphere (McKenzie, 1989), and/or (2) hydrous fluids driven off subducted slabs (Fitton et al., 1988). In the western United States, the geochemical imprint of the latter form of metasomatism is directly related to the history of subduction along the west coast (e.g., Lipman, 1980; Fitton et al., 1991) and has produced a lithospheric reservoir(s) with subduction zone characteristics (e.g. enrichment in Ba, depletion in Nb). The establishment of the subduction-related reservoir occurs through accretion of metasomatized mantle wedge material to the base of the lithosphere (Othman et al., 1989), or continued infiltration of the established lithosphere by slab-derived fluids (Leat et al., 1988a). The lower region of the TBL, if not undergoing rigorous convection (Parsons and McKenzie, 1978), also has the potential to develop a distinct geochemical signature. However, given the transitory nature of the lower region of the TBL, the time period over which geochemical signatures may evolve is considerably less than that of the overlying conductive regions of the lithosphere. Anderson (1994) argues that the lower portion of the TBL should not be referred to as "lithosphere" as it does not have the correct rheological properties, and has introduced the term "perisphere" to refer to this layer. This work follows the terminology and definitions of Gibson et al. (1992) and Harry and Leeman (1995): the SCLM is that portion of the mantle that moves with the plate and includes the MBL and the upper part of the TBL. The lower region of the TBL is transitory and may be considered part of the SCLM if it becomes strong enough to undergo extensional deformation. Lithospheric melts are derived via melting of basaltic-melt-metasomatized regions, producing basaltic magmas (Harry and Leeman, 1995), or through melting of incompatible-element-rich vein networks to produce potassic melts (Foley, 1992).

5.4 Regional setting

Theories on the exact cause of continental extension in the southwest and western U.S.A. are under debate. A widely held view relates the initiation of rifting to the tectonic regime along the west coast of North America (e.g. Lipman, 1980). Between 40-30 Ma, a decrease in the rate at which the eastward-dipping Farallon plate was subducted beneath the North American plate occurred (Atwater, 1970; Severinghaus and Atwater, 1990). By 30 Ma, the subduction boundary was replaced by the strike-slip San Andreas fault system. Lipman (1980) argues that this change in tectonic regime caused foundering of the subducted Farallon plate and subsequent counterflow in the asthenosphere, thus initiating uplift, extensional faulting, and magmatism in the RGR region. Alternative models have been developed for the Pacific Northwest region and the Basin and Range Province. Wernicke et al. (1987) view extension of the lithosphere as resulting primarily from gravitational spreading and thermal relaxation of previously thickened crust, although the effects of plate interactions may also be involved. In contrast, Gans et al. (1989) consider extension in the Basin and Range to be an active process initiated by asthenospheric upwelling, as the earliest magmatism began prior to extension. More recently, Hawkesworth et al. (1995) have revived a theory based on convective thinning of the lithosphere. In this model, convective thinning, or delamination, of the lithosphere occurred following lithospheric thickening during the Laramide and Sevier orogenies. Regional isostatic uplift took place as a result, thereby promoting an extensional regime by increasing the potential energy of the region. Uplift following delamination of the subcontinental lithosphere of the Rocky Mountains-Great Plains region has also been proposed by Angevine and Flanagan (1987) to explain sub-surface mass anomalies, however a relationship to extension in the adjacent RGR

has not been clearly defined. The convective thinning model promoted by Hawkesworth et al. (1995) additionally provides a convincing explanation of topography, present-day heat flow, and the timing and composition of magmatism associated with extension in the Basin and Range.

The RGR has developed along an axis of regional uplift in the south-central U.S.A. between the Colorado Plateau and the Great Plains (Fig. 5.1). Eaton (1987) has shown that the basins of the RGR constitute the axial graben of a continental ridge, termed the Alvarado Ridge (Fig. 5.1). For the purposes of this paper, the RGR is divided into three segments (Fig. 5.1): northwest Colorado (NWCO; 39-41°N), southern Colorado and northern New Mexico (CNM; 35-39°N), and southern New Mexico (SNM; 31.5-35°N). Localized uplift beginning in the Late Oligocene and continuing into the Pliocene has obliterated the rift basin structure in NWCO, however the RGR fault system can be traced to the Wyoming border (Tweto, 1979; Keller et al., 1991). In contrast, the physiographic expression of the rift in the central CNM is one of well-developed, right-stepping en echelon basins. South of 34°N, the RGR widens into a series of parallel basins which extend into Mexico.

Development of the RGR is considered a two phase process. Initial rifting occurred in SNM between 31-28 Ma (Chapin and Seager, 1975). In CNM and NWCO, rifting began shortly afterwards, c. 27 Ma (Lipman and Mehnert, 1975; Baldridge et al., 1980). Morgan et al. (1986) have documented several geophysical characteristics of the rift phases. The early phase of extension, from c. 30-18 Ma, is recognized by the development of broad basins along low-angle faults, with magnitudes of regional and local NE-SW extension approaching 30% and 100%, respectively. Tectonism slowed after 18 Ma, but was renewed by 10 Ma, and was accompanied by epeirogenic uplift.

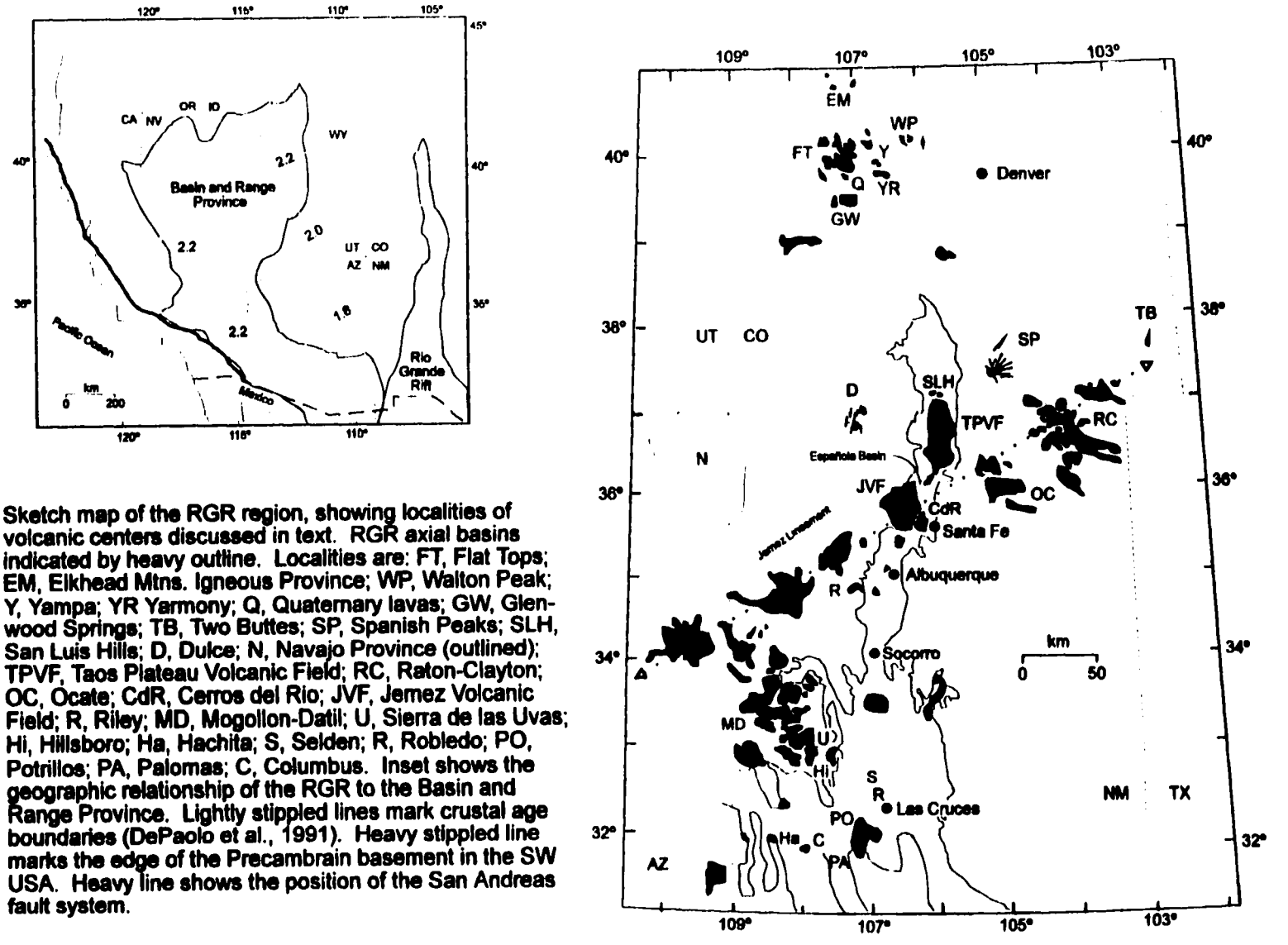

Fig. 5.1 Sketch map of the RGR region, showing localities of volcanic centers discussed in text. RGR axial basins indicated by heavy outline. Localities are: FT, Flat Tops; EM, Elkhead Mtns. Igneous Province; WP, Walton Peak; Y, Yampa; YR Yarmony; Q, Quaternary lavas; GW, Glenwood Springs; TB, Two Buttes; SP, Spanish Peaks; SLH, San Luis Hills; D, Dulce; N, Navajo Province (outlined); TPVF, Taos Plateau Volcanic Field; RC, Raton-Clayton; OC, Ocate; CdR, Cerros del Rio; JVF, Jemez Volcanic Field; R, Riley; MD, Mogollon-Datil; U, Sierra de las Uvas; Hi, Hillsboro; Ha, Hachita; S, Selden; R, Robledo; PO, Potrillos; PA, Palomas; C, Columbus. Inset shows the geographic relationship of the RGR to the Basin and Range Province. Lightly stippled lines mark crustal age boundaries (DePaolo et al., 1991). Heavy stippled line marks the edge of the Precambrain basement in the SW USA. Heavy line shows the position of the San Andreas fault system.

This late phase of extension resulted in the segmentation of earlier rift basins into narrow horsts and grabens in addition to the creation of new uplifts along high-angle faults. The amount of lateral extension thus far does not exceed 20%, however vertical displacements far exceed that of the initial rift phase.

Recent geophysical modeling of the RGR region suggests initial lithospheric thinning was accompanied by propagation of fractures through the lithosphere (Bussod and Williams, 1991; Davis, 1991). Subsequent injection of the asthenosphere into these fractures generated partial melts in the lower lithosphere, initiating uplift with potential small-scale convection in the asthenosphere. Forcible dike injection in the upper lithosphere is considered responsible for crustal thinning, graben formation, and rift shoulder uplift. This 'dike-injection' model also accounts for the observed upwarping of the Moho beneath the rift axis as the asthenosphere continues to intrude the lithosphere and lower crust (Parker et al., 1984). Nicolas et al. (1994) have proposed a similar model for the East African Rift.

5.4.1 Rift segments

As noted above, we have divided the RGR into three segments for ease of discussion. The following sections briefly introduce the volcanic fields included in this compilation. Localities were chosen for inclusion primarily on the basis of the availability of Sr, Nd, and Pb isotope data. However, incompatible trace element data from localities for which isotope data are not available are also discussed to emphasized mantle source characteristics in the rift segments.

5.4.1.1 Northwest Colorado (NWCO: 39-41°)

Volcanic centers in NWCO developed primarily to the west of faults recognized as an extension of the RGR system. In the early Miocene, volcanism

resulted in the formation of successions of lavas at Flat Tops, Walton Peak, and the area around Yarmony Mountain (Fig. 5.1). Alkalic and tholeiitic lavas were emplaced at all three localities (Leat et al., 1990; Gibson et al., 1991; Thompson et al., 1993). Caution is advised however in interpreting the normative compositions from Yarmony, as the samples have been affected by carbonation. Previous work on the major and incompatible trace element variations as well as Sr-Nd isotopic data have shown that the Flat Tops and Yarmony magmas were derived from the SCLM (Leat et al., 1990; Gibson et al., 1991). The lithospheric source of these magmas has an unusual incompatible trace element signature, combining low Nb/La and low K/La (e.g., Leat et al., 1988a). This source was initially defined by Leat et al. (1988a) as one of three potential mantle sources for NWCO lavas. Group 1 mantle represents the convecting asthenosphere and has oceanic island basalt (OIB) characteristics. Group 2, a strongly potassic magma source, and Group 3, the primary component of the Flat Tops and Yarmony magmas described above, are both lithospheric. Thompson et al. (1993) predicted that the magma types encountered at Walton Peak were also derived from the Group 3 source. However, on the basis of newly acquired Pb isotope data, it has been suggested (Chapter 3) that the Walton Peak magmas may be asthenosphere-derived.

Following the rift-wide lull in extension and magmatism, volcanic activity continued at scattered localities in NWCO, including the Elkheads Igneous Province, Yampa, and Glenwood Springs (Fig. 5.1). Minor outcrops of Quaternary lavas are also found. The primary magma source at each of these localities, with the exception of the Elkheads Igneous Province, has been interpreted as asthenospheric (Group 1; e.g., Leat et al., 1988a; 1989; 1991). Minettes from the Elkheads Igneous Province, including the Elk Mountain Sill, are defined by Leat et al. (1988b) and Thompson et al. (1989) as

most clearly representing the strongly potassic Group 2 source in NWCO.

5.4.1.2 Southern Colorado and Northern New Mexico (CNM; 35-39°)

The central segment of the rift region is divided by the Jemez Lineament (Fig. 5.1), a Precambrian structural flaw along which several volcanic centers have developed. Although few of these fields show a clear relationship to the RGR, data from them are useful for monitoring the geochemical characteristics of the SCLM on the rift flanks and shoulders. To the north of, and sub-parallel to, the Jemez Lineament are several volcanic fields (Navajo, Dulce, Spanish Peaks, and Two Buttes) which are also included here as monitors of the SCLM.

Magmatism during the early stage of rifting produced lavas and associated products of mafic to intermediate character. Included in this work are data from the San Luis Hills, Española Basin, Spanish Peaks, the Navajo Province, Dulce, Two Buttes, and Riley (Fig. 5.1). Johnson and Thompson (1991) studied the observed geochemical variations in mafic rocks from the San Luis Hills, concluding that two lithospheric components contributed to the observed magmatism. One of these lithospheric components may contain a contribution from the asthenosphere, similar to that identified at Los Mogotes volcano, San Juan Volcanic Field, c. 25 km west of the San Luis Hills. Gibson et al. (1993) describe a broad geochemical transect across the rift region, including the Navajo Province, Dulce, lava flows within the Española Basin, Spanish Peaks, and Two Buttes. It was observed that early rift under- and oversaturated lavas emplaced within and immediately outside the Española Basin are the clearest representation of an asthenospheric source during this time period. Gibson et al. (1992) noted the importance of previous magmatism in this area in allowing the asthenosphere-derived magmas to ascend to the surface with only minor contamination from the crust

or SCLM. In contrast, potassic samples included here from the Navajo Province and Two Buttes represent a SCLM component, whereas Dulce and Spanish Peaks reflect mixtures of asthenospheric and SCLM.

Late stage magmatism in the central rift segment produced several large volcanic fields; included here are Taos, Cerros del Rio, Ocate, and Raton-Clayton (Fig. 5.1). Minor lava flows were also erupted at scattered localities within the Española and Albuquerque Basins. Dungan et al. (1986) convincingly argued that a depleted mantle source yielded the extensive lavas which created the Taos Volcanic Field. Using isotope data, including Pb, Dungan et al. also showed that the primary contaminant of these lavas was lower crust. Nielsen and Dungan (1985) and more recently Housh et al. (1991) describe the petrologic character of the Ocate Volcanic Field, and describe the mafic components as originating within enriched lithosphere. Stormer (1972) and Phelps et al. (1985) initially characterized the geochemical variations in lavas from the Raton-Clayton Volcanic Field, concluding the source as being metasomatized mantle. Housh et al. (1991) expanded this work using Pb isotopes, which strongly suggest a lithospheric origin for the Raton lavas. The petrology of magma types encountered at Cerros del Rio was described by Baldridge (1979) and enhanced by Duncker et al. (1991). Using O isotope data in conjunction with incompatible trace element variations and Sr-Nd isotopes, Duncker et al. characterized the undersaturated component within the Cerros del Rio as having a lithospheric source, and the saturated component as being asthenospheric. The crustal contamination history of the Cerros lavas was also discussed by Duncker et al., and is further detailed using Pb isotopes (Chapter 4). Late stage lava flows in the Española and Albuquerque Basins have been described by Gibson et al. (1992) as having an asthenospheric origin.

5.4.1.3 Southern New Mexico (SNM; 31.5-35°)

Until recently, the southern segment of the RGR has received the least attention in terms of petrologic studies. Included in this compilation are data from the Mogollon-Datil, Potrillos, and Uvas Volcanic Fields, as well as minor lava flows in the Jornado and Tularosa Basins (Fig. 5.1). Early rift stage volcanic activity occurred within the Mogollon-Datil Volcanic Field, as well as to the southeast in the Sierra de las Uvas (Fig. 5.1). Davis and Hawkesworth (1993, 1994, 1995) discuss the petrogenesis of the early Mogollon-Datil volcanics, concluding that the lithosphere was the dominant source of the magmas. The influence of OIB-like asthenosphere in the Mogollon-Datil field did not begin until after the peak of extension in the area (c. 28.5 Ma). Davis and Hawkesworth (1995) note that the rate at which the transition from lithospheric to asthenospheric sources occurred was variable, but peaked at 20-14 Ma. Additional volcanic activity in the Sierra de las Uvas area produced rhyolites, basalts, and basaltic andesites of the Bell Top Formation (36-28 Ma) and basaltic andesites of the Uvas Volcanic Field (Seager and Clemons, 1975; Clemons, 1979; McMillan and Dickin, 1990; McMillan et al., in prep.). McMillan et al. (in prep.) discuss the geochemistry of Bell Top and Uvas suites, which are interpreted as being lithospheric in character.

Following eruption of the Uvas volcanics, magmatism in southern New Mexico was sparse until after 10 Ma. An 11.8 Ma basalt flow near Hachita, New Mexico (Fig. 5.1) has trace element and isotopic characteristics interpreted by McMillan et al. (in prep.) to represent a partial melt of the asthenosphere-lithosphere boundary. Anthony et al. (1992) briefly discuss the major element and selected trace element geochemistry of nine younger volcanic fields in the region. Lavas from the Animas, Deming, and Jornado del Muerto fields are primarily alkaline, whereas subalkaline chemistry

dominates at Columbus, Hillsboro, Black Mesa, Elephant Butte, Palomas, and Portrillo. McMillan and co-workers (Haag and McMillan, 1990; McMillan et al., 1992; McMillan et al., in prep.) have conducted more detailed work at Columbus and Hillsboro. In addition, Gibson et al. (1992) have analyzed lavas from the Potrillo field, the Jornado Basin, as well as the Tularosa Basin. Collectively, all of the late stage mafic lavas from southern New Mexico, with the exception of the Hachita flow, are interpreted as asthenospheric in origin. All samples from the late stage activity for which isotope and trace element data are available are included in this work.

5. 5 Geochemistry

The major and trace element variations, as well as Sr-Nd isotope data for the samples included in this report are discussed by the authors cited in the previous sections which describe magmatism in the RGR segments. Below aspects of the major and trace element data are reviewed. The data have been divided based on rift segment and rift stage (i.e., early or late). Diagrams for Sr-Nd isotope data have been omitted for several reasons. In many cases, Sr-Nd isotopic data for the samples considered here are similar, except in obvious cases of crustal contamination. Second, the Sr-Nd isotope variations tend to confirm previous theories already established using the major and trace element relationships in individual suites. Finally, and most importantly, Sr-Pb and Nd-Pb diagrams are better suited for documenting the isotope variations in the RGR segments due to the larger geographic variation in Pb isotope ratios.

5.5.1 Major elements

A summary of the major element composition of RGR magmas is conveniently described using normative compositions. Following Fitton et al. (1988),

only those samples with MgO > 4 wt.% have been included, in an effort to minimize the effects of crystal fractionation. All norms were calculated using Fe_2O_3/(total iron) = 0.15, and are plotted in Fig. 5.2.

In Fig. 5.2, a similar distribution of normative compositions relative to age in NWCO and SNM is observed. Early rift stage activity in these segments produced mainly saturated and oversaturated magmas, whereas later rift activity was predominantly undersaturated. The weakly *ol*-normative late stage samples in NWCO are crustally contaminated compositions from Glenwood Springs. In SNM, data points from the Uvas and Mogollon-Datil Volcanic Fields cluster in the oversaturated region of the diagram, due primarily to the slightly evolved state of the samples. In the central rift segment (CNM), a wide range of compositions was erupted throughout its magmatic history. The late rift stage data set is dominated by tholeiites from the Taos Plateau. Extreme undersaturated late stage compositions from the Raton-Clayton Volcanic Field (olivine melilite nephelinites and olivine nephelinites) are not plotted on this projection, as they lack modal plagioclase. With the exception of the Taos Plateau volcanics, their is a tendency for most late stage magmas from all segments of the rift to plot in the undersaturated region of this projection. This is a reflection of the increased importance of small degree asthenospheric partial melts in contributing to the magmatism throughout the development of the RGR.

5.5.2 Trace elements

In this section, data from evolved compositions as well as more mafic samples are examined to fully document the range in trace element variation from the RGR region. Normalized incompatible element or "spider-diagram" plots are an almost ubiquitous component of contemporary petrologic studies, and are used to compare

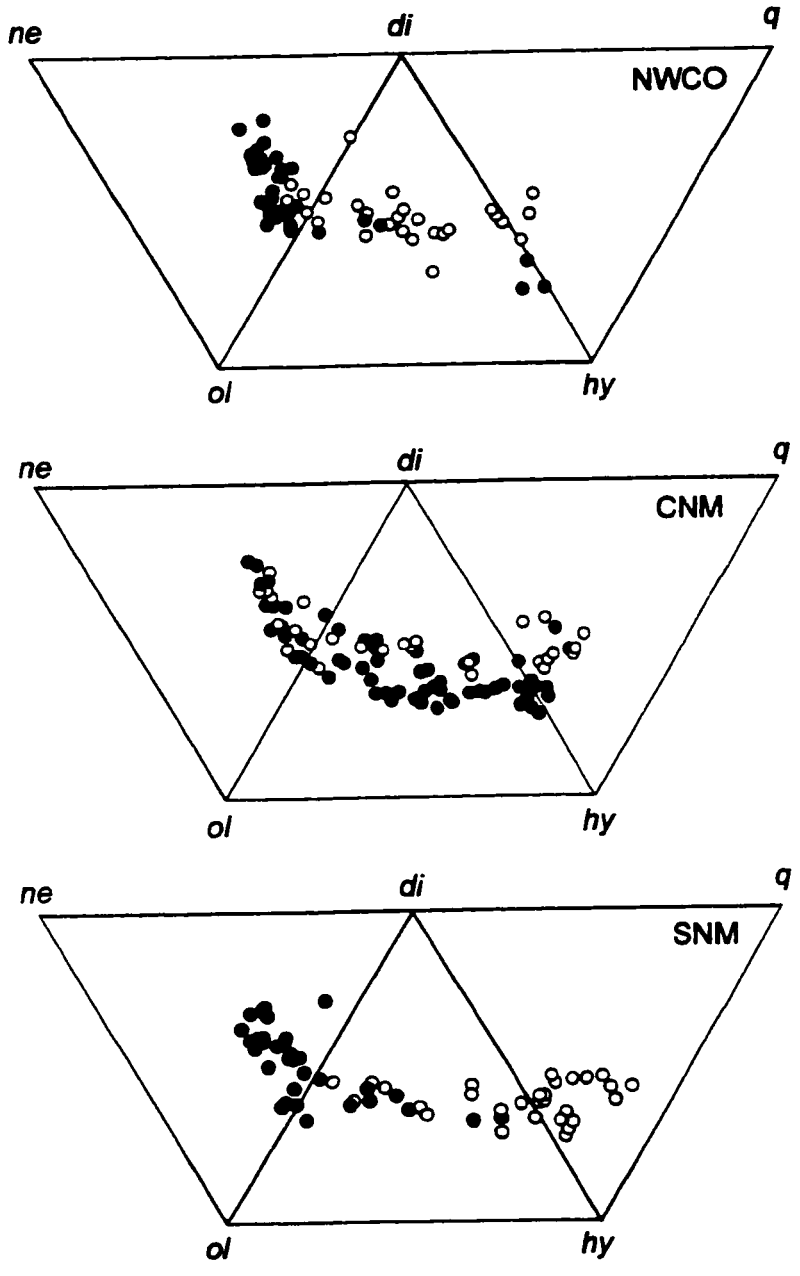

Fig. 5.2 Variations in normative composition in RGR magmas. Open circles - early rift stage, filled circles - later rift stage. Norms calculated using total Fe/Fe_2O_3=0.15 on samples with MgO > 4.0 wt.%. Data sources are (1) NWCO - Leat et al. (1988a,b, 1989, 1990, 1991), Gibson et al. (1991, 1992), Thompson et al. (1989, 1993), (2) CNM - Duncker et al. (1991), Thompson et al. (1991), Gibson et al. (1992, 1993), Dungan et al. (1986), Phelps et al. (1985), Nielsen and Dungan (1985), (3) SNM - Davis and Hawkesworth (1993, 1994, 1995), McMillan et al. (in prep.), Gibson et al. (1992)

individual samples to potential mantle parental material, or to examine trace element variations within suites of rocks. However, in order to clearly present the range in compositional variation encountered within RGR magmas would require a large number of such plots. Normalized incompatible element patterns for most RGR magmas have overall similar shapes which differ in terms of enrichment or depletion of large-ion-lithophile (LILE), rare earth (REE), and high field strength (HFSE) elements, and element concentrations. For clarity, the following discussion is divided into a description of rare earth element variations throughout the RGR, and an analysis of La/Ba and La/Nb ratios in each rift segment as a reasonable alternative to normalized incompatible element diagrams.

5.5.2.1 Rare earth elements

Fig. 5.3 is a graphical description of the degree of REE enrichment in RGR magmas using Ce/Yb ratios from published analytical data. Typical values for MORB and OIB taken from Sun and McDonough (1989) are also shown for comparison. From north to south, there is a slight decrease in the degree of REE enrichment in both the early and late stage magmas. However, within individual rift segments, the degree of enrichment within the early and late rift stage lavas combined is approximately constant. Data from CNM is highly variable, displaying the greatest range in Ce/Yb of all rift segments. This data suite is biased as it also includes analyses from rift flank and rift shoulder localities, which are more likely to reflect the composition of non-extended lithosphere. These localities would have experienced variable degrees of REE enrichment over time, due to metasomatic infiltration of small-volume melts from the asthenosphere. OIB-like magmas erupted at Yampa (NWCO) have higher Ce/Yb than typical OIB (Sun and McDonough, 1989), whereas lavas from the Española Basin

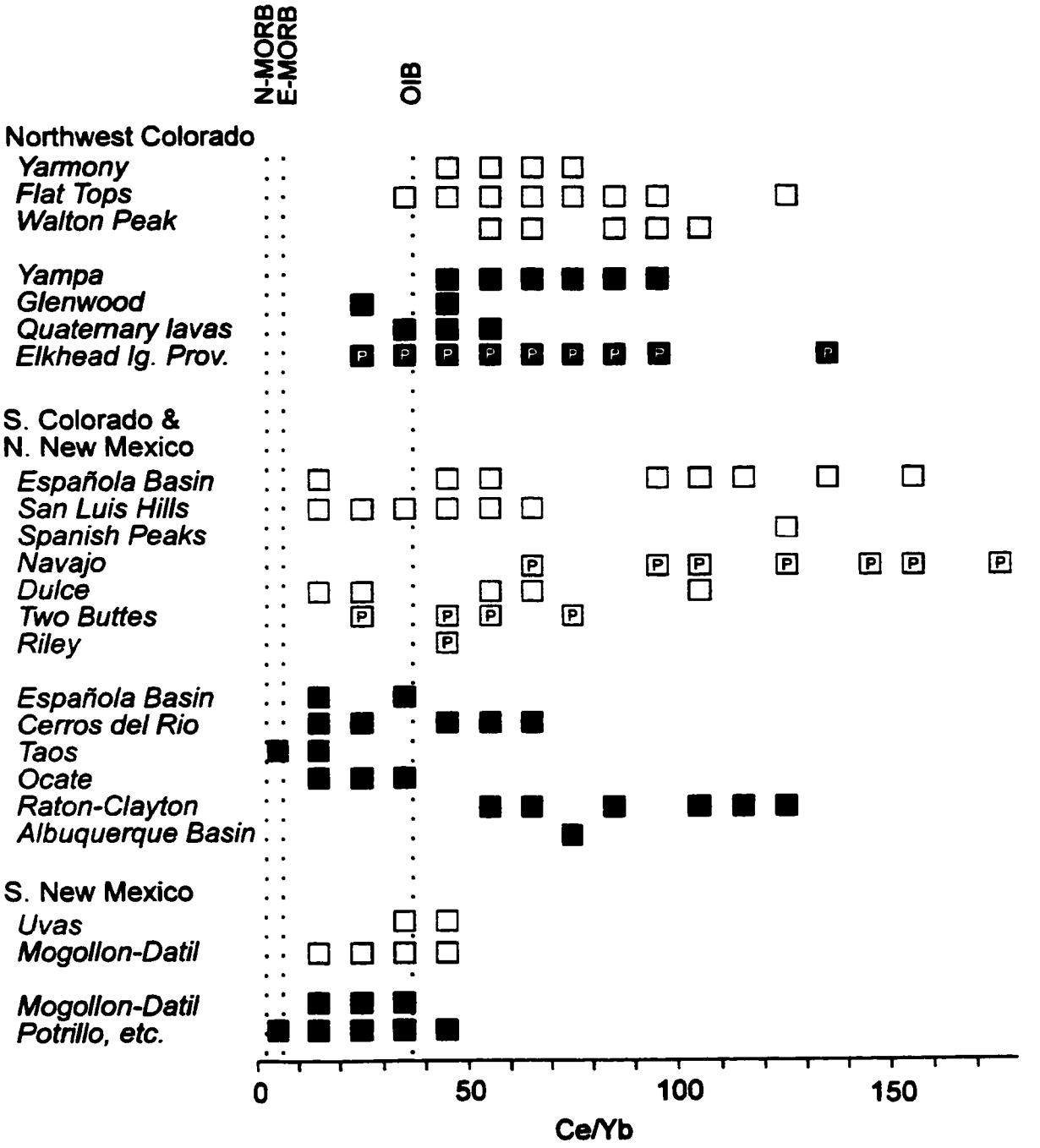

Fig. 5.3 Ce/Yb in RGR magmas, relative to typical MORB and OIB (Sun and McDonough, 1989). This diagram, divided by intervals of Ce/Yb=10, reflects the ranges of REE enrichment encountered at different rift localites, and is not dependent on the number of samples which plot within an interval. Open squares - early rift stage magmas, filled squares - later rift stage magmas. P indicates a potassic composition. Data sources as in Fig. 5.2. Potrillo, etc. includes all rift data other than Mogollon-Datil in southern New Mexico.

(CNM) and scattered localities in southern New Mexico (Potrillo, etc.; SNM) have similar values at or slightly below the OIB value. The enrichment at Yampa may be an effect of advection of asthenosphere beneath NWCO with the mantle volume feeding the Yellowstone plume (Leat et al., 1991). Data from the Taos Volcanic Field (CNM) fall within or just outside the range for depleted mantle (MORB), as expected from previous interpretations (Dungan et al., 1986).

5.5.2.2 La/Nb versus La/Ba

Fitton et al. (1991) have shown that a La/Nb vs.La/Ba diagram is useful for discriminating between those magmas similar to OIB, and those which have been influenced by the lithosphere. This is because all three elements are incompatible in mineral phases predicted to be in equilibrium with basaltic melt. Therefore, the ratios of the elements will reflect source characteristics as they are insensitive to low pressure fractionation, and for the most part the degree of partial melting. As a result of slight differences in the distribution coefficients for La, Nb, and Ba in potential asthenospheric mantle sources, OIB compositions tend to plot within a positively correlated ellipsoid on this type of diagram. Lithospheric sources influenced by episodes of subduction will accumulate Ba and to a lesser degree La, relative to Nb. Therefore, subduction-processed lithospheric sources will plot at relatively high La/Nb and relatively low La/Ba, in the lower right portion of the diagram. This relationship is more applicable to silica undersaturated basalts which tend to have higher concentrations of Nb relative to saturated or oversaturated varieties, and are thus more resistant to crustal contamination.

In Fig. 5.4 La/Nb vs. La/Ba data are plotted for each segment of the RGR relative to the field for OIB, and are further divided according to age; i.e., early versus

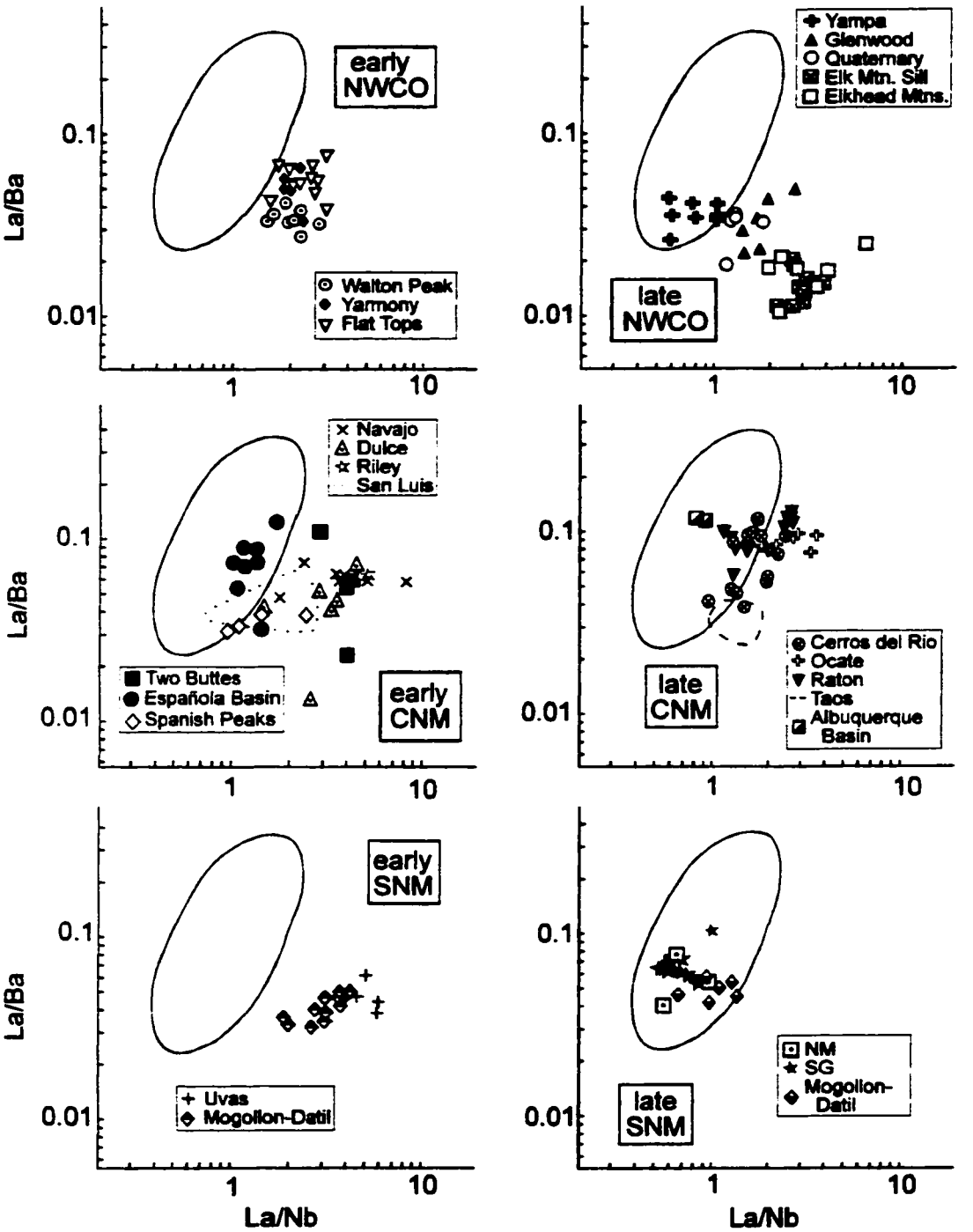

Fig. 5.4 La/Ba vs. La/Nb in RGR magmas. Data are separated in terms of latitudinal segments defined in text, and age. Ellipsoid represents OIB compositions (Fitton et al., 1991). Data sources as in Fig. 5.2. See text for discussion.

late rift activity. For the early rift stage, data from the San Luis Hills and scattered lava flows in the Española Basin plot within the OIB field. This is in keeping with previous conclusions by Johnson and Thompson (1991) and Gibson et al. (1992) regarding the asthenospheric component present in lavas at these localities. Potassic magmas erupted during the early rift stage show considerable scatter on this diagram, but all plot outside the OIB field. It was proposed in Chapter 3 that compositions from Walton Peak in NWCO are also asthenosphere-derived; however, interaction with strongly potassic components in the lithosphere have affected the ratios such that the data points plot just outside the OIB field. All other data from the early rift stage, including SNM are considered lithospheric.

Data for late rift stage localities show an overall increase in the involvement of the asthenosphere in the RGR magmas. In NWCO, samples from Yampa plot within the OIB field, consistent with previous interpretations presented by Leat et al. (1991). With the exception of samples from the Elk Mountain Sill, other data from the Elkheads Igneous Province, and possibly one Quaternary lava, late stage magmas in NWCO originated in the asthenosphere. However, interaction with strongly potassic lithospheric components have shifted the trace element ratios from these localities away from the OIB array towards the Elkheads compositions. In CNM, the data are scattered within and just outside the OIB field. A number of samples from the Cerros del Rio data set (Duncker et al., 1991) and all published samples from Raton-Clayton (Phelps et al., 1985) lack Nb concentration analyses. To estimate the Nb concentrations, I first assumed the Nb-Ta depletion was equal, i.e., on a normalized incompatible element diagram, the Nb-Ta trough would have a flat bottom. Using chondrite normalization factors (e.g. Thompson et al., 1984) and the available Ta data, I back-calculated

approximate Nb values. Accordingly, any conclusions drawn on the position of the Raton-Clayton and Cerros del Rio data on this plot should at best be considered an approximation. Data from Taos trend to lower La/Nb values as a result of crustal contamination. Data from SNM are most coherent and are primarily enclosed by the OIB field. Samples from south of 32° latitude (SNM) discussed by McMillan and co-workers are hereafter referred to as NM, and are distinguished on Fig. 5.4 and succeeding diagrams from those initially discussed by Gibson et al. (1992), hereafter termed SG.

5.5.3 Pb isotopes

Pb isotope analyses were performed using standard ion exchange techniques on approximately 100 samples covering the latitudinal range of the RGR. Analytical details are described in Appendix 1. A complete listing of the newly acquired data is given in Appendix 2, along with references to additional published data sources.

5.5.3.1 Pb isotope variations

Pb isotope data from each segment of the rift are shown in Figs. 5.5 and 5.6 relative to the 4.55 Ga Geochron and the Northern Hemisphere Reference Line defined by Hart (1984) for oceanic basalts. Data for each segment are also divided according to early or late stage rift activity.

NWCO. The Pb isotope systematics of this segment of the RGR are explored in detail in Chapter 3 and are reviewed here. Overall, the data from NWCO straddle the Geochron, with specific localities plotting as elongated fields approximately parallel to the NHRL. Data from the Elkheads Igneous Province also straddle the NHRL on a plot of $^{206}Pb/^{204}Pb$ vs. $^{208}Pb/^{204}Pb$ (Fig. 5.6). Early rift stage data generally plot to the left of the Geochron, with the exception of samples that have experienced crustal

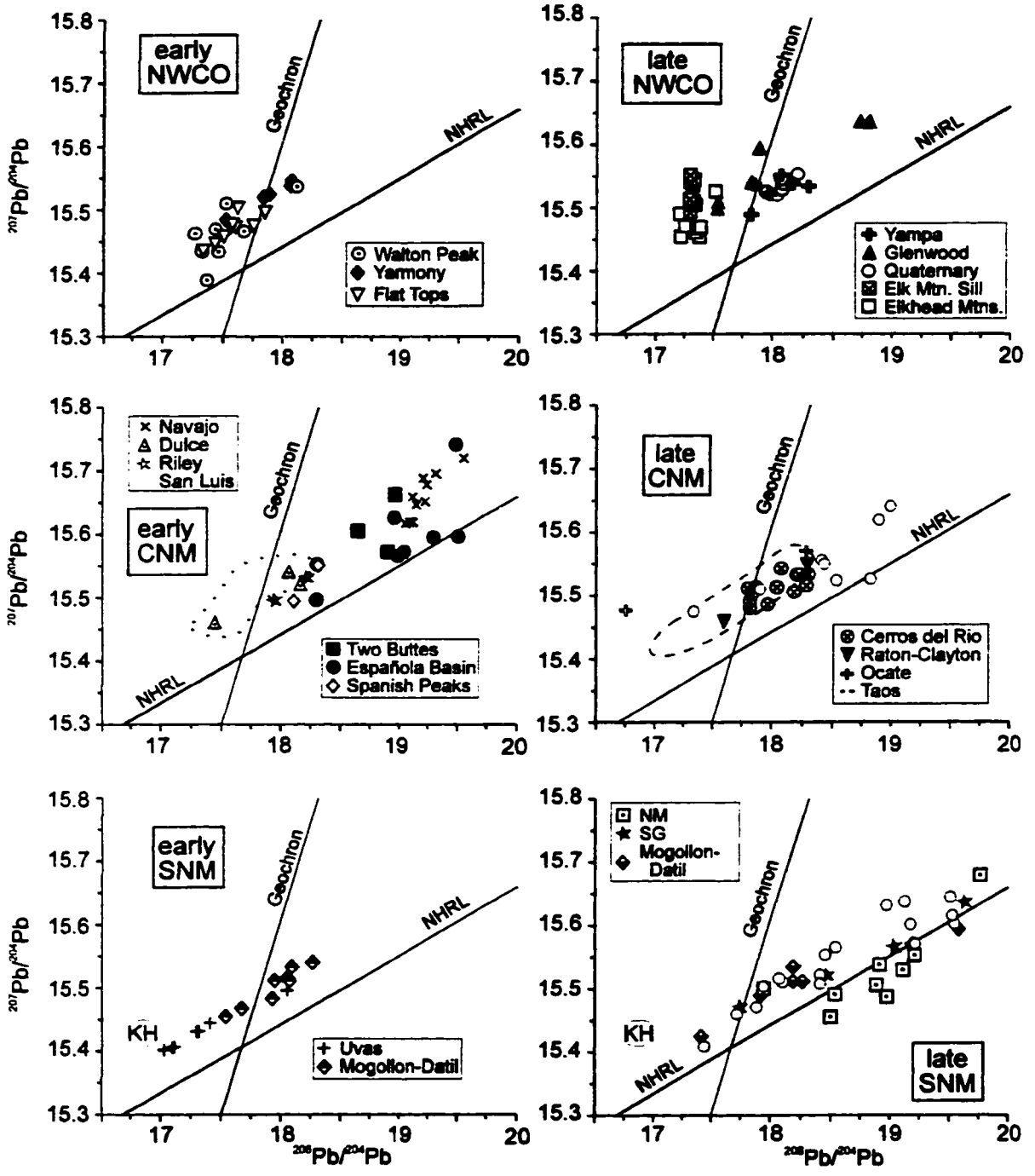

Fig. 5.5 $^{208}Pb/^{204}Pb$ versus $^{207}Pb/^{204}Pb$, relative to the NHRL (Hart, 1984) and the Geochron (Faure, 1986). Data are divided as in Fig. 5.4. KH=Kilbourne Hole in the SNM plots is the representative pelitic paragneiss analyzed by Reid et al. (1989). Lightly filled circles in CNM and SNM late stage rift plots represent analyses from Everson (1979). Other data sources given in Fig. 5.2.

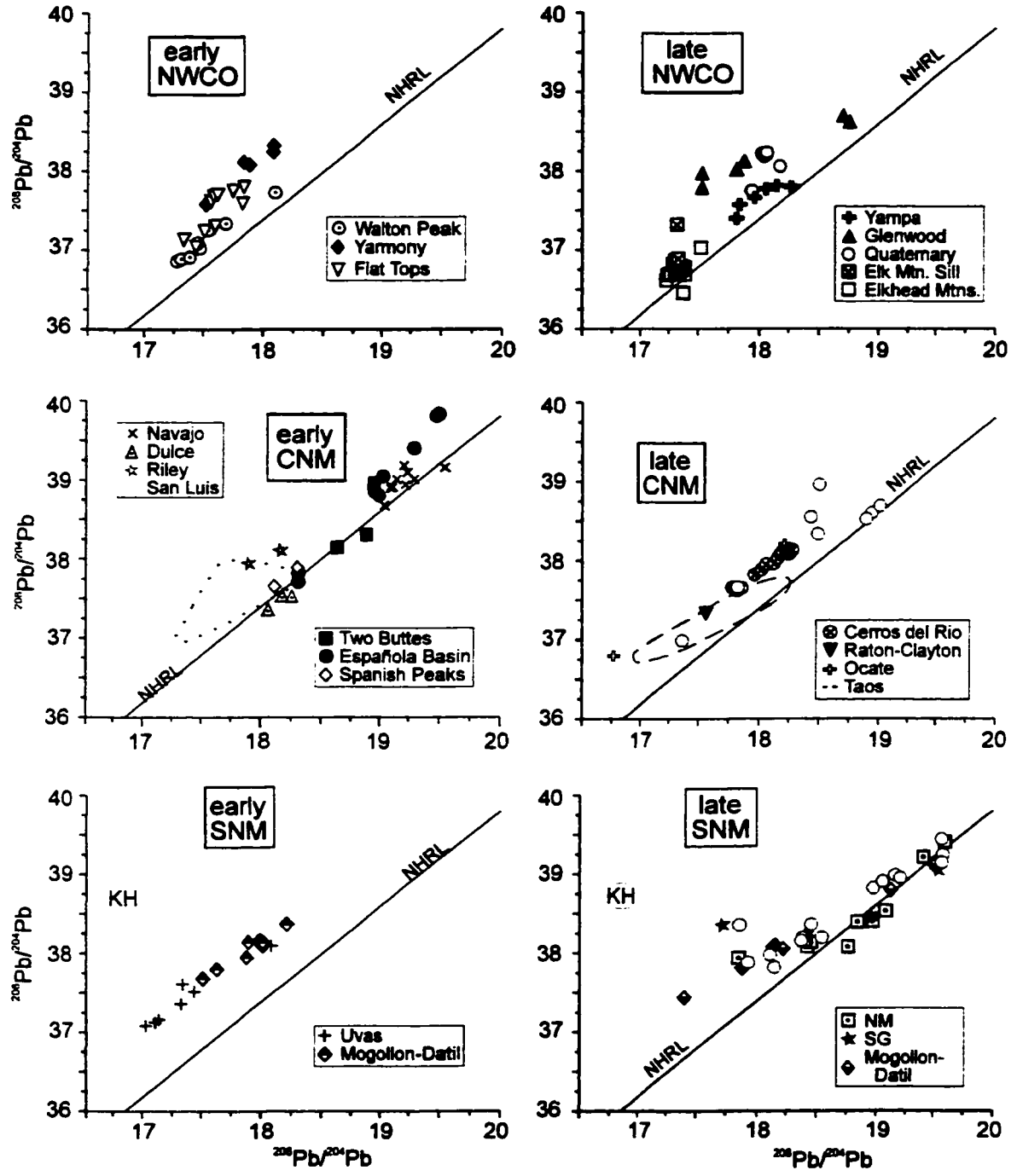

Fig. 5.6 $^{206}Pb/^{204}Pb$ versus $^{208}Pb/^{204}Pb$, relative to the NHRL (Hart, 1984). Data are divided as in Fig. 5.4. The representative pelitic paragneiss analyzed by Reid et al. (1989) is denoted as KH, and is plotted with the SNM data. Analyses from Everson (1979) in CNM and SNM late rift stage plots are shown as lightly filled circles. Other data sources given in Fig. 5.2.

contamination. Samples from Yampa represent an asthenospheric component affected by minor lithospheric contamination that is dominant in late rift stage magmas. Leat et al. (1991) likened the trace element and Sr-Nd isotopic composition of Yampa basalts to those from Loihi, Hawaii. Pb data from Yampa are generally similar to data from Loihi (Staudigel et al., 1984), but with slightly higher $^{207}Pb/^{204}Pb$ at comparable $^{206}Pb/^{204}Pb$. Crustal contamination in the Glenwood Springs data is evident by the trend to more radiogenic Pb (and Sr) values with increasing differentiation. Using Sr isotope data (below), crustal contamination becomes evident for several other sample sets, including Yarmony and the Quaternary lavas. The strongly potassic component found in the Elkheads Igneous Province represents the least radiogenic component of this sample suite. The non-radiogenic character of data from the Elkheads Igneous Province reflects derivation from a relatively old lithospheric source.

CNM. The central segment of the RGR also contains components of variable isotopic composition. Data from the early rift stage plot mostly to the right of the Geochron, and above the NHRL. As in NWCO, the strongly potassic magmas in this rift segment straddle the NHRL in $^{206}Pb/^{204}Pb$ vs. $^{208}Pb/^{204}Pb$ space (Fig. 5.6). Pb isotope ratios in samples from asthenosphere- derived early rift stage lava flows within the Española Basin are similar in composition to basalts from Cape Verde (see Zindler and Hart, 1986), and are considered to be affected by small degrees of upper crustal contamination (Chapter 4). Lithospheric components from both the east and west shoulders (Spanish Peaks; Riley and Dulce) of the RGR generally have less radiogenic Pb values then data from the rift flanks (Two Buttes; Navajo). Data from Riley have $^{208}Pb/^{204}Pb$ ratios comparable to those from Two Buttes. The relationship illustrated by the rift shoulder and flank data may be the result of mixing between radiogenic potassic

components ($^{206}Pb/^{204}Pb > 19$) in the lithosphere with an asthenospheric endmember having a $^{206}Pb/^{204}Pb$ closer to 18.0. In fact, the asthenospheric component identified by Johnson and Thompson (1991) in the 26 Ma San Luis Hills data set has a $^{206}Pb/^{204}Pb$ ratio of c.18.2. However, this postulated asthenospheric component is similar to MORB, and therefore has a $^{207}Pb/^{204}Pb$ value too low ($^{207}Pb/^{204}Pb \sim 15.45$) to act as an appropriate endmember.

In contrast, late rift stage data plot largely above the NHRL, and close to the Geochron, primarily reflecting contamination of all the data sets by a non-radiogenic (lower crustal) component. Individual data points from Everson (1979) plot as high as $^{206}Pb/^{204}Pb = 19.0$. Asthenospheric magmas from the Taos Plateau Volcanic Field have Pb isotope values comparable to mid-ocean ridge basalt, and have been interpreted as having undergone lower crustal contamination (Dungan et al., 1986). Components of the Cerros del Rio Volcanic Field are modeled as having experienced contamination by lower crust and possibly non-radiogenic upper crust. Housh et al. (1991a,b; 1992) explain the isotopic variation encountered at the Ocate and Raton-Clayton Volcanic Fields as resulting from mixing between an enriched lithospheric component and non-radiogenic lower crust. Housh et al. (1991a; 1992) suggest the trend produced by the Taos Plateau volcanics is also the result of this mixing scenario and further that there is no evidence for the involvement of a depleted mantle component. However, one could argue against this interpretation, as the mafic components from the Taos Plateau field are tholeiitic basalts with La/Sm values < 4.5, Sr concentrations c. 350 ppm (Dungan et al., 1986), and Pb concentrations probably no greater than 3 ppm. This implies that small degrees of contamination by crustal components with higher Nd, Sr, and Pb concentrations could easily alter the isotopic signature of these magmas,

thereby masking the depleted mantle component signature. In addition, the normalized incompatible element patterns of the least evolved Taos compositions are MORB-like (Dungan et al., 1986).

SNM. Similar to the central and northern segments of the RGR, Pb isotope data for localities in the southern segment plot to the left and right of the Geochron. The majority of early rift stage magmas from the Uvas and Mogollon-Datil Volcanic Fields lie along a trend parallel to the NHRL. Davis and Hawkesworth (1995) argue that the Pb isotope ratios in the Mogollon-Datil lavas maintain their lithospheric mantle source signature and are not the result of crustal contamination. These lavas may also contain a small asthenospheric component. In contrast, McMillan et al. (1992; in prep.) argue for lower crustal contamination of lithosphere- derived magmas to explain some of the Pb isotope variation in the Uvas data set.

Late rift stage magmas in SNM are interpreted as being derived primarily from the asthenosphere (Gibson et al., 1992; Davis and Hawkesworth, 1995; McMillan et al., in prep.). The variation in Pb isotopes in these lavas is more extensive than in any asthenospheric data from other segments of the rift. Data from Everson (1979) encompasses the range of newly aquired Pb data. NM samples plot below or only slightly above the NHRL and are isotopically similar to Icelandic basalts (see Zindler and Hart, 1986). SG samples show a similar range in $^{206}Pb/^{204}Pb$ to NM's group. The least radiogenic SG sample may have been contaminated by a lower crustal component isotopically similar to the representative pelitic paragneiss from Kilbourne Hole (Reid et al., 1989). According to Davis and Hawkesworth (1995) the most radiogenic sample in the Mogollon-Datil late rift stage data set has the highest proportion of an asthenospheric component. The less radiogenic members in this suite probably contain

a less radiogenic lithospheric component and may also have experienced small degrees of crustal contamination.

5.5.3.2 Nd-Pb and Sr-Pb isotope variations

Inter-isotope variations in magmas from the different RGR segments are shown in Figs. 5.7 and 5.8. As in the previous Pb isotope diagrams, the data are divided according to rift stage and latitude.

NWCO. Early rift stage magmas in this rift segment plot in a cluster on a $^{143}Nd/^{144}Nd$ vs. $^{206}Pb/^{204}Pb$ diagram, however two separate trends to lower $^{143}Nd/^{144}Nd$ can be discerned. The first trend is within the Walton Peak data, and involves decreasing $^{206}Pb/^{204}Pb$ with decreasing Nd isotope values. This has been interpreted as mixing between parental Walton Peak magmas and strongly potassic components prominently represented by the late rift stage Elkheads Igneous Province data suite (Chapter 3). The second trend, exhibited by Walton Peak and Yamony lavas, shows decreasing $^{143}Nd/^{144}Nd$ with increasing $^{206}Pb/^{204}Pb$, and is considered to be the result of crustal contamination. This hypothesis is confirmed upon examination of the $^{87}Sr/^{86}Sr$ and $^{206}Pb/^{204}Pb$ which are positively correlated for the Yarmony suite, and to a much lesser degree the Walton Peak data.

Late rift stage magmas in NWCO show considerably more scatter than the earlier compositions. Strongly potassic samples from the Elkheads Igneous Province are the least radiogenic component in terms of Sr, Nd, and Pb isotopes. Data from Yampa, reflecting the composition of the asthenosphere, generally have the most enriched isotopic signature in terms of Nd and Pb, with the exception of samples suspected of having been contaminated by radiogenic upper crust. A conspicuous upper crustal contamination trend in this data is defined by samples from the Glenwood

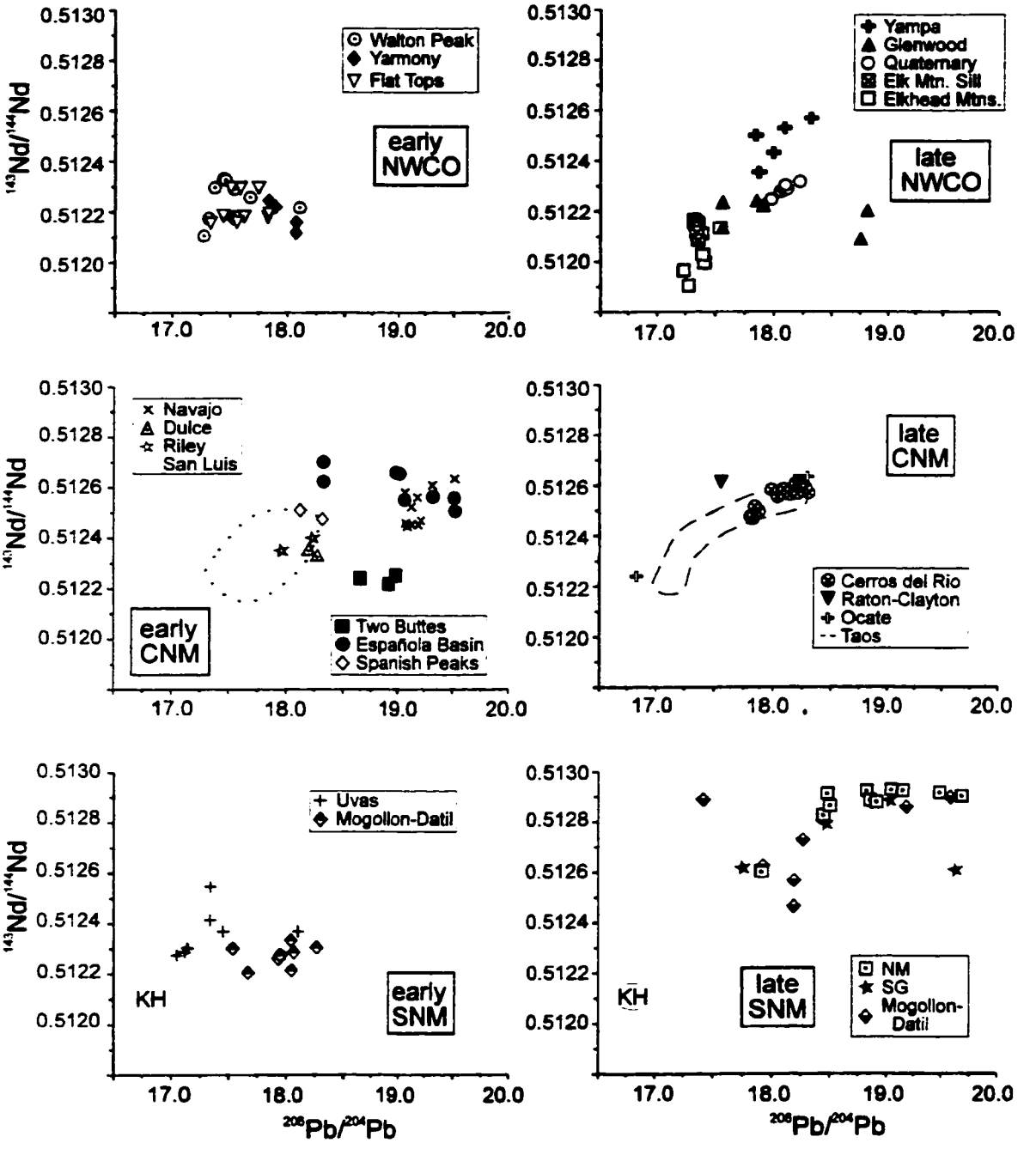

Fig. 5.7 $^{208}Pb/^{204}Pb$ - $^{143}Nd/^{144}Nd$ relationships in RGR compositions. KH is the representative pelitic paragneiss analyzed by Reid et al. (1989). Data sources as in Fig. 5.2.

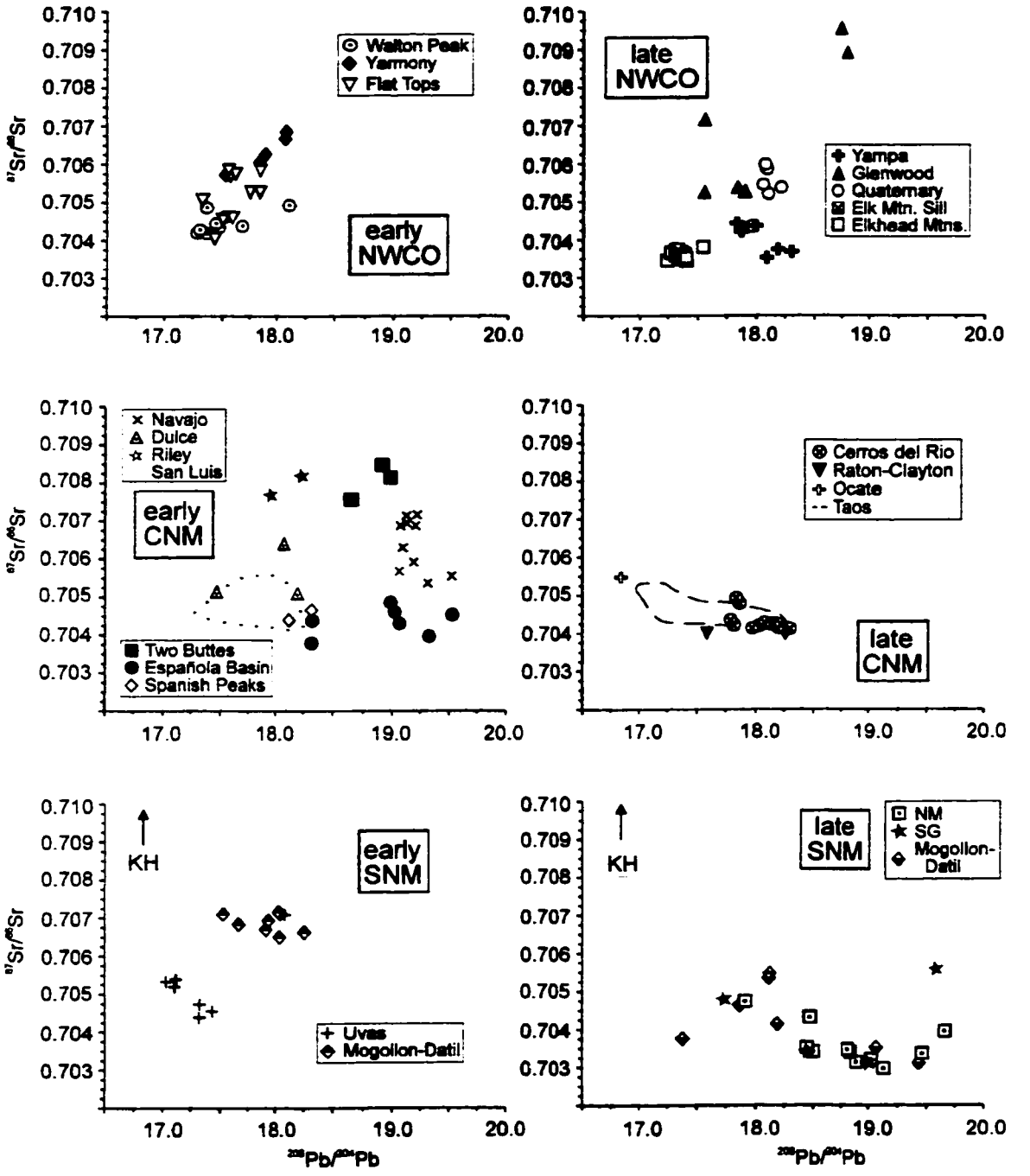

Fig. 5.8 Variation of $^{208}Pb/^{204}Pb$ and $^{87}Sr/^{86}Sr$ in RGR magmas. The representative pelitic paragneiss from Kilbourne Hole (Reid et al., 1989) is denoted as KH. Data sources listed in Fig. 5.2.

Springs suite, which display increasing $^{87}Sr/^{86}Sr$ and decreasing $^{143}Nd/^{144}Nd$ with increasing $^{206}Pb/^{204}Pb$. Samples within the Quaternary suite show a slightly convex, positive correlation on the $^{143}Nd/^{144}Nd$ vs. $^{206}Pb/^{204}Pb$ plot as a result of minor mixing with strongly potassic components with low isotopic Nd and Pb (Chapter 3).

CNM. Within the central rift segment, Sr-Nd-Pb isotope values exhibit much variation. Early rift stage lavas included within the Española data set have high $^{143}Nd/^{144}Nd$ and low $^{87}Sr/^{86}Sr$ coupled with relatively high $^{206}Pb/^{204}Pb$, consistent with their derivation from OIB-like asthenosphere. The potential asthenospheric component recognized in the San Luis Hills data has similar properties ($^{206}Pb/^{204}Pb$ >18.0, $^{143}Nd/^{144}Nd$ ~ 0.5127). Potassic magmas erupted during this rift stage have extremely variable isotopic compositions. Rift shoulder data from Spanish Peaks are isotopically similar to the asthenospheric component identified in the nearby San Luis Hills (Fig. 5.1), whereas data from Riley and Dulce have higher $^{87}Sr/^{86}Sr$ and lower $^{143}Nd/^{144}Nd$ at comparable $^{206}Pb/^{204}Pb$. As noted in Figs. 5.5 and 5.6 rift flank data are more radiogenic in $^{206}Pb/^{204}Pb$ than that from the rift shoulder localities. In addition, data from the Navajo Province have similar $^{143}Nd/^{144}Nd$, but more radiogenic $^{87}Sr/^{86}Sr$ relative to the asthenospheric lavas from the Española Basin. In contrast, $^{87}Sr/^{86}Sr$ isotopes from Two Buttes are comparable to Riley, but with $^{143}Nd/^{144}Nd$ values among the least radiogenic for this rift stage.

Paired isotopic data for samples from the Raton-Clayton and Ocate Volcanic Fields have not yet been published; however the least evolved (or contaminated) samples from these fields tend to have the highest $^{206}Pb/^{204}Pb$ and $^{143}Nd/^{144}Nd$, and lowest $^{87}Sr/^{86}Sr$. The range in isotopic composition at these localities is portrayed in Figs. 5.7 and 5.8 by using symbols representative of the endmembers at each locality. The

overall trend exhibited by magmas erupted during the late rift stage is one of increasing $^{87}Sr/^{86}Sr$ coupled with decreasing $^{143}Nd/^{144}Nd$ and $^{206}Pb/^{204}Pb$. Both the Raton-Clayton and Ocate data have been interpreted by Housh et al. (1991a,b, 1992) as examples of lower crustal contamination of lithosphere-derived melts. Similarly, the isotopic composition of the Cerros del Rio lavas are considered to result from contamination of asthenospheric and lithospheric magmas with lower crust, or possibly non-radiogenic upper crust (Duncker et al., 1991; Chapter 4). Housh et al. consider the Taos Plateau Volcanics to have a lithospheric source. However, based on the arguments presented above, the initial interpretation by Dungan et al (1986) regarding these lavas is preferred; that is derivation from a depleted mantle source followed by lower crustal contamination (and differentiation).

SNM. Early rift stage compositions in the southern rift segment plot in two clusters in $^{87}Sr/^{86}Sr$ vs. $^{206}Pb/^{204}Pb$ space, but form a continuum from relatively non-radiogenic to radiogenic $^{206}Pb/^{204}Pb$ with decreasing $^{143}Nd/^{144}Nd$. In both the Mogollon-Datil and Uvas suites, there is a tendency for the $^{206}Pb/^{204}Pb$ to be negatively correlated with $^{87}Sr/^{86}Sr$, and positively correlated with $^{143}Nd/^{144}Nd$. These trends support the contention by McMillan et al. (in prep.) that the Uvas lavas experienced lower crustal contamination upon ascent from the lithosphere. Also, the correlations uphold the conclusions by Davis and Hawkesworth (1993) that the isotopic composition of the early rift stage lavas result from mixing of 5 - 20% asthenospheric melt with a predominantly lithospheric component.

Pb isotopes within the late rift stage data set form a convex pattern with $^{143}Nd/^{144}Nd$ and a concave pattern with $^{87}Sr/^{86}Sr$. These patterns could be a reflection of the effects of both upper and lower crustal contamination in the Mogollon-Datil, NM, and

SG suites. However, Davis and Hawkesworth (1995) have found that mixing between an asthenospheric component and a lithospheric component isotopically similar to early rift stage Mogollon-Datil lavas satisfactorily accounts for the observed isotopic and trace element variations.

5.5.4 Pb isotope transects

In order to assess the variation of Pb isotopes with latitude, $^{206}Pb/^{204}Pb$ data from each rift segment that represent predominant lithospheric or asthenospheric components are plotted (Fig. 5.9a,b). The RGR developed within Proterozoic terranes which decrease in age from north to south (Fig. 5.1). As a comparison, data from mantle derived magmas erupted onto the Archean craton directly to the north of the rift region (Fig. 5.1) are included on Fig. 5.9. Also presented in Fig. 5.9 is a longitudinal transect from ~ 110° - 102° W, using the available Pb isotope data from 36° - 38° latitude (Fig 5.9c)

In Fig. 5.9a, data from predominant lithospheric sources from both major stages of rift activity are shown. Using MgO, Cr, and $^{87}Sr/^{86}Sr$ values as indicators of differentiation and contamination, respectively, the least evolved basaltic samples from each locality have been identified, and are connected with a solid line. Within the early rift stage lithospheric lavas, there is an apparent increase in $^{206}Pb/^{204}Pb$ from north to south between 40° and 34°, south of which $^{206}Pb/^{204}Pb$ shows a marked decrease. Lower Pb ratios are present in the Uvas and Mogollon-Datil basaltic suites, and are interpreted to reflect a strong influence of non-radiogenic (lower) crust on the lavas. One exception this is a sample from Mogollon-Datil, which is considerably more radiogenic than the remaining samples in the suite, and has probably been influenced by upper crust. Potassic magmas erupted during the early rift stage, believed to be derived from

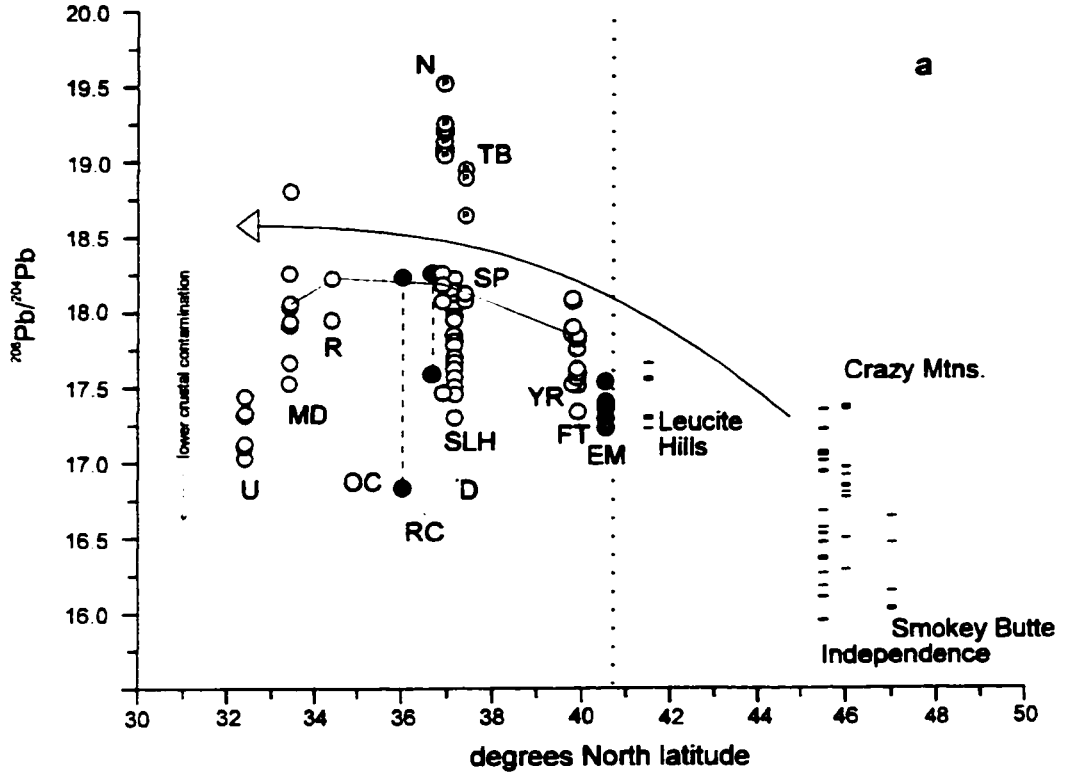

Fig. 5.9 Pb isotope transects. Symbols and locality abbreviations as in previous figures. a) Lithospheric data versus latitude. Included are data from the Archean craton (Fraser et al., 1985/1986; Dudas et al., 1987; Meen and Eggler, 1987). Dotted line marks the position of the Cheyenne Belt, a crustal suture separating the Archean and Proterozoic terranes. Arrow indicates general trend of data. See text for discussion.

complex incompatible-element-rich vein networks in the lithosphere (e.g. Foley, 1992), are considerably more radiogenic than the other lithospheric magmas. Alibert et al. (1986) have interpreted the isotopic signature of the potassic (minette) samples from the Navajo Province as reflecting a component of subducted sediment in their source. In contrast, late rift stage basaltic lithospheric magmas erupted within the central rift segment show little variation in $^{206}Pb/^{204}Pb$. The ranges in isotopic Pb expressed by data from the Ocate and Raton-Clayton fields are indicative of lower crustal contamination. An overall increase in $^{206}Pb/^{204}Pb$ is continuous from the Archean craton (north of ~41°) to southern New Mexico. Gibson et al. (1992) have noted an analogous relationship between $^{143}Nd/^{144}Nd$ and latitude in rift-related lithospheric magmas. The overall increase in $^{206}Pb/^{204}Pb$ from north to south in basaltic components derived from the lithosphere may, in part, be a reflection of the decreasing age of the lithosphere along this transect (Fig. 5.1).

Within asthenosphere-derived magmas (Fig. 5.9b) there is also an slight apparent increase in $^{206}Pb/^{204}Pb$ from within the Archean craton southward into New Mexico. The general scatter displayed by the asthenospheric compositions can be attributed to mantle heterogeneity as well as crustal and/or lithospheric contamination. Gibson et al. (1992) have noted a similar relationship in $^{143}Nd/^{144}Nd$ with latitude for asthenosphere-derived lavas. The apparent increase in $^{143}Nd/^{144}Nd$, and also $^{206}Pb/^{204}Pb$ in the asthenospheric lavas is directly related to the change in the Nd-Pb isotopic character of the lithosphere. In other words, the asthenospheric magmas erupted along the rift have all experienced similar but variable degrees of lithospheric contamination. The resultant isotopic Nd-Pb signatures of the lavas is dependent on the local isotopic character of the lithospheric contaminants.

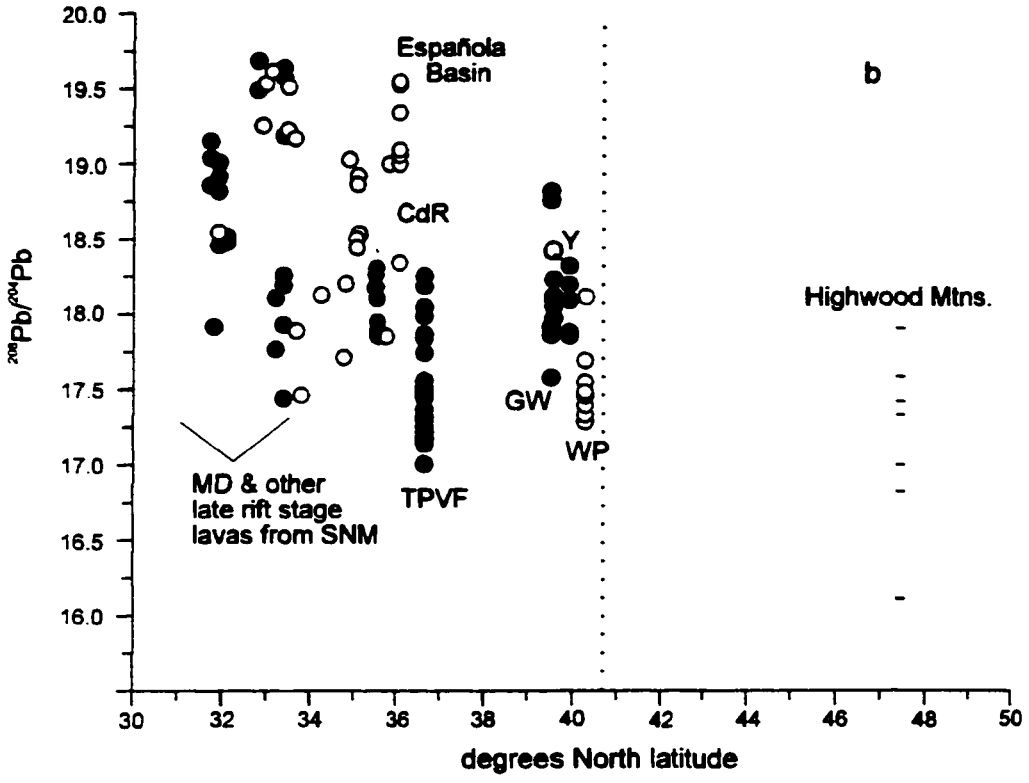

Fig. 5.9 (cont.) b) Asthenospheric data versus latitude. Symbols and abbreviations as in previous diagrams. Highwoods Mtns. data from O'Brien et al. (1995). Lightly filled circles are data from Everson (1979).

A longitudinal transect of the central rift region is shown in Fig. 5.9c. Plotted on the diagram are Pb isotopic data from potassic and basaltic lithospheric magmas erupted in both rift stages. $^{206}Pb/^{204}Pb$ data produce a concave pattern, with decreasing isotopic Pb signatures as the rift axis at ~106° is reached. As noted above, potassic samples (minettes) from the Navajo Province are believed to contain a subducted sediment component (Alibert et al., 1986), which has resulted in radiogenic isotopic Pb ratios. This interpretation may be applied to the data from Two Buttes as well. It is evident from Fig. 5.9a and 5.9c that the two lithospheric components envisaged to have contributed to magmatism in the RGR region have distinct isotopic signatures. The potassic component is radiogenic, with $^{206}Pb/^{204}Pb$ ~ 19.0-19.5, whereas the lithospheric basalt component is signficantly less radiogenic, with $^{206}Pb/^{204}Pb$ ~ 18.2.

5.5.5 Mantle source characteristics: summary

Many authors regard the metasomatic enrichment of the lithosphere beneath the RGR region to be, in part, a direct result of Mesozoic and/or Cenozoic subduction off of the west coast of the United States (e.g., Lipman, 1980; Fitton et al., 1988, 1991). This enrichment would be characterized for example by increases in Rb and Ba, and depletions in Nb, Ta, and Ti, and could potentially maintain characteristics similar to subducted sediments. However, the observed $^{143}Nd/^{144}Nd$ ratios in some lithosphere-derived magmas from the western United States require times of isolation from the convective asthenosphere exceeding 1 Ga (DePaolo, 1988a; Kempton et al., 1991; Gallagher and Hawkesworth, 1992). In order to more clearly establish the geochemical attributes of the mantle sources contributing to RGR magmatism, combined plots of $^{143}Nd/^{144}Nd$ and $^{206}Pb/^{204}Pb$ versus La/Nb (Fig. 5.10) have been constructed. Also, data from subducted Pacific pelagic sediments, which may have influenced the fluid flux from

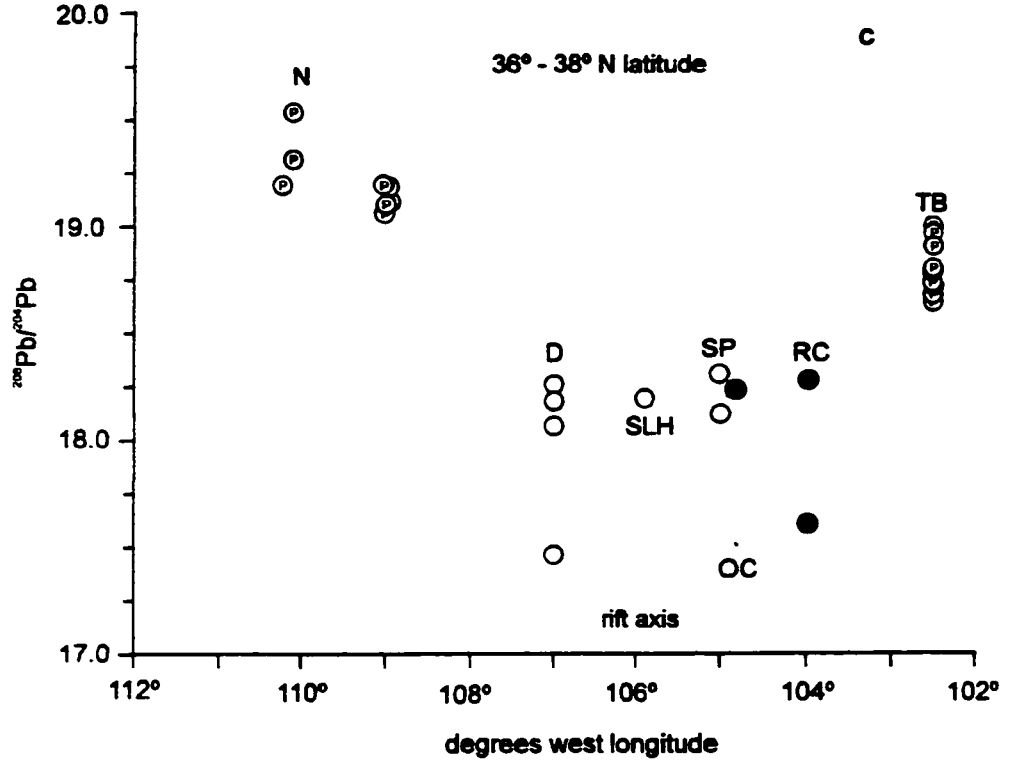

Fig. 5.9 (cont.) c) Longitudinal transect of lithospheric data from the central rift region. Potassic compositions from the rift flanks are more radiogenic than basaltic compositions from the rift axis.

the slab, are used as a proxy for the more recent subduction-related source.

In Fig. 5.10, the majority of data seen on previous diagrams is plotted, emphasizing data sets that most clearly represent asthenospheric or lithospheric sources. As noted above, there is an increase in $^{143}Nd/^{144}Nd$ and $^{206}Pb/^{204}Pb$ ratios from north to south among compositions representing the asthenosphere. La/Nb ratios in all of these magmas generally do not exceed 1.5.

In contrast, there is a large spread of data among the lithospheric data sets. The only clear evidence for an ancient component in these magmas is in the Elkheads Igneous Province data set in NWCO. The Elkheads data show a steady decrease in $^{143}Nd/^{144}Nd$ with increasing La/Nb, with $^{206}Pb/^{204}Pb$ remaining virtually constant. These trends are consistent with mixing of an old lithospheric component, similar to that found at Leucite Hills (Vollmer et al., 1984; O'Brien et al., 1995), with partial melts from the asthenosphere (Leat et al., 1988a). The $^{143}Nd/^{144}Nd$ ratios in the Flat Tops data set are similar to those of recent pelagic sediments, however, the $^{206}Pb/^{204}Pb$ of the magmas are considerably lower.

Within the CNM data, the rift flank data from the Navajo Province and Two Buttes display variations similar to pelagic sediments. The relationship between the remaining lithospheric data suites and an ancient versus recent metasomatizing agent/event are less clear. Although magmas from Cerro del Rio, the San Luis Hills, Riley, Dulce, and Spanish Peaks have $^{143}Nd/^{144}Nd$ vs. La/Nb variations indicative of recent subduction influence, their $^{206}Pb/^{204}Pb$ are lower than expected. Likewise, in SNM, the lithospheric component found with the Mogollon-Datil Volcanic Field and the Uvas suite have lower $^{206}Pb/^{204}Pb$ than required for a recent subduction affect.

The lack of correspondence between the RGR lithospheric data and

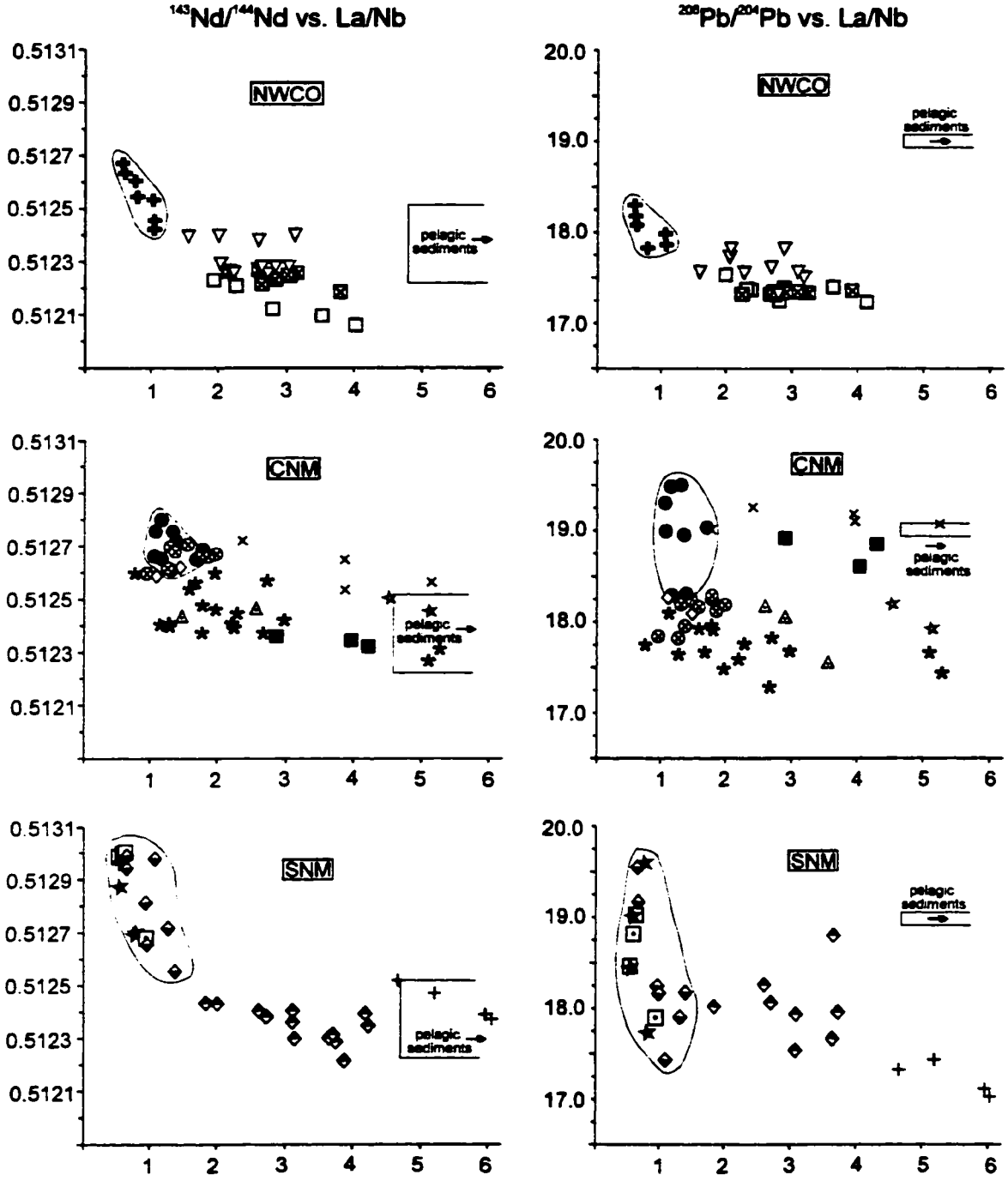

Fig. 5.10 Isotopic Nd and Pb versus La/Nb in representative mantle-derived lavas from the RGR. Asthenospheric compositions are enclosed in fields. Data for pelagic sediments from Sun (1980), Hole et al. (1984), and Goldstein and O'Nions (1981). See text for discussion.

representative compositions of ancient and recent metasomatizing events or agents, respectively, may be the result of several things. First, the assumption that pelagic sediment has, in the past, actively influenced the geochemistry of the fluids released from the subducted slab, may be incorrect. Second, the isotopic composition of the pelagic sediment may not be constant over time. Third, episodes of magmatism prior to rifting may have tapped the more volatile/ancient components within local lithospheric volumes, such that their ability to influence ascending magmas was reduced. Finally, the resultant trace element and isotopic signature exhibited by many of the lithospheric magmas erupted within the RGR region may be the products of mixing between ancient and recent metasomatic components.

5.6 Applicability of extension models

Recently published models that explore petrologic and geochemical changes in magmas produced during continental rifting include those of McKenzie and Bickle ([MB]; 1988), Perry et al. (1987) and Leeman and Harry (1993). We agree with Leeman and Harry (1993) and Harry and Leeman (1995) that the [MB] model is more constructively applied in areas experiencing the advanced stages of extension and which also are underlain by hot, plume-like, asthenosphere. As no convincing evidence for a mantle plume beneath the RGR region is available, we focus on the applicability of the models proposed by Perry et al. and Leeman and Harry to the magmatic history of the RGR.

Perry et al. (1987) have identified two mantle sources within RGR magmas that are generally < 5 Ma. The first source, which they refer to as "depleted mantle" or DM, has a $^{143}Nd/^{144}Nd$ ratio c. 0.5130 (ε_{Nd} ~ +7 to +8). This source is prevalent in magmas erupted in Southern New Mexico. Their second source experienced a history

of lower Sm/Nd relative to DM, and therefore has a $^{143}Nd/^{144}Nd$ ratio closer to 0.5127 (ε_{Nd} ~ 0 to +2.2); this source is called "enriched mantle" or EM. Perry et al. propose that the evolution of RGR magma sources proceeds as follows. Prior to extension (stage 1), EM resides within the lithosphere and DM represents the convecting asthenosphere. Following the initiation of rifting (stage 2), the rheological boundary separating the lithosphere and asthenosphere rises to the base of the crust, and EM begins to erode. At this point, EM behaves as asthenosphere but still retains its "enriched" geochemical signature. At an advanced stage of extension (stage 3), convective mixing has scoured much of the local EM volume and incorporated it into DM as blobs or plums. In this scenario, alkali basalts are progressively tapped from EM-lithosphere (stage 1), EM-asthenosphere or the EM/DM boundary (stage 2), then DM (stage 3). In contrast, Perry et al. consider all tholeiitic magmas to be derived from within EM. This model has been applied by Perry et al. (1988) and Daley and DePaolo (1992) to explain the observed local variation in $^{143}Nd/^{144}Nd$ in mafic rocks from Lucero, New Mexico and near Las Vegas, Nevada, respectively. In a more regional context, the central segment of the RGR, as defined here (CNM), is recognized by Perry et al. as currently experiencing stage 2, i.e., *all* magmas (tholeiites an alkali basalts) have been derived from the EM source. In SNM, the rift has reached stage 3, such that all magmas (alkali basalts) < 5 Ma were derived from DM. Relative to Pb isotopes, the EM source, prominent in CNM, has a $^{206}Pb/^{204}Pb$ ratio of 18.2, whereas the DM source, noted in SNM has a $^{206}Pb/^{204}Pb$ c. 19.0.

Perry et al. (1987) do not use incompatible trace elements to characterize their mantle sources, but instead rely on Nd, and to a lesser extent, Sr isotopes. While we agree with the assertion that crustal contamination has not greatly affected most of

Perry et al.'s data set, we do not support the contention that all individual magmas were derived exclusively from EM, DM, or the EM/DM boundary during specific stages of rift evolution, and that these sources can be distinguished solely using $^{143}Nd/^{144}Nd$ ratios. For example, Leat et al. (1991) and Thompson et al. (1993) have demonstrated the effects on Sr-Nd isotopes and incompatible trace elements by mixing of OIB-like asthenosphere and potassic lithospheric sources. Magmas from Walton Peak and Yampa are believed to have originated in the asthenosphere during early and late rift activity (Chapter 3), respectively. According to the Perry et al. model, the NWCO volcanics should be tapped from sources established within stage 2, or possibly a transition from stage 1 to stage 2. The magmas erupted at Walton Peak (23 Ma) and Yampa (7 Ma) have $^{143}Nd/^{144}Nd$ ratios indicative of EM, therefore they should also display incompatible trace element variations reflecting long-term isolation from the asthenosphere. In other words, the metasomatism which resulted in light REE enrichment (low Sm/Nd) invariably must have affected other trace elements as well. As noted earlier, this metasomatism commonly produces subduction-related geochemical attributes (e.g., Fitton et al., 1991). However, the incompatible trace element variations exhibited by the Yampa and Walton Peak magmas are primarily OIB-like, and are convincingly modeled as mixtures of OIB and potassic components within the NWCO lithosphere. These mixing models are also supported by the available Pb data (Chapter 3).

Work by Gibson et al. (1992, 1993) on early rift stage mafic lavas from the Española Basin (CNM; Fig. 5.1) also reveals a discrepancy in the Perry et al. (1987) model. Gibson et al. have shown that asthenosphere-derived, OIB-type magmas were erupted as early as c. 22 Ma in CNM (Perry et al.'s northern rift). Similar to the Walton

Peak and Yampa magmas described above, the Española Basin mafic lavas have $^{143}Nd/^{144}Nd$ indicative of EM , which may be the result of mixing with a low $^{143}Nd/^{144}Nd$ component in the lithosphere (Gibson et al., 1993). However, Perry et al. (1987) stress that CNM is at stage 2 in their extension model. Alternatively, we would argue that given the eruption of OIB-like asthenospheric magmas in both CNM and NWCO during the early rift stage, stage 3 of Perry et al. had been achieved by c. 25 Ma. The variations in $^{143}Nd/^{144}Nd$ (and $^{206}Pb/^{204}Pb$) can be explained by invoking contamination by local lithosphere, as discussed in section 5.5.4. Perry et al. (1988) suggest the time lag between thermal conversion of EM to its replacement by DM is approximately 10 Ma. If so, this indicates that rifting began earlier than previously believed in NWCO and CNM. Because little petrologic work has been done in the southern segment of the rift, we are unable at this time to apply this proposed model to SNM.

Although we disagree with some aspects of the extension model of Perry et al. (1987), it does provide a framework in which changes to the subcontinental lithosphere during rifting can be viewed. If we are correct in our proposal that the RGR achieved stage 3 of Perry et al. earlier that previously thought, evidence of extensional activity must be identified. Previous estimates of the onset of rifting were based on the simultaneous occurrence of basaltic volcanism and subsidence (e.g. Lipman and Mehnert, 1975). However, Leeman and Harry (1993) and Harry and Leeman (1995) argue that the first indications of extension in the Great Basin region of the Basin and Range Province, i.e., listric normal faults, are accompanied by large volume silicic to intermediate magmatism and minor contemporaneous mafic volcanics. This magmatic/extensional episode is considered to have initiated by partial melting of basaltic components in the lithosphere, and would take place in stage 2 of Perry et al.

(1987). Upwelling of the asthenosphere provides heat to melt the basaltic components within the lithosphere, thereby promoting anatexis. Applying this reasoning to the RGR region, evidence for extensive silicic to intermediate volcanism and rare mafic lavas is found in a large region of Colorado, and also in southern New Mexico. In Colorado, Steven (1975) describes an extensive mid-Tertiary volcanic field, with source regions in the San Juan Mountains (35 Ma), Thirty Nine Mile Volcanic Field (35-36 Ma), Elk and West Elk Mountains (34 Ma), and the Colorado Mineral Belt (39 Ma). Intermediate and silicic activity took place at the Ortiz, Cerrillos, and Espinaso volcanic centers in northern New Mexico (Kautz et al., 1981). In southern New Mexico, extensive outpourings of silicic and intermediate volcanics occurred in and around the Mogollon-Datil Volcanic Field, e.g. Rubio Peak Formation (35-40 Ma; Davis and Hawkesworth, 1994; McMillan et al, in prep.). Yet, published observations describe the initiation of faulting to be c. 28 Ma (Lipman and Mehnert, 1975); it should be noted that this estimate is based also on the appearance of *basaltic* lavas, as opposed to more siliceous compositions. The primary extension directions in the Basin and Range and RGR regions at this time was NE - SW.

Harry and Leeman (1995) note that mafic lavas older than 15 Ma are quite rare in the Great Basin region. In contrast, basaltic volcanism is widespread during the early phases of rifting in the Rio Grande region. It was noted earlier that the RGR is located along the axis of the Alvarado Ridge (section 5.4; Eaton, 1987). This ridge is coincident with a region that had previously undergone deformation and igneous activity during Laramide times (Lipman and Mehnert, 1975). It is plausible that basaltic lavas were more voluminous in the early history of the RGR because they could ascend to the surface along reactivated fault planes. Also, previous episodes of magmatism helped to remove fusible components in the lithosphere which might impede or contaminate

ascending basaltic magmas (Gibson et al., 1993).

The extension model of Leeman and Harry (1993) predicts that for lithosphere with an initial thickness of 125 km, the rate of melt production in the lithosphere will peak within the first 10-20 Ma, then decrease rapidly. For thinner lithosphere, the rate of melt production decreases almost immediately after the onset of extension. If it is assumed that the initial lithospheric thickness of the RGR prior to extension was ~100 km, then the latter scenario applies. A decrease in melt production would be accompanied by a decrease in volcanism related to anatexis. An apparent lull in volcanism would thus take place as the rift region underwent a transition from Perry et al.'s stage 2 to stage 3. A lull in activity is noted in both the Basin and Range from 20 - 17 Ma, and in the RGR region, from 18 - 13 Ma. Relative to Perry et al.'s model, a large volume of the SCLM (EM) has been eroded and entrained within the convecting asthenosphere (DM). The DM/asthenosphere is now in close proximity to the base of the crust, and within the depth range for equilibration of alkali basalt melts with mantle mineral assemblages (Takahashi and Kushiro, 1983). Upwelling asthenosphere also provides heat to induce partial melting of the substantially thinned EM lithosphere. Following the lull in activity in both regions, rifting and volcanism increased in intensity. Magmatism produced basaltic/bimodal assemblages, faulting produced horst and graben structures, and the primary extension direction had changed to E - W.

This combined version of the models proposed by Perry et al. (1987) and Leeman and Harry (1993) can also explain the trace element and isotopic variations exhibited by RGR mafic volcanics. In NWCO, early rift stage activity yielded partial melts of EM lithosphere which erupted at the Flat Tops and Yarmony volcanic centers. Asthenospheric melts mixed with potassic components in the EM lithosphere, producing

lava flows at Walton Peak. $^{206}Pb/^{204}Pb$ ratios in the least evolved samples from each of these localities is < 18.0 (Fig. 5.9a). Late rift stage magmas erupted at scattered localities in the Quaternary, and earlier at Yampa, and Glenwood were primarily derived from the asthenosphere, generally with $^{206}Pb/^{204}Pb$ values of ~18.2 (Fig. 5.9b). Crustal contamination and interaction with the ancient potassic component acted to increase or decrease the Pb isotopic ratios, respectively at these localities. This potassic component is best represented by minettes from the Elkheads Igneous Province, with $^{206}Pb/^{204}Pb$ ratios c. 17.4. The $^{143}Nd/^{144}Nd$ ratios of the early and late rift stage asthenosphere-derived magmas are depressed (0.5122 - 0.5126; Fig. 5.7) relative to the ratio defined by Perry et al. (1987) for DM asthenosphere (0.5130). As modeled by Leat et al. (1991), this discrepancy is easily explained by invoking mixing with the lithospheric minette component within the Elkheads Igneous Province that has a $^{143}Nd/^{144}Nd$ closer to 0.5121.

In the central rift segment, early rift stage activity produced lavas at the San Luis Hills and within the Española Basin. The majority of lavas erupted at the San Luis Hills were derived from basaltic EM lithosphere, with $^{143}Nd/^{144}Nd$ ratios close to 0.5125, and $^{206}Pb/^{204}Pb$ near 18.2 (Fig. 5.7). The isotopic signature of a minor DM asthenospheric component (with $^{143}Nd/^{144}Nd$ ~0.513 and $^{206}Pb/^{204}Pb$ ~ 19.0) present in some of the San Luis Hills lavas has been masked by the EM lithospheric contribution. Over- and undersaturated lavas in the Española Basin have similar $^{143}Nd/^{144}Nd$ near 0.5127. However, the oversaturated lavas have $^{206}Pb/^{204}Pb$ of 18.3, which is less than the undersaturated lava average of 19.2. As noted above, Gibson et al (1992, 1993) have argued that the Española Basin lavas are asthenosphere-derived, and that some of the undersaturated lavas with elevated $^{87}Sr/^{86}Sr$ have been contaminated by

radiogenic crust. In order to place these lavas within the context of Perry et al.'s model, we suggest that these magmas originated as partial melts from a volume of DM that had subsequently mixed with a small proportion of lithospheric EM (Chapter 4), similar to the petrogenesis of the Yampa magmas in NWCO. The EM component is isotopically similar to that erupted in the San Luis Hills, and would result in a $^{206}Pb/^{204}Pb$ close to 18.2. Thus, this initial mixing event would act to decrease both Nd and Pb isotope ratios. We believe that the process which subsequently resulted in elevated $^{87}Sr/^{86}Sr$ in the Española Basin undersaturated lavas also caused a shift in their Pb isotope ratios to more radiogenic values and a potentially a further decrease in $^{143}Nd/^{144}Nd$ (Figs. 5.7, 5.8).

Other lithospheric magmas were erupted during this time period on the shoulders and flanks of the central rift segment. Potassic magmas from the Navajo Province and Two Buttes, representing components of non-extended EM lithosphere, have $^{143}Nd/^{144}Nd$ between ~0.5123 and ~0.5126 (Fig. 5.7), and isotopic Pb ratios close approaching those for Pacific sediments (~19.0; Sun, 1980). These observations, in concert with the trace element-isotope relationships discussed in Fig. 5.10, imply that a recent metasomatic event has influenced the geochemistry of the potassic magma source at these localities. Samples analyzed here that were erupted at Dulce and Spanish Peaks have been interpreted by Gibson et al. (1993) to be mixtures of potassic and basaltic lithospheric components. These lavas have $^{206}Pb/^{204}Pb$ ratios close to 18.2, analogous to the EM lithosphere tapped at the San Luis Hills. Potassic magmas from Riley have Nd and Pb signatures comparable to Dulce, but with higher $^{208}Pb/^{204}Pb$ at a given $^{206}Pb/^{204}Pb$ ratio, indicating that the Pb isotopic character of lithospheric components changes with latitude.

Within the CNM segment, late rift stage activity produced magmas at the Cerros del Rio, Raton-Clayton, Ocate, and Taos Plateau volcanic fields. The least evolved components in all of these groups have similar $^{206}Pb/^{204}Pb$ of 18.3. This suggests that all were derived from an EM lithospheric source. However, it was remarked above (section 5.5.3.1) that there is a substantial body of evidence to suggest that the Taos Plateau magmas are MORB-like (DM), and were influenced by lower crust during their ascent to the surface. The Cerros del Rio lavas have trace element ratios and isotopic signatures very similar to the earlier erupted lavas in the Española Basin. In Chapter 4 it was suggested that both the saturated and undersaturated components of the Cerros field originated within the convecting DM asthenosphere. Both of these components are suspected of being contaminated (e.g. Duncker et al., 1991). Further, it was proposed that, like the early Española Basin magmas, the Cerros del Rio magmas mixed with a minor proportion of EM lithosphere prior to ascent. $^{87}Sr/^{86}Sr$ data for the tholeiites also require a small amount of contamination by a relatively non-radiogenic component. Undersaturated Cerros magmas also interacted with EM lithosphere, resulting in reductions of $^{143}Nd/^{144}Nd$ ratios to ~0.5126 (Chapter 4).

SNM early rift stage volcanics are interpreted to be lithosphere-derived. We commented above that there is a distinct lack of petrologic information available from the southern rift segment, thus it may be difficult to tie in the combined rift evolution model described above. The least evolved lavas in the Mogollon-Datil volcanics have an EM $^{206}Pb/^{204}Pb$ lithospheric signature of 18.2, whereas $^{206}Pb/^{204}Pb$ in the Uvas suite is closer to 17.3. It is likely that this isotopic signature does not represents a true source value, but rather extensive contamination by lower crust. Presently available data do not indicate the presence of an asthenospheric component in this rift segment during early

rift activity. However, convecting DM asthenosphere must have been present to act as a heat source to induce melting in the EM lithosphere, and its signature may be masked by high degrees of crustal and/or lithospheric contamination.

Late rift stage magmas in the southern rift are, by contrast, dominated by a DM asthenospheric component. The least evolved lavas in the Mogollon-Datil volcanics and the NM, SG rock suites all have values close to 19.2. Deviations from this value can be explained by variable amounts of crustal contamination. This is supported by variations in Sr-Nd-Pb isotopes. Future work in the southern rift segment will help to establish whether or not the proposed extension model is valid.

Chapter 6: Radiogenic isotopic evidence for mantle derivation of monzonites from the Colorado Mineral Belt

6.1 Abstract

A group of monzonite intrusions of early Tertiary age emplaced near Central City, Colorado, in the northern Colorado Mineral Belt, have geochemical characteristics that imply differentiation from mantle-derived magmas. Trace element data together with Sr, Nd and Pb isotopic compositions suggest that the monzonite parental magmas resulted from mixing of partial melts from the convecting asthenosphere with potassic melts from the sub-continental lithosphere. Differentiation of the magmas took place at depth, allowing the Sr concentrations in the monzonites to approach 2500 ppm. Following ascent to upper crustal levels, the monzonite magmas were contaminated by partial melts of upper crust, producing radiogenic Sr and Pb isotopic signatures, and elevated $\delta^{18}O$. As such, a major role for lower crust in either the origin or subsequent contamination of the monzonite magmas is not supported.

6.2 Introduction

The Colorado Mineral Belt (CMB) is a northeast-trending zone characterized by Late Cretaceous-Tertiary ore deposits and intrusions (Tweto and Sims, 1963; Stein and Crock, 1990) and is contained within the Colorado Lineament (Fig. 6.1). A system of Precambrian shear zones associated with the Colorado Lineament traverses the CMB (Warner, 1978), and is thought to have played an active part in its origin. Leake (1990) emphasizes this hypothesis by stating that major crustal lineaments play a major role in controlling the emplacement of granitoid intrusions. Tweto and Sims (1963)

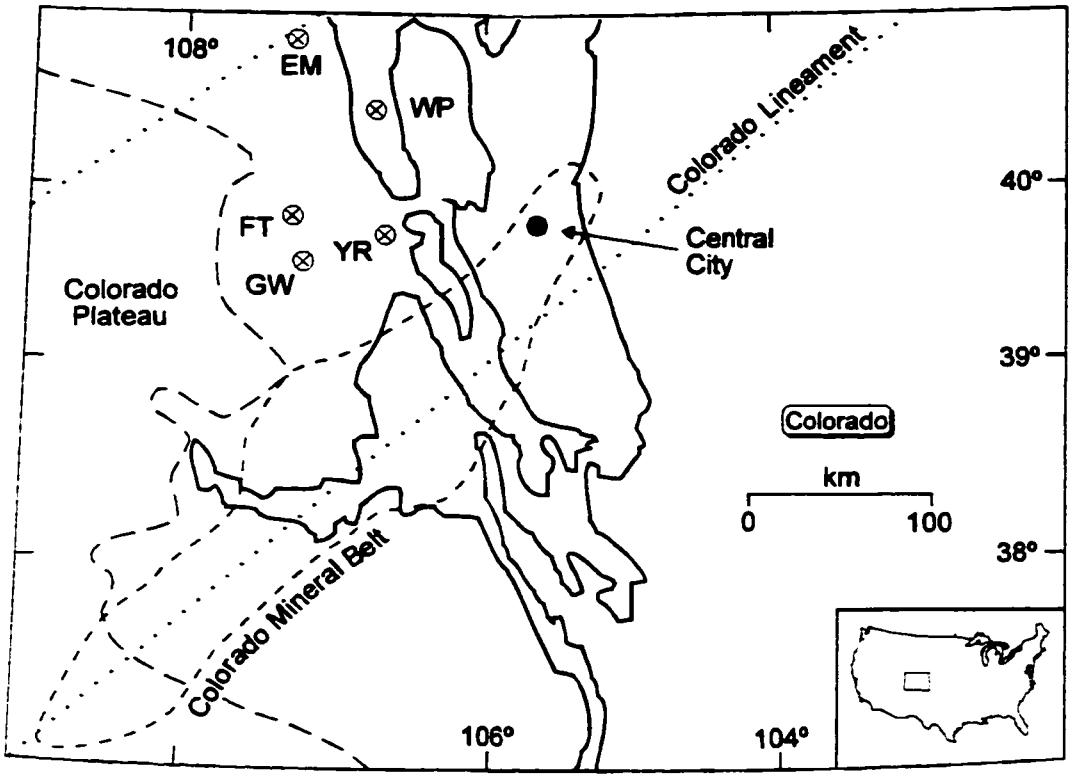

Fig. 6.1 Location map showing geographic relationships of Central City to the Colorado Mineral Belt (shaded), the Colorado Lineament (dotted lines), the Colorado Plateau (dashed line), and Proterozoic uplifts (heavy solid line). Neogene volcanic fields discussed in text are: EM=Elkhead Mountains Igneous Province; FT=Flat Tops; YR=Yarmony; WP=Walton Peak; GW=Glenwood.

suggested that the proximity of intrusions within the CMB together with petrographic similarities between the intrusions and ore deposits indicate that a single body of magma or chain of closely related magmas existed beneath the CMB in Late Cretaceous time. Subsequent work by Simmons and Hedge (1978) indicated that a co-magmatic origin for some of the larger plutons within the CMB is plausible, however, geochemical, mineralogical, and textural evidence from smaller plutons suggests that they are *not* high-level expressions of batholiths. Stein and Crock (1990) have divided the CMB into northern, central, and southern areas, and have classified the granitoids according to age and composition, however, not all CMB intrusions conform to this scheme.

Petrogenesis of CMB granitoids has been discussed by Simmons and Hedge (1978), Musselman and Simmons (1987), and Stein and co-workers (Stein and Fullagar, 1985; Stein et al., 1987; Stein and Crock, 1990). These workers advocate melting of Proterozoic mafic lower crustal source(s) to produce the monzonite component encountered in the CMB. Minor involvement of lithospheric mantle-derived melts was possible, but not required by the available data. Contrastingly, Leat et al. (1988b) have discussed the derivation of silicic magma from a minette parent in the Elkhead Mountains Volcanic Field (Fig. 6.1), c. 150 km northwest of the CMB. The trachydacitic Elk Mountain sill, part of the Elkhead Mountains Igneous Province (Fig. 6.1) contains ca. 10% by volume ellipsoidal minette inclusions. Bulk chemistry as well as Sr, Nd and Pb isotopic composition point strongly to a co-genetic relationship between the trachydacite and minette magmas. Although not located within the CMB, the Elkhead Mountains work by Leat et al. promotes an alternative mechanism for petrogenesis of intermediate composition intrusions of the CMB by showing that differentiation of mantle-derived melt with little involvement of crustal sources has occurred in northern Colorado.

The present work considers the petrogenesis of a group of intermediate composition intrusions near Central City, Colorado, located in the northern CMB (Fig. 6.1). Nd and Pb isotopic data and trace element data are given here along with Sr isotopic data previously reported by Dickin et al. (1986) and trace element data previously published by Rice et al. (1985) which support the potential derivation of the intrusions by fractionation of asthenosphere-derived basalt with potassic components in the lithospheric mantle of Colorado.

6.3 General Geology & Petrology

Intrusions in the Central City area may be classified into a calc-alkaline granodiorite or alkali-rich monzonite suite (Braddock, 1969; Simmons and Hedge, 1978; Rice et al. 1985). Rice et al. (1982) concluded that most intrusions in this area are of early Tertiary age (58-63 Ma). Representative samples from the "monzonite suite" were chosen for this study and include leucocratic monzonite and syenite from Central City, and one hornblende monzonite from the Ward district. Hereafter, they will collectively be referred to as monzonites. Table 6.1 lists available major and trace element data, along with Sr, Nd, and O isotope data for the selected samples. Pb data are listed in Appendix 2. Petrographic descriptions are given by Rice et al. (1985, and references therein).

Basement rocks, which may act as upper crustal contaminants to ascending magmas in the Central City area, consist principally of metavolcanic and meta-sedimentary quartzofeldspathic and biotite gneisses, with minor pegmatite (Sims, 1964; Taylor, 1976; Tweto, 1980). The entire CMB is contained within the Proterozoic Yavapai province (Condie, 1992), which includes the Pb isotopic province Ib of Zartman (1974), and the crustal age province 2 of Bennett and DePaolo (1987).

Table 6.1. Geochemical data for stocks near Central City

Sample#	135	282	296	419	W33	293B
Type[a]	lm	lm	lm	lm	hm	s
Major element oxides (wt. %)						
SiO_2	63.34	63.73	63.44	64.71	59.69	59.95
TiO_2	0.31	0.35	0.43	0.49	0.56	0.57
Al_2O_3	16.99	17.34	17.18	18.39	17.71	17.04
Fe_2O_3	3.94	3.73	4.36	3.03	5.72	4.92
MnO	0.01	0.15	0.17	0.01	0.07	0.24
MgO	0.41	0.84	0.93	0.27	1.73	0.80
CaO	2.69	3.17	3.68	0.97	3.30	3.99
Na_2O	4.87	5.53	5.04	5.42	4.62	5.13
K_2O	3.22	3.30	3.34	5.05	4.24	4.59
P_2O_5	0.17	0.18	0.19	0.12	0.31	0.18
Trace elements (ppm)						
Ba	2220	n.d.	n.d.	2400	n.d.	2530
Rb	58	181	65	61	103	90
Sr	2108	421	2043	2006	1639	4145
Nb	24	27	27	21	24	49
Y	54	44	38	37	51	33
Zr	539	290	593	563	544	285
Ce	149	74.6	144	140	139	300
Nd	62.5	27.1	62.2	59	59.5	115
Sm	10.32	4.61	9.50	9.49	9.96	17.30
Eu	2.66	1.09	2.62	2.49	2.59	4.11
Gd	6.30	n.d.	n.d.	n.d.	4.59	n.d.
Dy	5.17	n.d.	n.d.	n.d.	4.98	n.d.
Er	2.73	n.d.	n.d.	n.d.	2.63	n.d.
Yb	2.75	3.49	4.28	2.70	2.41	3.64
Th	18	n.d.	n.d.	29	n.d.	42
U	6	n.d.	n.d.	4	n.d.	9
Pb	22	n.d.	n.d.	25	n.d.	33
$\delta^{18}O$	9.6	11.7	9.2	9.1	n.d.	7.7
$^{87}Sr/^{86}Sr$	0.70470	0.70611	0.70505	0.70444	0.70570	0.70503
$^{143}Nd/^{144}Nd$	0.512508	0.512391	0.512365	0.512476	0.512341	0.512427

[a] lm=leucocratic monzonite; hm=hornblende monzonite; s=syenite
n.d.=not determined

6.4 Petrogenetic models

The work of Simmons and Hedge (1978), Musselman and Simmons (1987), and Stein and co-workers (Stein and Fullagar, 1985; Stein et al., 1987; Stein and Crock, 1990) represents a comprehensive overview of the geochemical variations within the CMB. Stein (1985) argues for a lower crustal origin for the CMB granitoids on the basis of relatively low Pb isotope ratios. However, this review did not take into account the potential effects of lower crustal or lithospheric contamination of an ascending asthenospheric magma in generating a proportion of the low Pb ratios in the data set. In light of the work by Leat et al. (1988b) on the Elk Mountain Sill, the conclusion by these workers of primary crustal derivation of CMB stocks thus requires more rigorous testing.

Recently published work by Wendlandt et al. (1993) offers insight into the incompatible element and Sr-Nd isotopic character of crustal compositions beneath the Colorado Plateau, located to the immediate west and southwest of the CMB (Fig. 6.1). Lipman (1980) has shown that the Colorado Plateau has remained devoid of large-scale volcanism despite its widespread occurrence throughout the western U.S. In addition, prior to the formation of the CMB, volcanism in the immediate area was negligible for at least 50 Ma (Lipman, 1980). With approximately average crustal thickness and low cratonic heat flow, it is unlikely that the Colorado Plateau has experienced substantial underplating following crustal formation c. 1.8 Ga (Wendlandt et al. 1993). As such, data from xenoliths representative of the unexposed crustal stratigraphy of the Colorado Plateau should provide useful analogs to crustal compositions beneath the CMB prior to magmatic activity there 55-65 Ma.

Eocene magmatism in Montana and Neogene volcanic activity associated with the northern Rio Grande Rift may provide clues to the possible types of mantle

compositions available in the area. Work by O'Brien et al. (1991, 1995) suggests that three source components were involved in the petrogenesis of 50-53 Ma extrusive and intrusive rocks from the Highwood Mountains, Montana: 1) ancient, subcontinental lithosphere, 2) asthenospheric mantle, and 3) a young, subduction-related component, which acted primarily to increase Rb concentrations. Similarly, three distinct mantle sources are thought to have contributed to the diversity of rift-related magma types recognized in Northwest Colorado (NWCO; Chapter 3; Leat et al., 1988a,b, 1990, 1991; Thompson et al.,1989). Specifically, Leat and co-workers have defined Groups that include younger, subduction-related (Group 3) and relatively old potassic components (Group 2; e.g., lamprophyre, leucitite) within the subcontinental lithosphere, and asthenospheric OIB. It was argued by O'Brien and co-workers and Leat and co-workers that mixing of asthenospheric melts with components of the overlying lithosphere is responsible for the resultant trace element and isotopic signatures in their respective data sets.

As a first step in determining the origin of the monzonites, their normalized incompatible element abundance patterns are compared to representative samples of mafic lower crust from the Colorado Plateau (Fig. 6.2a; Wendlandt et al., 1993), and Neogene mafic rocks from Northwest Colorado (Fig. 6.2b; e.g. Leat et al., 1988a). As noted above, mafic rocks from the Highwood Mountains in Montana are interpreted to be asthenospheric, but have interacted with the Archean lithosphere. Since the CMB is located entirely within Proterozoic terrane, a comparison of the normalized trace element abundances from the stocks to the Highwood rocks would not be valid. However, processes related to the petrogenesis of monzonites from Montana can be used to infer details regarding the evolution of the Central City monzonites. All monzonites from

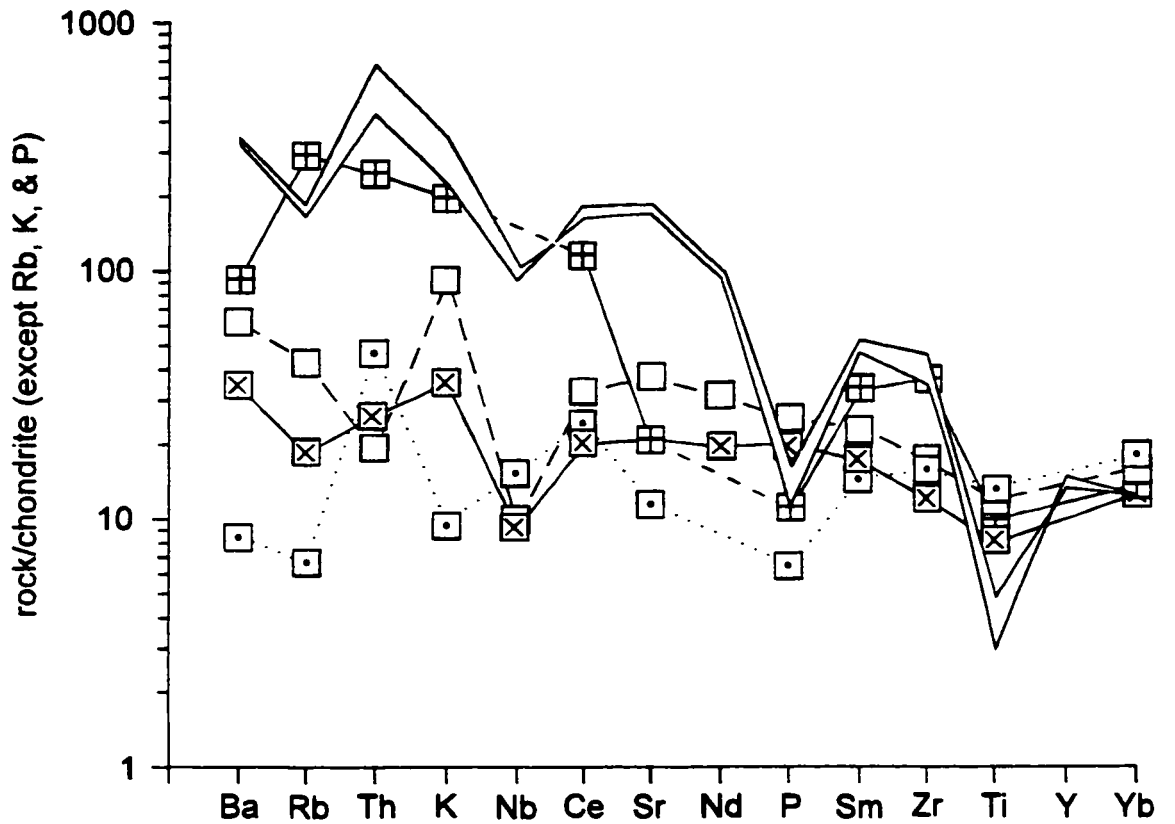

Fig 6.2 Normalized incompatible element diagrams showing potential monzonite source compositions relative to the monzonites (shaded). a) data for average lower crust from the Colorado Plateau (Wendlandt et al., 1993): ⊞=paragneiss; ⊠= granulite; ⊡=eclogite; □=garnet amphibolite. Normalization parameters from Thompson et al. (1984)

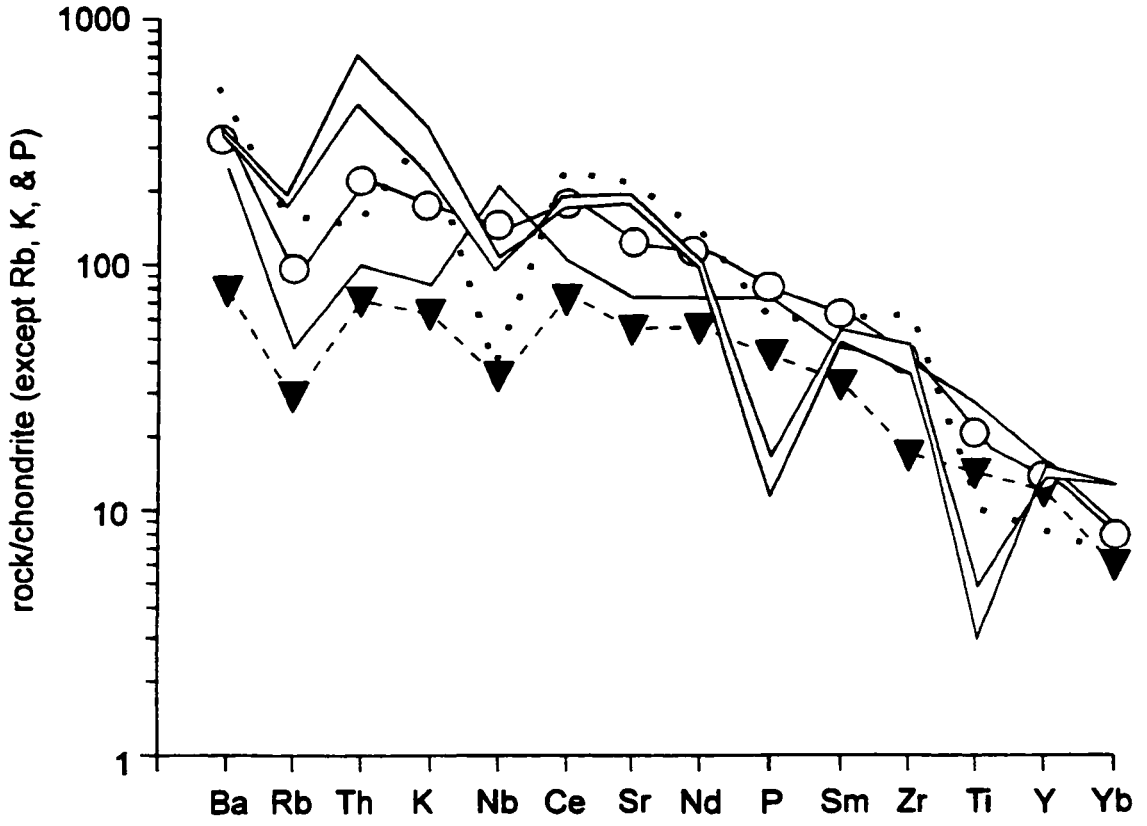

Fig. 6.2 (cont.) b) Normalized incompatible element data for monzonites (shaded region), versus representative data from mantle-derived Northwest Colorado volcanics: solid line=Group 1 OIB-like magma (5LT104, Leat et al., 1991); ▼=Group 3 subduction-processed magma (US78, Gibson et al., 1991); ○ = Group 1 + 2 (5LT160, Thompson et al., 1993); heavy dotted line=Group 2 minette (US102, Thompson et al., 1989). Normalization parameters from Thompson et al. (1984).

Central City included in this study have similar, overlapping incompatible element patterns except for sample 282, which displays a negative Sr anomaly.

As seen in Fig. 6.2a, potential crustal source compositions from the Colorado Plateau exhibit a range in normalized incompatible element abundances. The relative depletions of some elements in the monzonites compared with all potential sources (crust or mantle) reflects the crystallization of phases such as apatite, and Ti-magnetite, and the accumulation of plagioclase. No definitive pattern relationships exist between the Colorado Plateau samples and the monzonites, although the very low abundances of several incompatible trace elements in the eclogite xenoliths make them unlikely parental candidates. In Fig. 6.2b, the Central City monzonite patterns are shown relative to the NWCO mafic volcanic rocks. The monzonite patterns closely resemble two similar yet petrogenetically distinct examples from NWCO: one that is considered as representative of the young, metasomatized lithospheric Group 3 source (Flat Tops; e.g. Leat et al., 1988a; Gibson et al., 1991; Chapter 3), and one that has been proposed to result from mixing of the asthenospheric Group 1 with older lithospheric Group 2 source (Walton Peak; Thompson et al., 1993; Chapter 3). A pattern for the Group 2 source (minette) also displays similar characteristics to the monzonite patterns, yet the noticeable depletions in Rb and Th call into question the viability of Group 2 being the unique source of the monzonites. As the incompatible trace element relationships relay no definitive answers regarding possible source compositions, it is necessary to examine the available radiogenic isotope data to further refine the analysis.

6.5 Isotopic Relationships

Potential magma source(s) of the monzonites include mafic lower crust, lithospheric mantle, or asthenospheric mantle that has experienced contamination by a

relatively old potassic melt, also from the lithosphere. In Fig. 6.3, isotopic Sr and Nd data for the monzonites are shown, together with the published isotopic data for possible magma sources discussed above. For comparison, isotopic data for monzonites analyzed Stein and Crock (1990) are included on the diagram. These data exhibit more scatter but generally follow a potential crustal contamination trend of increasing $^{87}Sr/^{86}Sr$ with decreasing $^{143}Nd/^{144}Nd$, similar to the monzonites reported on here. The field labeled FT delineates the range in isotopic data from the metasomatized lithospheric Group 3 Flat Tops Volcanic Field, in NWCO (Fig. 6.1; Gibson et al., 1991). Similarly, data from Walton Peak (Group 1 + 2; OIB + old lithosphere) are represented by the field labeled WP. The effect of crustal contamination on either of these mantle magma sources is similar in Sr-Nd space, and is illustrated by the field for data from Yarmony Mountain (YR, Fig. 6.1; Leat et al., 1990).

The viability of lower crustal garnet amphibolite as a source can be effectively ruled out on the basis of their isotopic signatures, which are less radiogenic in $^{143}Nd/^{144}Nd$ than the monzonites. It should be noted that two additional samples of garnet amphibolite from Wendlandt et al. (1993; not shown) have similar or higher $^{143}Nd/^{144}Nd$ than the monzonites, but also have $^{87}Sr/^{86}Sr$ ratios > 0.706, thus making them improbable parental candidates. Similarly, the paragneiss component is also discounted, as it has Sr-Nd isotopes similar to upper crust: $^{87}Sr/^{86}Sr > 0.708$, $^{143}Nd/^{144}Nd < 0.5119$ (Wendlandt et al., 1993). The use of lower crustal mafic granulite as a source is questionable, as the average Sr concentration in the granulites is 256 ppm (N=9; Wendlandt et al., 1993); however, the choice of this component cannot be completely ruled out. Alternatively, it is suggested that a mantle-derived melt with an initial Sr concentration of ~1000 ppm is the probable source of the monzonites reported on here.

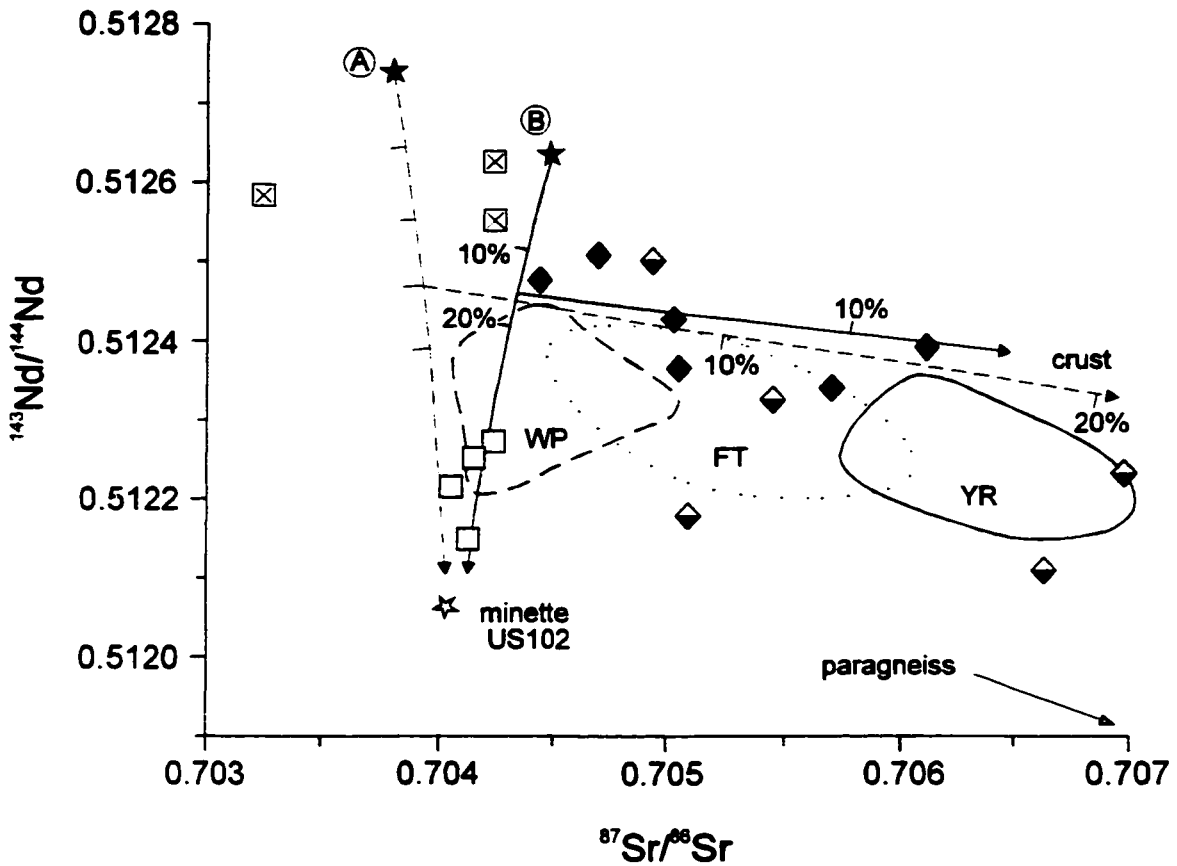

Fig. 6.3 Sr-Nd diagram showing mixing relationships between potential mantle sources and partial melt of crust, following initial contamination by minette. Sources A and B described in text. Minette (US102) data are from Thompson et al. (1989). Crustal contaminant composition is based on regional crustal data (Leat et al., (1991). ◆=monzonites, this study; ◈=monzonites from Stein and Crock (1990) □ =lower crustal garnet amphibolites and ⊠ =lower crustal granulites from Wendlandt et al. (1993). Field labeled WP is for Group 1+2 data from Walton Peak (Thompson et al., 1993), FT is for Group 3 compositions from Flat Tops (Gibson et al., 1991), and YR is for data from crustally-contaminated Group 3 compositions from Yarmony (Leat et al., 1990; Chapter 3).

Two hypothetical starting mantle compositions, one isotopically similar to that of Nelson and Davidson (1993) for 25-30 Ma intermediate composition intrusions from the Colorado Plateau, and the second roughly equivalent to the asthenospheric mantle component from the Highwood Mountains volcanics (O'Brien et al., 1995), are investigated (A and B, respectively in Fig. 6.3). Sr, Nd, and Pb concentrations and isotopic compositions of the source mantle as well as potential contaminants discussed below are listed in Table 6.2.

Given the apparent crustal contamination trend in the data set, mixing calculations were performed between the mantle sources and a potential upper crustal contaminant. The resultant mixing trends are parallel to, but well above the field of data defined by the monzonites. A more convincing fit to the data set would be achieved by invoking a mixed mantle source, similar to that illustrated by the Highwood Mountains and Walton Peak (NWCO) data. The process of mixing a partial melt from the asthenosphere (Group 1) with an ancient potassic component in the lithospheric mantle (Group 2) has been identified in the Neogene volcanics of Northwest Colorado (e.g., Leat et al., 1991) as a viable process for reducing the $^{143}Nd/^{144}Nd$ signature of a magma at relatively constant $^{87}Sr/^{86}Sr$, with the added effect of increasing incompatible element concentrations. An isotopically extreme minette from the Elkhead Mountains Volcanic Field (Fig. 6.1) is used as the Group 2 component in the mixing models. In lieu of using minette, mixing of a mantle-derived melt with lower crustal garnet amphibolite could also provide the necessary reduction in $^{143}Nd/^{144}Nd$ (Fig. 6.3), but the incompatible trace element abundances would not greatly increase.

Following the addition of 30% minette to mantle source A (Colorado Plateau intrusives; Nelson and Davidson, 1993), approximately 40% contamination by simple

Table 6.2 Mixing parameters

	minette[a]	mantle A[b]	mantle B[b]	partial melt of crust[c]	minette mixture A[d]	minette mixture B[d]
[Sr], ppm	2351	1000	816	350	2700	2500
$^{87}Sr/^{86}Sr$	0.704048	0.7038	0.7045	0.8	0.703924	0.70435
[Nd], ppm	82	60	37.89	60	66	45
$^{143}Nd/^{144}Nd$	0.512005	0.51274	0.512638	0.5117	0.512468	0.512463
[Pb], ppm	30	5	11.5	40	12	20
$^{206}Pb/^{204}Pb$	17.28	18.2	18.6	21.115	17.538	18.184
$^{207}Pb/^{204}Pb$	15.47	15.45	15.55	15.874	15.464	15.525
$^{208}Pb/^{204}Pb$	36.70	37.4	38.0	46.332	38.816	37.590

[a] minette (US102) data from Thompson et al. (1989). [Pb] based on isotope dilution data from other minettes in the Elkheads Igneous Province (C. Heikoop, unpubl. data)

[b] mantle values: model A - Nelson and Davidson (1993), model B - O'Brien et al. (1995)

[c] Pb isotope data are from a whole rock analysis of a quartz monzonite from the Boulder Creek Batholith (#12), published in Aleinikoff et al. (1993); remaining data are estimates

[d] concentration data are estimated; isotope ratios are the result of mixing minette with source mantles as described in text

mixing with a single crustal component would be required to reproduce the isotopic compositions of the monzonites. However, the Sr concentrations in such melts only approach 1000 ppm, which is considerably lower than the observed Sr concentrations in most of the monzonites (Table 6.1). In a similar fashion, addition of 15% minette to mantle source B (Highwood Mountains parental melt), followed by at least 30% bulk crustal contamination can reproduce the isotopic signatures of the monzonites, but not the Sr concentrations. In order to achieve high Sr concentrations at relatively low Sr isotope ratios, the parental monzonite magmas must have fractionated at sufficient depth such that plagioclase crystallization was suppressed (Green and Ringwood, 1967; Elthon and Scarfe, 1984). Magma mixing and fractionation of mafic phases, unaccompanied by plagioclase, is recognized in the Highwood Mountains volcanics as a viable process to achieve the more evolved magmas in the suite, including syenite and monzonite (O'Brien et al., 1991). Assuming the average Sr concentration in the monzonites approached 2500 ppm prior to crustal contamination, addition of at least 25% crust by bulk assimilation would be necessary in order to reproduce the isotopic values of the monzonites. Alternatively, if contamination by a partial melt of upper crustal wall rock (Table 6.2) occurred, less than 10% crustal melt would be needed to adequately generate the Sr concentrations as well as the isotope compositions in three monzonites with $^{87}Sr/^{86}Sr < 0.705$ (Table 6.1). The effects of this mixing scenario are shown in Fig. 6.3. Two samples listed in Table 6.1 have Sr concentrations less than 2000 ppm and have probably been affected by AFC, and one has a Sr concentration over 4000 ppm. These differences illustrate the variable nature of the contamination process and emphasize that the monzonites discussed here are probably not cogenetic, as suggested by Rice et al. (1985).

Pb-Pb data for the monzonites are plotted in Fig. 6.4. All data plot to the right of the Geochron, and trend in an approximate straight line to more radiogenic values. Applying the mixing models described above for the monzonites, contamination by c. 10% of a partial melt of upper crust is again suggested. The Pb data follow the contamination trends from either proposed mantle source fairly well in $^{206}Pb/^{204}Pb$ vs. $^{207}Pb/^{204}Pb$ space, however, the best model fit to the monzonite $^{206}Pb/^{204}Pb$ - $^{208}Pb/^{206}Pb$ data ia arrived at using mantle source B (Highwood Mountains parental melt). Also shown are fields for uncontaminated (WP) and contaminated (Glenwood=GW, Fig. 6.1; Chapter 3) 'Group 1 + 2' mixed magma source, and the contaminated Group 3 source (YR) in NWCO. The relative orientation of the NWCO data fields imply that the isotopic composition of upper crust in Colorado is variable.

As a further check on the above model, the relationships between $^{206}Pb/^{204}Pb$ and isotopic Sr - Nd were considered (Fig. 6.5a,b, respectively). Both mantle source models produce similar results, with c. 10% crustal melt as the radiogenic contaminant. There is an overall trend of increasing isotopic Pb with Sr in the monzonites (Fig. 6.5a), similar to that indicated by the crustally contaminated NWCO data. The relationship between Pb and Sr isotopes in the monzonites is somewhat decoupled at higher $^{87}Sr/^{86}Sr$, suggesting that more than one contaminant was available. For $^{143}Nd/^{144}Nd$, the mixing relationships are somewhat clearer, with a definite trend to lower isotopic Nd with increasing $^{206}Pb/^{204}Pb$ (Fig. 6.5b). Upper crustal contamination in the NWCO volcanics has produced a similar result.

6. 6 Conclusions

Isotopic relationships in monzonites from the Central City area within the CMB are consistent with derivation from a mantle source. Available geochemical data

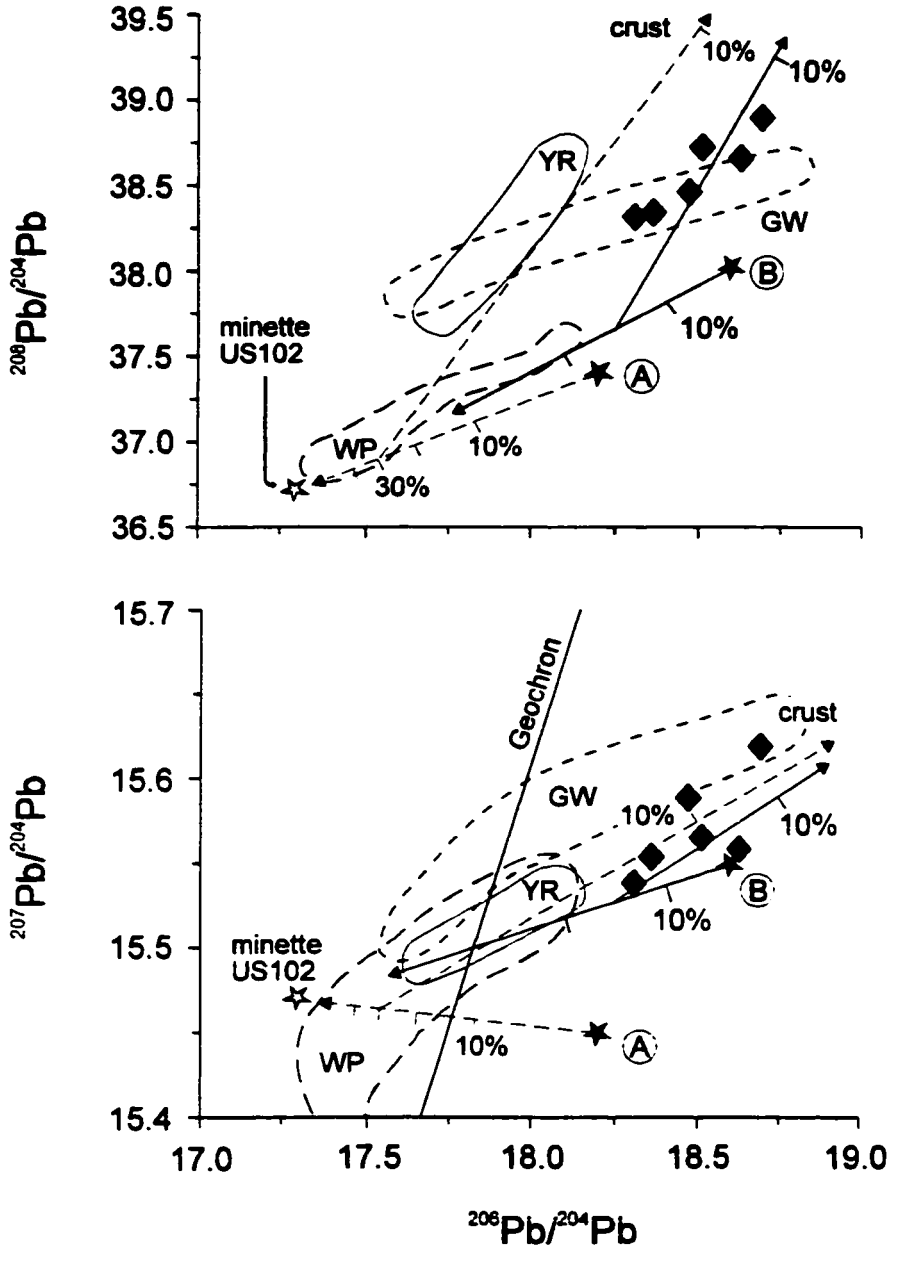

Fig. 6.4 Pb-Pb isotopic relationships for Central City monzonites, relative to mixing models discussed in text. The crustal contaminant is an isotopically extreme composition from the Boulder Creek Batholith (#12WR, Aleinikoff et al., 1993). Fields for Northwest Colorado volcanics described in Fig 6.3.

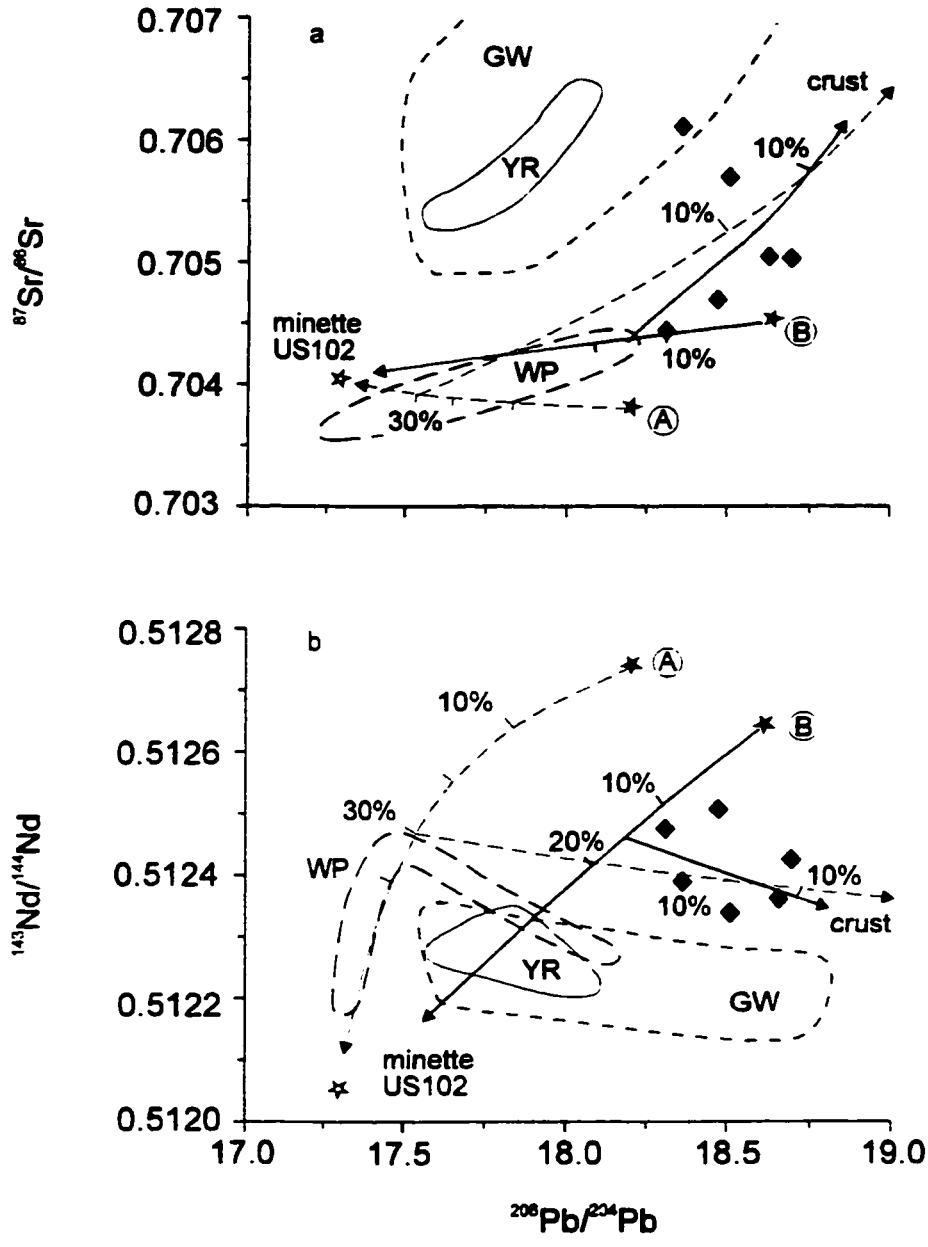

Fig. 6.5 Isotopic relationships in a) Pb versus Sr and b) Pb versus Nd space. Minor decoupling of Sr and Pb isotopes relative to the mixing models implies that more than one contaminant has influenced the isotopic composition of the monzonites. Fields for Northwest Colorado volcanics are described in Fig. 6.3.

suggest that partial melts from the convecting asthenosphere interacted with ancient potassic components in the mechanical boundary layer of the lithosphere, similar to the mantle mixing process recognized in the Highwood Mountains intrusive and extrusive volcanics in Montana, and Neogene basic volcanic rocks to the west and northwest of Central City, in Colorado. Significant differentiation of the magmas occurred prior to their ascent along pre-existing crustal flaws associated with the Colorado Lineament. Fractionation at depth suppressed the crystallization of plagioclase, allowing the Sr concentrations in several of the monzonites to approach 2500 ppm. Contamination by partial melts of upper crust resulted in $\delta^{18}O \sim 9.5$ per mille, which is higher than typical mantle $\delta^{18}O$ of 5 per mille. Sr and Pb isotopic ratios in the data set trend towards more radiogenic values, implying a limited if not negligible role for lower crust in the petrogenesis of the monzonites. The results of this study imply that other intrusive bodies in the Colorado Mineral Belt may also have a dominant mantle origin, as opposed to lower crust.

Chapter 7: Conclusions

7.1 Applications of Pb isotopes to continental basalt studies

Lead isotopes are useful tools in studies of continental basalt petrogenesis. This is primarily due to the inherently large differences in the concentration of Pb in the convecting mantle versus the continental crust. As a result of this difference, Pb isotopes often reflect contamination or mixing processes otherwise overlooked by studies which focus on Sr-Nd isotopes only. The basaltic compositions at Yarmony Mountain, discussed in Chapter 3, serve as an example of this application.

Lead isotope evolution in the Earth's continental lithosphere has created distinct radiogenic and non-radiogenic reservoirs at upper and lower crustal levels, respectively. In general, the lower crust maintains a non-radiogenic Sr, Nd, and Pb isotopic character relative to the upper crust. This distinction often becomes apparent when Sr-Nd-Pb inter-isotope relationships are considered. Use of combined isotope plots in an analysis of mafic magmas erupted in the Española Basin, north-central New Mexico (Chapter 4), lead to the conclusion that the dominant crustal contaminants affecting early and late rift stage magmas were upper and lower crust, respectively.

Metasomatic events affecting the subcontinental lithospheric mantle throughout the lifetime of a region have also created isotopically diverse domains, represented by potassic and ultrapotassic magmas. The isotopic signature of these metasomatized areas is dependent on the age of the metasomatic event. Older events, essentially concurrent with the age of the lithosphere, have relatively non-radiogenic isotopic Pb and Nd values, such as the minette component in the Elkheads Igneous

Province of Northwest Colorado (Chapter 3). Younger metasomatic events, possibly related to the history of subduction off of the west coast of the USA, would result in more radiogenic values, such as those encountered in the minettes from the Navajo Province, Arizona, and Two Buttes, Colorado (Chapter 5).

7.2 Related studies

The isotopic composition of relatively non-contaminated continental basalts are of use in examining the petrogenetic histories of regional intermediate and silicic volcanics. Evolved magmas may be generated through crustal anatexis, or fractionation of a mantle-derived parent. The geochemical trends encountered within the Elk Mountain Sill in Northwest Colorado have been successfully modeled as resulting from fractional crystallization of a mantle-derived mafic (minette) parent to a silicic trachydacite. Intermediate composition stocks near Central City, Colorado may also be the products of such a process. In this instance, the mantle source is inferred to be a hybrid mixture of asthenosphere and potassic lithosphere components, similar to the parental material suggested for the Walton Peak mafic magmas (Chapter 3). The isotopic and trace element characteristics of the intermediate composition stocks developed through fractionation of the hybrid source volume, followed by contamination of partial melts of upper crust.

7.3 The Rio Grande Rift

Past regional studies of the Rio Grande Rift have overlooked the application of Pb isotopes as useful petrogenetic indicators. This may be due to a general lack of Pb isotope analyses. Local studies which include document Pb isotope variations, are an important component of the synthesis presented in Chapter 5.

The $^{206}Pb/^{204}Pb$ ratios of basaltic components from the subcontinental lithosphere beneath the rift region increase from north to south, in concert with the observed decrease in age of the lithosphere from north to south. Potassic components from the lithosphere show distinct isotopic differences. In Northwest Colorado, a region suspected of partially overlying Archean craton, the $^{206}Pb/^{204}Pb$ of the potassic component is c. 17.4. In contrast, the potassic component encountered in the central rift region (Arizona, Southern Colorado) is considerably more radiogenic, with $^{206}Pb/^{204}Pb$ ~19.0. Nd-Pb isotopes and incompatible trace element variations in the central rift region potassic magmas suggest a link to recent metasomatic events, whereas the Northwest Colorado component is considered to be ancient. The asthenospheric component in the rift-related magmas probably had a $^{206}Pb/^{204}Pb$ ~18.5-19.0, throughout the history of the rift.

Future work will undoubtedly fill in the noticeable gaps in the regional synthesis. Coverage in Northwest Colorado is good, however, a younger series of lavas at Flat Tops, as well as several other fields remain to be analyzed. A similar situation exists in the Southern Colorado-Northern New Mexico region. Many of the larger volcanic fields along the Jemez Lineament (Chapter 5) have been studied, however, Pb isotope data is scarce to non-existent. Pb isotope data for the Ocate and Raton-Clayton fields are available in the form of ranges published in abstracts; hopefully complete data sets will be published soon. Many scattered lava flows, as well as larger volcanic fields in central and southern New Mexico, also remain to be analyzed.

Appendix 1: Analytical Procedures

Pb isotope dilution and ratio analysis was performed at McMaster University. Samples with LOI values > 2%, together with samples which were suspected of having undergone post-eruptive alteration, e.g.., carbonation, and those that required multiple analysis due to high Fe contents, were leached in warm 6 M HCl overnight and rinsed in quadrupley distilled water prior to digestion. Standard digestion techniques using HF, HNO_3, and HCl were employed. For isotope dilution, an enriched ^{208}Pb spike was introduced prior to digestion. Pb was separated using standard anion exchange techniques with 0.7 M HBr. Purified samples were then loaded on single Re filaments using the silica gel technique, and analyzed on a VG354 mass spectrometer using a single collector program. During the period of analysis, NBS981 yielded mean values of $^{206}Pb/^{204}Pb=16.901$, $^{207}Pb/^{204}Pb=15.447$, $^{208}Pb/^{204}Pb=36.558$ (N=111). Therefore, data have been corrected for fractionation of 0.1%/a.m.u. Within-run precision on isotope ratios averaged less than 0.03% (1σ). Total procedural blanks are less than 1 ng and are considered negligible.

Several sample suites in NWCO, interpreted as being primarily mantle-derived with only minor crustal contamination, have $^{87}Sr/^{86}Sr$ values > 0.705. The published analyses of these rocks did not include a pre-digestion leach procedure. To ensure that, for example, the effects of minor carbonation at Yarmony did not effect the Sr ratios, a subset was chosen for re-analysis following a pre-digestion leach. All repeat analyses were within analytical error of their initial results, confirming that post-eruptive alteration, if any, had an insignificant effect on $^{87}Sr/^{86}Sr$ ratios.

Representative samples of the monzonite suite discussed in Chapter 6 were analyzed for Nb, Rb, Sr, Y, and Zr by XRF at McMaster University. Data are listed in Table 6.1.

For REE and Nd isotope analysis of the monzonite suite, sample dissolution by standard techniques using HF and HNO_3 was employed. Samples were split and one aliquot spiked using a mixed REE spike. Standard cation and reverse phase column separation methods were used for bulk separation, followed by further separation of LREE from HREE. All samples were loaded on Re-center, Ta-side double filaments. Selected REE concentrations were determined using a modified "two-run" procedure for determination of Sm/Nd ratios. Average precision of Sm/Nd ratios was ca. 0.2% (2 SDM), based on analysis of replicate dissolutions. BCR-1 yielded a Sm/Nd ratio of 0.2280 ± 2. Nd isotopes were analyzed using a four collector peak switching algorithm. Measured ratios were normalized to $^{146}Nd/^{144}Nd = 0.7219$. Within run precision was ca. 0.003% (2 SEM). An average value of 0.511851 ±0.000025 (2σ) was obtained from the La Jolla standard.

Appendix 2: Pb isotope and concentration data

Locality	Age	$^{206}Pb/^{204}Pb$	$^{207}Pb/^{204}Pb$	$^{208}Pb/^{204}Pb$	[Pb], ppm
Northwest Colorado					
Walton Peak	22.8 Ma				
5LT160		17.682	15.469	37.354	
5LT161		18.110	15.539	37.724	
5LT162		17.536	15.511	37.283	
5LT165		17.273	15.466	36.885	
5LT166		17.315	15.439	36.900	
5LT167		17.448	15.470	37.112	13.7
US90		17.370	15.393	36.924	10.4
US91		17.466	15.437	37.049	7.7
Flat Tops	20.6-23 Ma				
5LT377		17.752	15.478	37.756	
5LT338		17.599	15.476	37.309	
5LT342		17.626	15.506	37.716	
5LT351		17.844	15.505	37.827	
5LT356		17.562	15.476	37.639	
5LT358		17.336	15.438	37.145	
5LT360		17.511	15.461	37.249	
US82		17.834	15.495	37.612	
US83		17.583	15.478	37.845	
Yarmony	21.5-24 Ma				
5LT119		17.837	15.523	38.114	
5LT121		17.897	15.525	38.081	
5LT124		17.522	15.486	37.574	
5LT125		18.082	15.549	38.324	
5LT128		18.078	15.538	38.232	
Yampa	5.8 Ma				
5LT87[a]		17.996	15.522	37.663	
5LT89		18.314	15.533	37.801	
5LT90		18.090	15.555	37.769	
5LT104		18.191	15.536	37.812	
5LT107		17.844	15.489	37.403	
US89		17.874	15.536	37.572	
Quaternary	4 ka-2 Ma				
5LT11		18.084	15.532	38.191	
5LT14		18.108	15.537	38.193	
5LT18		18.094	15.545	38.237	
5LT21		18.056	15.518	38.222	
US68		18.222	15.552	38.062	
US111		17.971	15.526	37.739	

Locality	Age	$^{206}Pb/^{204}Pb$	$^{207}Pb/^{204}Pb$	$^{208}Pb/^{204}Pb$	[Pb], ppm
Elk Mtn. Sill	7.6-11.1 Ma				
data from Leat et al. (1988b)					
Elkhead Mtns	8.7-11.6 Ma				
data from Thompson et al. (1989)					
Glenwood	7.9-11.1 Ma				
5LT1		17.560	15.506	37.956	7.1
5LT3		17.910	15.594	38.103	11.6
5LT5		17.848	15.538	38.000	10.3
5LT7		18.754	15.636	38.674	6.4
5LT9		18.814	15.637	38.599	
US73		17.562	15.499	37.764	
Southern Colorado & Northern New Mexico					
San Luis Hills	26 Ma				
data from Johnson and Thompson (1991)					
Navajo province	19-28 Ma				
US8		19.311	15.697	39.011	
89SB139		19.059	15.621	38.677	
89SB141		19.122	15.660	38.906	
additional data from Alibert et al. (1986)					
Dulce	24-27 Ma				
8LT188		18.191	15.522	37.517	
89SB122		18.265	15.500	37.525	
89SB123		18.074	15.541	37.344	
89SB124		17.467	15.461	36.934	
Española Basin	18-27 Ma				
8LT187[a]		19.020	15.569	38.811	
8LT192		19.514	15.748	39.808	5.4
89SB22		18.327	15.554	37.814	
89SB27		18.319	15.501	37.722	1.4
89SB29		19.526	15.600	39.836	5.2
89SB31		19.324	15.600	39.405	
89SB100		19.064	15.577	39.041	
89SB219		18.985	15.631	38.847	4.4
Spanish Peaks	20-27.5 Ma				
8LT20		18.314	15.553	37.882	
8LT36		18.122	15.496	37.654	
Two Buttes	27-35 Ma				
89SB234		18.903	15.574	38.285	
89SB235		18.970	15.664	38.948	
89SB236		18.645	15.608	38.141	
Riley	25-28 Ma				
89SB183		17.952	15.499	37.978	
89SB184		18.227	15.536	38.144	
Cerros del Rio	2-4 Ma				
6-7B		17.838	15.497	37.622	3.8

Locality	Age	$^{206}Pb/^{204}Pb$	$^{207}Pb/^{204}Pb$	$^{208}Pb/^{204}Pb$	[Pb], ppm
Cerros del Rio (cont.)					
6-15G		17.869	15.511	37.650	
6-15H		18.037	15.510	37.879	
6-19A		17.825	15.477	37.632	9.2
6-26C		17.975	15.482	37.815	
TA33[a]		18.202	15.529	38.068	
I-0		17.800	15.507	37.655	14.5
I-4		18.280	15.511	38.084	6.5[b]
I-5		18.305	15.529	38.129	10.0
I-6		18.223	15.530	38.096	2.8
SF-3[a]		18.083	15.540	37.963	
SF-5[a]		18.144	15.506	37.962	
SF-10[a]		18.185	15.503	38.032	
O-2		17.820	15.487	37.640	
Raton-Clayton	<10 ka-8 Ma				
data from Housh et al. (1991b)					
Ocate	0.8-8.3 Ma				
data from Housh et al. (1991a)					
Taos	3.5-5 Ma				
data from Dungan et al. (1986)					
Southern New Mexico					
Uvas	27-28 Ma				
UBA023		17.112	15.408	37.139	
UBA025		17.332	15.434	37.639	
UBA026		17.039	15.404	37.094	
UBA029		17.324	15.432	37.370	
UBA032		17.127	15.410	37.170	
UBA034		17.437	15.447	37.518	
UBA011		18.084	15.498	38.130	
Mogollon-Datil	20-30 Ma				
data from Davis and Hawkesworth (1995)					
	< 20 Ma				
data from Davis and Hawkesworth (1995)					
NM					
Hachita					
DH08	11.8 Ma	17.916	15.505	37.932	
Selden					
DH01	9.8 Ma	18.492	15.498	38.091	
SB018		18.520		38.134	
Robledo					
DH03	7.1 Ma	18.832	15.511	38.091	
Columbus					
DH06	5.2 Ma	19.161	15.556	38.537	
DH07	3.9 Ma	18.866	15.543	38.380	
DH05	3 Ma	19.054	15.534	38.421	

Locality	Age	$^{206}Pb/^{204}Pb$	$^{207}Pb/^{204}Pb$	$^{208}Pb/^{204}Pb$	[Pb], ppm
Hillsboro					
DH12	4.2 Ma	19.698	15.684	39.411	
DH14	4.2 Ma	19.500		39.207	
Aden					
WPB002	0.5 Ma	18.460	15.461	38.175	
WPB001		18.922	15.493	38.403	
SG					
Potrillo					
6LT99	<0.5 Ma	19.022	15.573	38.515	
6LT127	<0.5 Ma	18.462	15.525	38.275	
Malpais flow, Jornada Basin					
8LT54	0.2 Ma	19.612	15.645	39.094	
Valley of Fire lava, Tularosa Basin					
8LT167	0.001 Ma	17.745	15.475	38.396	

Additional Pb isotope for scattered lava flows from the rift were obtained from Everson (1979).

Colorado Mineral Belt					
Central City					
135	63 Ma	18.466	15.548	38.452	
282		18.357	15.549	38.334	
296		18.621	15.554	38.649	
419		18.304	15.534	38.310	
W33		18.502	15.561	38.710	
293B		18.687	15.614	38.878	

[a]within-run precision > 0.03% (1σ) for this sample
[b]this value is an average of hawaiites I-5 and I-6

References

Aleinikoff, J.N., Reed, J.C., Jr., and Wooden, J.L., 1993. Lead isotopic evidence for the origin of Paleo- and Mesoproterozoic rocks of the Colorado Province, U.S.A. Precambrian Res., 63:97-122.

Anderson, D.L., 1994. The sublithospheric mantle as the source of continental flood basalts: the case against continental lithosphere and plume head reservoirs. Earth Planet. Sci. Lett., 123:269-280.

Angevine, CL. and Flanagan, K.M., 1987. Buoyant sub-surface loading of the lithosphere in the Great Plains foreland basin. Nature, 327:137-139.

Atwater, T., 1970. Implications of plate tectonics for the Cenozoic tectonic evolution of Western North America. Geol. Soc. Am. Bull., 81:3513-3536.

Axen, G.J., Taylor, W.J., and Bartley, J.M., 1993. Space-time patterns and tectonic controls of Tertiary extension and magmatism in the Great Basin of the western United States. Geol. Soc. Am. Bull., 105:56-76.

Baldridge, W.S., 1979. Petrology and petrogenesis of Plio-Pleistocene basaltic rocks from the central Rio Grande rift, New Mexico, and their relation to rift structure. In: Riecker, R.E. (ed.), Rio Grande Rift: Tectonics and Magmatism. Am. Geophys. Union, Washington, D.C., pp323-353.

Baldridge, W.S., Damon, P.E., Shafiqullah, M. and Bridwell, R.J., 1980. Evolution of the central Rio Grande rift, New Mexico: new potassium-argon ages. Earth Planet. Sci. Lett., 51:309-321.

Baldridge, W.S., Perry, F.V., Vaniman, D.T., Nealey, L.D., Leavy, B.D., Laughlin, A.W., Kyle, P., Bartov, Y., Steinitz, G., and Gladney, E.S., 1991. Middle to late Cenozoic magmatism of the southeastern colorado Plateau and central Rio Grande rift (New Mexico and Arizona, U.S.A.): a model for continental rifting. Tectonophysics, 197:327-354.

Beard. B.L. and Johnson, C.M., 1993. Hf isotope composition of late Cenozoic basaltic rocks from northwestern Colorado, USA: new constraints on mantle enrichment processes. Earth Planet. Sci. Lett., 119:495-509.

Bennett, V.C. and DePaolo, D.J., 1987. Proterozoic crustal history of the western United States as determined by neodymium isotope mapping. Geol. Soc. Am. Bull., 99:674-685.

Braddock, W.A.., 1969 . Geology of the Empire quadrangle, Grand, Gilpin, and Clear Creek counties, Colorado. U.S.G.S. Prof. Paper 616, 56p.

Bradshaw, T.K., Hawkesworth, C.J., and Gallagher, K., 1993. Basaltic volcanism in the southern Basin and Range: no role for a mantle plume. Earth Planet. Sci. Lett., 116:45-62.

Brandon, A.D. and Goles, G.G., 1988. A Miocene subcontinental plume in the Pacific Northwest: geochemical evidence. Earth Planet. Sci. Lett., 88:273-283.

Bussod, G.Y.A. and Williams, D.R., 1991. Thermal and kinetic model of the southern Rio Grande Rift: inferences from crustal and mantle xenoliths from Kilbourne Hole, New Mexico. Tectonophysics, 197:373-389.

Camp, V.E., 1995. Mid-Miocene propagation of the Yellowstone mantle plume head beneath the Columbia River basalt source region. Geology, 23(5):435-438.

Chapin, E.E., 1979. Evolution of the Rio Grande Rift: a summary. In: Riecker, R.E. (ed.), Rio Grande Rift: Tectonics and Magmatism. Am. Geophys. Union, Washington, D.C., pp 1-6.

Chapin, C.E., and Cather, S.M., 1994. Tectonic setting of the axial basins of the Northern and Central Rio Grande rift. In: Keller, R.G., and Cather, S.M. (eds.), Basins of the Rio Grande Rift: Structure, Stratigraphy, and Tectonic Setting. Geol. Soc. Am. Spec. Pap. 291, pp 5-25.

Chapin, C.E. and Seager, W.R., 1975. Evolution of the Rio Grande rift in the Socorro and Las Cruces areas. New Mexico Geol. Soc. Guidebook 26, pp297-321.

Chen, C.-Y. and Frey, F.A., 1985. Trace element and isotopic geochemistry of lavas from Haleakala volcano, East Maui, Hawaii: implications for the origin of Hawaiian basalts. J. Geophys. Res., 90(B10):8743-8768.

Christiansen, R.L. and Lipman, P.W., 1972. Cenozoic volcanism and plate-tectonic evolution of the Western United States, II. Late Cenozoic. Phil. Trans. Roy. Soc. Lond., A271:249-284.

Clemons, R.E., 1979. Geology of the Good Sight Mountains, Luna County, New Mexico. New Mexico Bur. Mines Min. Res. Circular 169, 32pp.

Condie, K.C., 1992. Proterozoic terranes and continental accretion in southwestern North America. In: Condie, K.C. (ed.), Proterozoic Crustal Evolution. Elsevier, NY, pp 447-480.

Coney, P.J., 1987. The regional tectonic setting and tpossible causes of Cenozoic extension in the North American Cordillera. In: Coward, M.P., Dewey, J.F., and Hancock, P.L. (eds.), Continental Extensional Tectonics. Spec. Publ. Geol. Soc. Lond. 28, pp177-186.

Cumming, G.L. and Richards, J.R., 1975. Ore lead isotope ratios in a continuously changing Earth. Earth Planet. Sci. Lett., 28:155-171.

Daley, E.E. and DePaolo, D.J., 1992. Isotopic evidence for lithospheric thinning during extension: southern Great Basin. Geology, 20:104-108.

Davis, J. and Hawkesworth, C., 1993. The petrogenesis of 30-20 Ma basic and intermediate volcanics from the Mogollon-Datil Volcanic Field, New Mexico, USA. Contrib. Mineral. Petrol., 115:165-183.

Davis, J. and Hawkesworth, C., 1994. Early calc-alkaline magmatism in the Mogollon-Datil Volcanic Field, New Mexico, USA. J. Geol. Soc. Lond., 151:825-843.

Davis, J. and Hawkesworth, C., 1995. Geochemical and tectonic transitions in the evolution of the Mogollon-Datil Volcanic Field, New Mexico, U.S.A. Chem. Geol., 119:31-53.

Davis, P.M., 1991. Continental rift structures and dynamics with reference to teleseismic studies of the Rio Grande and East African rifts. Tectonophysics, 197:309-325.

Davis, P.M., Parker, E.C., Evans, J.R., Iyer, H.M., and Olsen, K.H., 1984. Teleseismic deep sounding of the velocity structure beneath the Rio Grande rift. In: Baldridge, W.S., Dickerson, P.W., Riecker, R.E., and Zidek, J. (eds.), Rio Grande Rift: Northern New Mexico. N.M. Geol. Soc. Guidebook 35, pp29-38.

DePaolo, D.J., 1988a. Age dependance of the composition of continental crust: evidence from Nd isotopic variations in granitic rocks. Earth Planet. Sci. Lett., 90:263-271.

DePaolo, D.J., 1988b. Neodymium Isotope Geochemistry. Springer-Verlag, New York, 187pp.

DePaolo, D.J. and Wasserburg, G.J., 1976. Inferences about magma sources and mantle structure from variations of $^{143}Nd/^{144}Nd$. Geophys. Res. Lett., 3:743-746.

DePaolo, D.J., Linn, A.M. and Schubert, G., 1991. The continental crustal age distribution: methods of determining mantle separation ages from Sm-Nd isotopic data and application to the southwestern United States. J. Geophys. Res., 96(B2):2071-2088.

Dickin, A.P., Rice, C.M., and Harmon, R.S., 1986 . A strontium and oxygen isotope study of Laramide magmatic and hydrothermal activity near Central City, Colorado. Econ. Geol., 81:904-914.

Dickin, A.P., 1995. Radiogenic Isotope Geology. Cambridge University Press, Cambridge, 452pp.

Doe, B.R. and Zartman, R.E., 1979. Plumbotectonics I, The Phanerozoic. In: Barnes, H.L.. (ed.), Geochemistry of Hydrothermal Ore Deposits, 2nd ed. Wiley, New York, New York, pp22-70.

Doe, B.R., Lipman, P.W., Hedge, C.E., and Kurasawa, H., 1969. Primitive and contaminated basalts from the southern Rocky Mountains, USA. Contrib. Mineral. Petrol., 21:142-156.

Draper, D.S., 1991. Late Cenozoic bimodal magmatism in the northern Basin and Range province of Southeastern Oregon. J. Volcanol. Geotherm. Res., 45:299-328.

Dudás, F.Ö., Carlson, R.W., and Eggler, D.H., 1987. Regional middle Proterozoic enrichment of the subcontinental mantle source of igneous rocks from central Montana. Geology, 15:22-25.

Duncker, K.E., Wolff, J.A., Harmon, R.S., Leat, P.T., Dickin, A.P., and Thompson, R.N., 1991. Diverse mantle and crustal components in lavas of the NW Cerros del Rio volcanic field, Rio Grande Rift, New Mexico. Contrib. Mineral. Petrol., 108:331-345.

Dungan, M.A., Lindstrom, M.M., McMillan, N.J., Moorbath, S., Hoefs, J., and Haskin, L.A., 1986. Open system evolution of the Taos Plateau Volcanic Field, Northern New Mexico 1. The petrology and geochemistry of the Servilleta basalt. J. Geophys. Res. 91(B6):5999-6028.

Dupré. B. and Allègre, C.J., 1983. Pb-Sr isotope variation in Indian Ocean basalts and mixing phenomena. Nature, 303:142-146.

Eaton, G.P., 1979. A plate-tectonic model for late Cenozoic crustal spreading in the western United States. In: Riecker, R.E. (ed.), Rio Grande Rift: Tectonics and Magmatism. Am. Geophys. Union, Washington, D.C., pp 7-32.

Eaton, G.P., 1986. A tectonic redefinition of the southern Rocky Mountains. Tectonophysics, 132:163-193.

Eaton, G.P., 1987. Topography and origin of the southern Rocky Mountains and Alvarado Ridge. In: Coward, M.P., Dewey, J.F., and Hancock, P.L. (eds.), Continental Extensional Tectonics. Spec. Publ. Geol. Soc. Lond. 28, pp355-369.

Ellisor, R., Wolff, J.A., Davidson, J.P., Kyle, P.R., and Gardner, J.N., 1995. Petrogenesis of Keres Group lavas, Jemez Mountains Volcanic Field, New Mexico. EOS, Trans. Am. Geophys. Union, pF665.

Everson, J. E., 1979. Regional variations in the lead isotopic characteristics of late Cenozoic basalts from the southwestern United States. Ph.D. thesis, Calif. Inst. Tech., Pasadena, California, 454pp.

Faure, G., 1986. Principles of Isotope Geology, 2nd ed. Wiley, New York, 589pp.

Fitton, J.G., and Dunlop, H.M., 1985. The Cameroon Line, West Africa, and its bearing on the origin of oceanic and continental alkali basalts. Earth Planet. Sci. Lett., 72:23-38.

Fitton, J.G., James, D., and Leeman, W.P., 1991. Basic magmatism associated with late Cenozoic extension in the western United States: compositional variations in space and time. J. Geophys. Res., 96:13693-13711.

Fitton, J.G., James, D., Kempton, P.D., Ormerod, D.S., and Leeman, W.P., 1988. The role of lithospheric mantle in the generation of late Cenozoic basic magmas in the western United States. J. Petrol. Spec. Lith. Issue, pp331-49.

Foley, S., 1992. Vein-plus-wall-rock melting mechanisms in the lithosphere and the origin of potassic alkaline magmas. Lithos, 28:435-453.

Foley, S. and Peccerillo, A., 1992. Potassic and ultrapotassic magmas and their origin. Lithos, 28:181-185.

Fraser, K.J., Hawkesworth, C.J. Erlank, A.J., Mitchell, R.H., and Scott-Smith, B.H., 1985/86. Sr, Nd, and Pb isotope and minor element geochemistry of lamproites and kimberlites. Earth Planet. Sci. Lett., 76:57-70.

Frey, F.A. and Clague, D.A., 1983. Geochemistry of diverse basalt types from Loihi seamount, Hawaii: petrogenetic implications. Earth Planet. Sci. Lett., 66:337-355.

Gallagher, K. and Hawkesworth, C., 1992. Dehydration melting and the generation of continental flood basalts. Nature, 358:57-59.

Gans, P.B., Mahood, G.A., and Schermer, E., 1989. Synextensional magmatism in the Basin and Range Province; a case study from the eastern Great Basin. Geol. Soc. Am. Spec. Paper 233, 53pp.

Gardner, J.N. and Goff, F., 1984. Potassium-argon dates from the Jemez Volcanic Field: implications for tectonic activity in the north-central Rio Grande Rift. In: Baldridge, W.S., Dickerson, P.W., Riecker, R.E., and Zidek, J. (eds.), Rio Grande Rift: Northern New Mexico. N.M. Geol. Soc. Guidebook 35, pp75-81.

Geist, D. and Richards, M., 1993. Origin of the Columbia Plateau and Snake River Plain: deflection of the Yellowstone plume. Geology, 21:789-792.

Gibson, S.A., Thompson, R.N., Leat, P.T., Morrison, M.A., Hendry, G.L., and Dickin, A.P., 1991. The Flat Tops Volcanic Field 1. Lower Miocene open-system, multisource magmatism at Flander, Trappers Lake. J. Geophys. Res., 96(B8):13609-13627.

Gibson, S.A., Thompson, R.N., Leat, P.T., Dickin, A.P., Morrison, M.A., Hendry, G.L., and Mitchell, J.G., 1992. Asthenosphere-derived magmatism in the Rio Grande rift, western USA, implications for continental break-up. Spec. Publ. Geol. Soc. Lond., 68:61-89.

Gibson, S.A., Thompson, R.N., Leat, P.T., Morrison, M.A., Hendry, G.L., Dickin, A.P., and Mitchell, J.G., 1993. Ultrapotassic magmas along the flanks of the Oligo-Miocene Rio Grande Rift, USA: monitors of the zone of lithospheric mantle extension and thinning beneath a continental rift. J. Petrol., 34(1):187-228.

Goldstein, S.L. and O'Nions, R.K., 1981. Nd and Sr isotopic relationships in pelagic clays and ferromanganese deposits. Nature, 292:324-327.

Golombek, M.P., 1983. Geology, structure, and tectonics of the Pajarito fault zone in the Española Basin of the Rio Grande rift, New Mexico. Geol. Soc. Am. Bull., 94:192-205.

Grambling, J.A., Williams, M.L., and Mawer, C.K., 1988. Proterozoic tectonic assembly of New Mexico. Geology 16:724-727.

Haag, D.M. and McMillan, N.J., 1990. Geochemistry of the Late Oligocene to Early Pleistocene basalts of southern New Mexico. Geol. Soc. Am. Abstr. Prog., 22:A345.

Hamilton, W., 1987. Crustal extension in the Basin and Range Province, southwestern United States. In: Coward, M.P., Dewey, J.F., and Hancock, P.L. (eds.), Continental Extensional Tectonics. Spec. Publ. Geol. Soc. Lond. 28, pp155-176.

Harry, D.L. and Leeman, W.P., 1995. Partial melting of melt metasomatized subcontinental mantle and the magma source potential of the lower lithosphere. J. Geophys. Res., 100(B7):10255-10269.

Harry, D.L., Sawyer, D.S., and Leeman, W.P., 1993. the mechanics of continental extension in western North America: implications for the magmatic and structural evolution of the Great Basin. Earth Planet. Sci. Lett., 117:59-71.

Hart, S.R., 1984. A large scale isotopic anomaly in the Southern Hemisphere mantle. Nature, 309:753-757.

Hawkesworth, C., Turner, S., Gallagher, K., Hunter, A., Bradshaw, T., and Rogers, N., 1995. Calc-alkaline magmatism, lithospheric thinning and extension in the Basin and Range. J. Geophys. Res., 100(B7):10271-10286.

Hedge, C.E., Houston, R.S., Tweto, O.L., Peterman, Z.E., Harrison, J.E., and Reid, R.R., 1986. The Precambrian of the southern Rocky Mountain region. U.S.G.S. Prof. Paper 1241-D, 17pp.

Hills, F.A. and Houston, R.S., 1979. Early Proterozoic tectonics of the central Rocky Mountains, North America. Contrib. Geol., 17:89-109.

Hofmann, A.W., Jochum, K.P., Seufert, M., and White, W.M., 1986. Nd and Pb in oceanic basalts: new constraints on mantle evolution. Earth Planet. Sci. Lett., 79:33-45.

Hole, M.J., Saunders, A.D., Mariner, G.F., and Tarney, J., 1984. Subduction of pelagic sediments: implication for the origin of Ce-anomaous basalts from the Mariana Islands. J. Geol. Soc. Lond., 141:453-472.

Holmes, A., 1946. An estimate of the age of the Earth. Nature, 157:680-684.

Housh, T., Bowring, S.A., and Dungan, M.A., 1991. Pb, Nd, and Sr isotopic data from the Ocate Volcanic Field: constraints on the role of enriched lithosphere in within-rift and off-axis magmatism in the northern Rio Grande Rift, New Mexico. Geol. Soc. Am. Abst. Progr., 23(5):133.

Housh, T., Bowring, S.A., Dungan, M.A., and Stormer, J.C., 1991. Enriched lithosphere in northern New Mexico: new Pb isotopic data from the Raton-Clayton Volcanic Field. Geol. Soc. Am. Abstr. Progr., 23(4):33.

Housh, T., Bowring, S.A., and Dungan, M.A., 1992. Isotopic and geochemical evidence for enriched lithospheric mantle beneath northern New Mexico and its role in the development of late Cenozoic magmatism. EOS, Trans. Am. Geophys. Union 73:338 (abstr.).

Houtermans, F.G., 1946. Die isotopen-haufigkeiten im naturlichen Blei und dasAalter des Urans. Naturwissenschaften, 33:185-187.

Ingersoll, R.V., Cavazza, W., Baldridge, W.S., and Shafiquillah, M., 1990. Cenozoic sedimentation and paleotectonics of north-central New Mexico: implications for initiation and evolution of the Rio Grande rift. Geol. Soc. Am. Bull., 102:1280-1296.

Izett, G.A. and Obradovich, J.D., 1994. $^{40}Ar/^{39}Ar$ age constraints for the Jaramillo normal subchron and the Matuyama-Bruhnes geometric boundary. J. Geophys. Res., 99:2925-2934.

Jaffey, A.H., Flynn, K.F., Glendenin, L.E., Bentley, W.C., and Essling, A.M., 1971. Precision measurement of the half-lives and specific activities of U235 and U238. Physics Reviews, C4:1889-1907.

Johnson, C.M. and Thompson, R.A., 1991. Isotopic composition of Oligocene mafic volcanic rocks in the Northern Rio Grande rift: evidence for contributions of ancient intraplate and subduction magmatism to evolution of the lithosphere. J. Geophys. Res., 96(B8):13593-13608.

Johnson, C.M., Lipman, P.W., and Czamanske, G.K., 1990. H, O, Sr, Nd, and Pb isotope geochemistry of the Latir volcanic field and cogenetic intrusions, New Mexico, and relations between evolution of a continental magmatic center and modifications of the lithosphere. Contrib. Mineral. Petrol., 104:99-124.

Johnson, R.A., Karlstrom, K.E., Smithson, S.B., and Houston, R.S., 1984. Gravity profiles across the Cheyenne Belt, a Precambrian crustal suture in southeastern Wyoming. J. Geodynam., 1:445-472.

Karlstrom, K.E. and Houston, R.S., 1984. The Cheyenne Belt: analysis of a Proterozoic suture in southern Wyoming. Precambrian Res., 25:415-446.

Keller, G.R., Khan, M.A., Morgan, P., Wendlandt, R.F., Baldridge, W. S., Olsen,, K.H., Prodehl, C. and Braile, L.W., 1991. A comparative study of the Rio Grande and Kenya rifts. Tectonophysics, 197:355-71.

Kempton, P.D., Fitton, J.G., Hawkesworth, C.J., and Ormerod, D.S., 1991. Isotopic and trace element constraints on the composition and evolution of the lithosphere beneath the southwestern United States. J. Geophys. Res., 96(B8):13713-13735.

Larsen, E.S., Irving, I., and Gonyer, F.A., 1938. Petrologic results from a study of the minerals from Tertiary volcanic rocks of the San Juan region, Colorado. Am. Mineral., 23:417-429.

Larson, E.E., Ozima, M., and Bradley, W.C., 1975. Late Cenozoic basin volcanism in northwestern Colorado and its implications concerning tectonics and the origin of the Colorado River system. In: Curtis, B.F. (ed.), Cenozoic History of the Southern Rocky Mountains, Geol. Soc. Am. Mem. 144:155-178.

Leake, B.E., 1990. Granite magmas: their sources, initiation and consequences of emplacement. J. Geol. Soc. Lond., 147:579-589.

Leat, P.T., Thompson, R.N., Morrison, M.A., Hendry, G.L., and Dickin, A.P., 1988a. Compositionally-diverse Miocene-Recent rift-related magmatism in northwest Colorado: partial melting, and mixing of mafic magmas from 3 different asthenospheric and lithospheric mantle sources. J. Petrol. Spec. Lith. Issue, pp.351-377.

Leat, P.T., Thompson, R.N., Morrison, M.A., Hendry, G.L., and Dickin, A.P., 1988b. Silicic magmas derived by fractional crystallization from Miocene minette, Elkhead Mountains, Colorado. Min. Mag., 52:577-585.

Leat, P.T., Thompson, R.N., Dickin, A.P., Morrison, M.A., and Hendry, G.L., 1989. Quaternary volcanism in northwestern Colorado: implications for the roles of asthenosphere and lithosphere in the genesis of continental basalts. J. Volcanol. Geotherm. Res., 37:291-310.

Leat, P.T., Thompson, R.N., Morrison, M.A., Hendry, G.L., and Dickin, A.P., 1990. Geochemisty of mafic lavas in the early Rio Grande Rift, Yarmony Mountain, Colorado, U.S.A. Chem. Geol., 81:23-43.

Leat, P.T., Thompson, R.N., Morrison, M.A., Hendry, G.L., and Dickin, A.P., 1991. Alkaline hybrid mafic magmas of the Yampa area, NW Colorado, and their

relationship to the Yellowstone mantle plume and lithospheric mantle domains. Contrib. Mineral. Petrol., 107:310-327.
Leeman, W.P. and Harry, D.L., 1993. A binary source model for extension-related magmatism in the Great Basin, western North America. Science, 262:1550-1554.
LeMaitre, R.W., 1989. A Classification of Igneous Rocks and Glossary of Terms: Recommendations of the International Union of Geological Sciences Subcommission on the Systematics of Igneous Rocks. Blackwell, Oxford, 193pp.
Leudke, R.G. and Smith, R.L., 1978. Map showing distibution, composition, and age of late Cenozoic volcanic centers in Colorado, Utah, and southwestern Wyoming. U.S.G.S. Map I-1091-B (1:1,000,000).
Lipman, P.W., 1980. Cenozoic volcanism in the western United States: implications for continental tectonics. In: Studies in Geophysics, Continental Tectonics. Nat. Acad. Sci., Washington, D.C., pp.161-174.
Lipman, P.W. and Mehnert, H.H., 1975. Late Cenozoic basaltic volcanism and development of the Rio Grande depression in the southern Rocky Mountains. In: Curtis, B.F. (ed.), Cenozoic History of the Southern Rocky Mountains, Geol. Soc. Am. Mem.144:119-154.
Lugmair, G.W. and Marti, K., 1978. Lunar initial $^{143}Nd/^{144}Nd$: differential evolution of the lunar crust and mantle. Earth Planet. Sci. Lett., 39:349-357.
Mack, G.H., Seager, W.R., and McIntosh, W.C., 1996. Evolution of the southern Rio Grande Rift, south-central New Mexico. Geol. Soc. Am. Abstr. Progr., p.A516.
Manley, K., 1979. Stratigraphy and structure of the Española Basin, Rio Grande Rift, New Mexico. In: Riecker, R.E. (ed.), Rio Grande Rift: Tectonics and Magmatism. Am. Geophys. Union, Washington, D.C., pp 71-86.
McKenzie, D., 1989. Some remarks on the movement of small melt fractions in the mantle. Earth Planet. Sci. Lett., 95:53-72.
McKenzie, D. and Bickle, M.J., 1988. The volume and composition of melt generated by extension of the lithosphere. J. Petrol., 29(3):625-679.
McMillan, N.J. and Dickin, A.P., 1990. The Uvas Basaltic Andesit, southern New Mexico: Magmagenesis during initial Rio Grande Rift extension. Geol. Soc. Am. Abstr. Prog., 22:A345.
McMillan, N.J., Dickin, A.P., and Skuba, C., 1992. Pb-Sr-Nd isotopic constraints on Cenozoic mantle and crustal magma sources, southern New Mexico. EOS, Trans. Am. Geophys. Union, 73:338 (abstr.).
Meen, J.K. and Eggler, D.H., 1987. Petrology and geochemistry of the Cretaceous Independence volcanic suite, Absaroka Mountains, Montana: clues to the composition of the Archean sub-Montanan mantle. Geol. Soc. Am. Bull., 98:238-247.
Miller, D.M., Nilsen, T.H., and Bilodeau, W.L., 1992. Late Cretaceous to early Eocend geologic evolution of the United States Cordillera. In: Burchfiel, B.C., Lipman, P.W., and Zoback, M.L. (eds.), The Cordilleran Orogene: Conterminous U.S., vol. G3, The Geology of North America. Geol. Soc. Am., Boulder, CO, pp205-260.
Morgan, P., Seager, W., and Golombek, M.P., 1986. Cenozoic thermal, mechanical and tectonic evolution of the Rio Grande Rift. J. Geophys. Res., 91(B6):6263-6276.
Muehlberger, W.R., 1979. The Embudo fault between Pilar and Arroyo Hondo, New Mexico: an active intracontinental transform fault. N.M. Geol. Soc. Guidebook 30, pp77-82.

Musselman, T.E. and Simmons, E.C., 1987. Crustal source for a mafic alkalic suite from the Colorado Mineral Belt, with evidence for regional metamorphism. Geol. Soc. Am. Abstr. Prog., 19:783.

Nelson, D.R., 1992. Isotopic characteristics of potassic rocks: evidence for the involvement of subducted sediments in magma genesis. Lithos, 28:403-420.

Nelson, S.T. and Davidson, J.P., 1993. Interactions between mantle-derived magmas and mafic crust, Henry Mountains, Utah. J. Geophys. Res., 98(B2):1837-1852.

Nicholls, J., Carmichael, I.S.E., and Stormer, J.C., Jr., 1971. Silica activity and P_{total} in igneous rocks. Contrib. Mineral. Petrol., 33:1-20.

Nielsen, R.L. and Dungan, M.A., 1985. The petrology and geochemistry of the Ocate volcanic field, north-central New Mexico. Geol. Soc. Am. Bull., 96:296-312.

Nicolas, A., Achauer, U., and Daignieres, M., 1994. Rift initiation by lithospheric rupture. Earth Planet. Sci. Lett., 123:281-298.

O'Brien, H.E., Irving, A.J., and McCallum, I.S., 1991. Eocene potassic magmatism in the Highwood Mountains, Montana: petrology, geochemistry, and tectonic implications. J. Geophys. Res., 96(B8):13237-13260.

O'Brien, H.E., Irving, A.J., McCallum, I.S., & Thirwall, M.R., 1995. Strontium, neodymium, and lead isotopic evidence for the interaction of post-subduction asthenospheric potassic mafic magmas of the Highwood Mountains, Montana, USA, with ancient Wyoming craton lithospheric mantle. Geochim. Cosmochim. Acta, 59:4539-4556.

Othman, D. B., White, W.M., and Patchett, P.J., 1989. The geochemistry of marine sediments, island arc magma genesis, and crust-mantle recycling. Earth Planet. Sci. Lett., 94:1-21.

Oversby, V.M., 1974. A new look at the lead isotope growth curve. Nature, 248:132-133.

Parker, E.C., Davis, P.M., Evans, J.R., Iyer, H.M., and Olsen, K.H., 1984. Upwarps of anomalous asthenosphere beneath the Rio Grande rift. Nature, 312:354-356.

Parsons, B. and McKenzie, D., 1978. Mantle convection and the thermal structure of the plates. J. Geophys. Res., 83:4485-4496.

Patterson, C.C., 1956. Age of meteorites and the Earth. Geochim. Cosmochim. Acta, 10:230-237.

Pearce, J.A., 1983. The role of sub-continental lithosphere in magma genesis at destructive plate margins. In: C.J. Hawkesworth and M.J. Norry (eds.), Continental Basalts and Mantle Xenoliths. Shiva, Nantwich, pp.230-249.

Perry, F.V., Baldridge, W.S., and DePaolo, D.J., 1987. Role of asthenosphere and lithosphere in the genesis of Late Cenozoic basaltic rocks from the Rio Grande Rift and adjacent regions of the southwestern United States. J. Geophys. Res., 92(B9):9193-9213.

Perry, F.V., Baldridge, W.S., and DePaolo, D.J., 1988. Chemical and isotopic evidence for lithospheric thinning beneath the Rio Grande rift. Nature, 332:432-434.

Phelps, D.W., Gust, D.S., and Wooden, J.L., 1985. Petrogenesis of the mafic feldspathoidal lavas o fthe Raton-Clayton volcnaic field, New Mexico. Contrib. Mineral. Petrol., 84:182-190.

Prodehl, C. and Pakiser, L.C., 1980. Crustal structure of the southern Rocky Mountains from seismic measurements. Geol. Soc. Am. Bull., 91:147-155.

Reid, M.R., Hart, S.R., Padovani, E.R., and Wandless, G.A., 1989. Contribution of metapelitic sediments to the composition, heat production, and seismic velocity of the lower crust of southern New Mexico, U.S.A. Earth Planet. Sci. Lett., 95:367-381.

Rice, C.M., Lux, D.R., and MacIntyre, R.M., 1982. Timing of mineralization and related intrusive activity near Central City, Colorado. Econ. Geol., 77:1655-1666.

Rice, C.M., Harmon, R.S., and Sheperd, T.J., 1985. Central City, Colorado: the upper part of an alkaline porphyry molybdenum system. Econ. Geol., 80:1769-1796.

Rinehart, E.J., Sanford, A.R., and Ward, R.W., 1979. Geographic extent and shape of an extensive magma body at midcrustal depths in the Rio Grande Rift near Socorro, New Mexico. In: Riecker, R.E. (ed.), Rio Grande Rift: Tectonics and Magmatism. Am. Geophys. Union, Washington, D.C., pp 237-252.

Robertson JM, Grambling JA, Mawer CK, Bowring SA Williams ML, Bauer PW, Silver LT (1993). Transcontinental Proterozoic provinces: Precambrian geology of New Mexico. In: Reed Jr., J.C., Bickfor, M.E., Houston, R.S., Link, P.K., Rankin, D.W., Sims, P.K., and Van Schmus, W.R. (eds.), Precambrian: Conterminous U.S., vol. C-2, The Geology of North America, Geol. Soc. Am., Boulder, CO, pp228-238.

Roden, M.F., Frey, F.A., and Clague, D.A., 1984. Geochemistry of tholeiitic and alkalic lavas from the Koolau Range, Oahu, Hawaii: implications for Hawaiian volcanism. Earth Planet. Sci. Lett., 69:141-158.

Salters, V.J.M. and Barton, M. 1985. The geochemistry of ultrapotassic lavas from the Leucite Hills, Wyoming. EOS, Trans. Am. Geophys. Union, 66(46):1109.

Salyards, S.L., Ni, J.F., and Aldrich, Jr., M.J., 1994. Variation in paleomagnetic rotations and kinematics of the north-central Rio Grande rift. In: Keller RG, Cather SM (eds) Basins of the Rio Grande Rift: Structure, Stratigraphy, and Tectonic Setting. Geol. Soc. Am. Spec. Pap. 291, pp59-71.

Seager, W.R. and Clemons, R.E., 1975. Middle to Late Tertiary geology of the Cedar Hills-Selden Hills area, New Mexico. New Mexico Bur. Mines Min. Res. Circular 133, 24 pp.

Seager, W.R. and Morgan, P., 1979. Rio Grande Rift in southern New Mexico, west Texas, and Northern Chihuahua. In: Riecker, R.E. (ed.), Rio Grande Rift: Tectonics and Magmatism. Am. Geophys. Union, Washington, D.C., pp 87-106.

Severinghaus, J. and Atwater, T., 1990. Cenozoic geometry and thermal state of the subducting slabs beneath western North America. In: Wernicke, B.P. (ed.), Basin and Range Extensional Tectonics near the Latitude of Las Vegas, Nevada. Geol. Soc. Am. Mem. 176, pp 1-22.

Sims, P.K., 1964. Geology of the Central City quadrangle, Colorado. U.S.G.S. Quad. Map 267.

Simmons, E.C. and Hedge, C.E., 1978. Minor-element and Sr-isotope geochemistry of Tertiary stocks, Colorado Mineral Belt. Contrib. Mineral. Petrol., 67:379-396.

Smith, R.B. and Braile, L.W., 1994. The Yellowstone hotspot. J. Volcanol. Geotherm. Res., 61:121-187.

Smith, R.L., Bailey, R.A., and Ross, C.S., 1970. Geologic map of the Jemez Mountains, New Mexico. USGS Misc. Geol. Invest., Map I-571, scale 1:125,000.

Snyder, G.L. and Hedge, C.E., 1978. Intrusive rocks northeast of Steamboat Springs, Park Range, Colorado. U.S.G.S. Prof. Pap. 1041, 42pp.

Spell, T.L., Kyle, P.R., and Thirwall, M. (in press). $^{40}Ar/^{39}Ar$ geochronology and geochemistry of the Cerro Toledo Rhyolite. NMGS Bull.

Stacey, J.S. and Kramers, J.D., 1975. Approximation of terrestrial lead isotope evolution by a two-stage model. Earth Planet. Sci. Lett., 26:207-221.

Stanton, R.L. and Russell, R.D., 1959. Anomalous leads and the emplacement of lead sulphide ores. Econ. Geol., 54:588-607.

Staudigel, H., Zindler, A., Hart, S.R., Leslie, T., Chen, C.-Y., and Clague, D., 1984. The isotope systematics of a juvenile intraplate volcano: Pb, Nd, and Sr isotope ratios of basalts from Loihi seamount, Hawaii. Earth Planet. Sci. Lett., 69:13-29.

Steiger, R.H. and Jager, E., 1977. Subcommission on geochronology: convention on the use of decay constants in geo- and cosmo-chronology. Earth Planet. Sci. Lett., 36:359-362.

Stein, H.J., 1985. A lead, strontium, and sulfur isotope study of Laramide-Tertiary intrusions and mineralization in the Colorado Mineral Belt with emphasis on Climax-porphyry molybdenum systems plus a summary of other newly acquired isotopic and rare earth element data. Unpubl. Ph.D. thesis, Chapel Hill, Univ. North Carolina, 493pp.

Stein, H.J. and Fullagar, P.D., 1985. Origin of Colorado Mineral Belt Laramide-Tertiary magmatism: lead and strontium isotopes. Geol. Soc. Am. Abstr. Prog., 17:727.

Stein, H.J. and Hannah, J.L., 1985. Movement and origin of ore fluids in Climax-type systems. Geology, 13:469-474.

Stein, H.J. and Crock, J.G., 1990. Late Cretaceous-Tertiary magmatism in the Colorado Mineral Belt: rare earth element and samarium-neodymium isotopic studies. In: The nature and origin of Cordilleran magmatism. Geol. Soc. Am. Mem. 174, pp195-223.

Stein, H.J., Fullagar, P.D., and Hannah, J.L., 1987. Source of Colorado Mineral Belt Late Cretaceous-Tertiary intrusions: regional Pb, Sr, and O isotope studies. Geol. Soc. Am. Abstr. Prog., 19:336.

Steven, T.A., 1975. Middle Tertiary volcanic field in the southern Rocky Mountains. In: Curtis, B.F. (ed.), Cenozoic History of the Southern Rocky Mountains, Geol. Soc. Am. Mem.144:75-94.

Stille, P., Unruh, D.M, and Tatsumoto, M., 1983. Pb, Sr, Nd, and Hf isotopic evidence of multiple sources for Oahu, Hawaii basalts. Nature, 304:25-29.

Stormer, J.C., Jr., 1972. Mineralogy and petrology of the Raton-Clayton volcanic field, northeastern New Mexico. Geol. Soc. Am. Bull., 83:3299-3322.

Sun, S.-S., 1980. Lead isotopic study of young volcanic rocks from mid-ocean ridges, ocean islands and island arcs. Phil. Trans. Roy. Soc. Lond., .A 297:409-445.

Sun, S.-S. and McDonough, W.F., 1989. Chemical and isotopic systematics of oceanic basalts: implications for mantle composition and processes. In: Saunders, A.D. and Norry, M.J. (eds.), Magmatism in the Ocean Basins. Geol. Soc. Spec. Publ. 42, pp313-345.

Sun, S.-S., Nesbitt, R.W., and Sharaskin, A.Y., 1979. Geochemical characteristics of mid-ocean ridge basalts. Earth Planet. Sci. Lett., 44:119-138.

Takahashi, E. & Kushiro, I., 1983. Melting of dry peridotite at high pressures and basalt magma genesis. Am. Min., 68:859-879.

Tatsumoto, M., Unruh, D.M., and Patchett, P.J., 1981. U-Pb and Lu-Hf systematics of Antarctic meteorites. National Institute for Polar Research, Tokyo.

Taylor, R.B., 1976. Geologic map of the Black Hawk quadrangle, Gilpin, Jefferson, and Clear Creek counties, Colorado. U.S.G.S. Quad. Map 1248.

Thompson, R.A., Johnson, C.M., and Mehnert, H.H., 1991. Oligocene basaltic volcanism of the northern Rio Grande Rift: San Luis Hills, Colorado. J. Geophys. Res., 96(B8):13577-13592.

Thompson, R.N., 1982. Magmatism of the British Tertiary Volcanic Province. Scott. J. Geology, 18:50-107.

Thompson, R.N. and Gibson, S.A., 1991. Subcontinental mantle plumes, hotspots and pre-existing thinspots. J. Geol. Soc. Lond., 148:973-977.

Thompson, R.N., Leat, P.T., and Humphreys, E., 1989a. What is the influence of the Yellowstone plume on Pleistocene-Recent western USA magmatism? In:Continental Magmatism (Abs.), Bull. N.M. Bur. Mines Min. Res., 131:268.

Thompson, R.N., Morrison, M.A., Dickin, A.P., and Hendry, G.L., 1983. Continental flood basalts...arachnids rule, OK? In: Hawkesworth, C.J. and Norry, M.J. (eds.), Continental Basalts and Mantle Xenoliths. Shiva, Nantwich, pp.158-185.

Thompson, R.N., Morrison, M.A., Hendry, G.L., and Parry, S.J., 1984. An assessment of the relative roles of crust and mantle in magma genesis: an elemental approach. Phil. Trans. Roy. Soc. Lond., A 310:549-590.

Thompson, R.N., Leat, P.T., Dickin, A.P., Morrison, M.A., and Hendry, G.L., and Gibson, S.A., 1989b. Strongly potassic mafic magmas from lithospheric mantle sources during continental extension and heating:evidence from Miocene minettes of northwest Colorado, U.S.A. Earth Planet. Sci. Lett., 98:139-153.

Thompson, R.N., Gibson, S.A., Leat, P.T., Mitchell, J.G., Morrison, M.A., Hendry, G.L., and Dickin, A.P., 1993. Early Miocene continental extension-related basaltic magmatism at Walton Peak, northwest Colorado: further evidence on continental basalt genesis. J. Geol. Soc. Lond., 150:277-292.

Tweto, O., 1979. The Rio Grande Rift system in Colorado. In: Riecker, R.E. (ed.), Rio Grande Rift: Tectonics and Magmatism. Am. Geophys. Union, Washington, D.C., pp33-56.

Tweto, O., 1980. Precambrian geology of Colorado. In: H.C. Kent and K.W. Porter (eds.), Colorado Geology: Denver. Colorado Rocky Mtn. Ass. Geol., pp37-46.

Tweto, O. and Sims, P.K., 1963. Precambrian ancestry of the Colorado Mineral Belt. Geol. Soc. Am. Bull., 74:991-1014.

Vollmer, R., Ogden, P., Schilling, J-G., Kingsley, R.H., and Waggoner, D.G., 1984. Nd and Sr isotopes in ultrapotassic rocks from the Leucite Hills, Wyoming. Contrib. Mineral. Petrol., 87:359-368.

Warner, L.A., 1978. The Colorado lineament: a middle Precambrian wrench fault system. Geol. Soc. Am. Bull., 89:161-171.

Weaver, B., 1991. Trace element evidence for the origin of ocean-island basalts. Geology, 19:123-126.

Wendlandt, E., DePaolo, D.J., and Baldridge, W.S., 1993. Nd and Sr isotope chronostratigraphy of Colorado Plateau lithosphere: implications for magmatic and tectonic underplating of the continental crust. Earth Planet. Sci. Lett., 116:23-43.

Wernicke, B.P., Christiansen, R.L., England, P.C., and Sonder, L.J., 1987. Tectonomagmatic evolution of Cenozoic extension in the North American Cordillera. In: Coward, M.P., Dewey, J.F., and Hancock, P.L. (eds.), Continental Extensional Tectonics. Spec. Publ. Geol. Soc. Lond. 28, pp203-221.

White, W.M., 1985. Sources of oceanic basalts: radiogenic isotope evidence. Geology, 13:115-118.

White, W.M. and Hofmann, A.W., 1982. Sr and Nd isotope geochemistry of oceanic basalts and mantle evolution. Nature, 296:821-825.

Wolff, J.A. and Gardner, J.N., 1995. Is the Valles caldera entering a new cycle of activity? Geology, 23:411-414.

York, D., Strangway, D.W., and Larson, E.E., 1971. Preliminary study of a Tertiary magnetic transition in Colorado. Earth Planet. Sci. Lett., 11:33-38.

Zartman, R.E., 1974. Lead isotopic provinces in the cordillera of the western United States and their geologic significance. Econ. Geol., 69:792-805.

Zindler, A. and Hart, S.R., 1986. Chemical geodynamics. Ann. Rev. Earth Planet. Sci., 14:493-571.

Zindler, A., Jagoutz, E., and Goldstein, S., 1982. Nd, Sr, and Pb isotopic systematics in a three-component mantle: a new perspective. Nature, 298:519-523.

IMAGE EVALUATION TEST TARGET (QA-3)

150mm

6"

APPLIED IMAGE . Inc
1653 East Main Street
Rochester, NY 14609 USA
Phone: 716/482-0300
Fax: 716/288-5989